$5

January/February 2015

www.arrl.org

QEX

A Forum for Communications Experimenters

Issue No. 288

VE2AZX built this "Low Frequency Adapter for Your Vector Network Analyzer" to extend the range of his HP VNA to include audio frequencies. With a 1 to 30 MHz signal generator it can even serve as a wideband direct conversion receiver.

ARRL The national association for AMATEUR RADIO™
225 Main Street
Newington, CT USA 06111-1494

The Legend Continues

The TS-590SG

Back in 1973, Kenwood introduced the first affordable HF radio to the world, the legendary TS-520... 27 years later, the TS-570D and the TS-570S with 6 meters were by far the most popular HF and HF+6 transceivers on the market.

Be witness to the evolution of KENWOOD's pride and joy - the TS-590S HF transceiver - pushing performance and technology to its utmost limit, with the receiver configured to capitalize on roofing filter performance and IF AGC controlled through advanced DSP technology. Enter the TS-590SG. A new generation of high performance transceiver, with the type of high level response to meet DX'ers needs.

Don't be fooled by big boxes, high price tags, complex operation and broken promises. As Kenwood continues to build outstanding products with unparalleled performance and great value, it's no surprise Kenwood is rated as one of the leading choices for HF radios.

It's not too late to own an HF legend because we still build them today.

KENWOOD

Customer Support: (310) 639-4200
Fax: (310) 537-8235

www.kenwood.com/usa

ISO9001 Registered

ADS#43214

QEX (ISSN: 0886-8093) is published bimonthly in January, March, May, July, September, and November by the American Radio Relay League, 225 Main Street, Newington, CT 06111-1494. Periodicals postage paid at Hartford, CT and at additional mailing offices.

POSTMASTER: Send address changes to: QEX, 225 Main St, Newington, CT 06111-1494
Issue No 288

Harold Kramer, WJ1B
Publisher

Larry Wolfgang, WR1B
Editor

Lori Weinberg, KB1EIB
Assistant Editor

Zack Lau, W1VT
Ray Mack, W5IFS
Contributing Editors

Production Department

Steve Ford, WB8IMY
Publications Manager

Michelle Bloom, WB1ENT
Production Supervisor

Sue Fagan, KB1OKW
Graphic Design Supervisor

David Pingree, N1NAS
Senior Technical Illustrator

Brian Washing
Technical Illustrator

Advertising Information Contact:

Janet L. Rocco, W1JLR
Business Services
860-594-0203 – Direct
800-243-7768 – ARRL
860-594-4285 – Fax

Circulation Department

Cathy Stepina, *QEX Circulation*

Offices

225 Main St, Newington, CT 06111-1494 USA
Telephone: 860-594-0200
Fax: 860-594-0259 (24 hour direct line)
e-mail: **qex@arrl.org**

Subscription rate for 6 issues:

In the US: ARRL Member $24, nonmember $36;

US by First Class Mail:
ARRL member $37, nonmember $49;

International and Canada by Airmail: ARRL member $31, nonmember $43;

Members are asked to include their membership control number or a label from their QST when applying.

In order to ensure prompt delivery, we ask that you periodically check the address information on your mailing label. If you find any inaccuracies, please contact the Circulation Department immediately. Thank you for your assistance.

Copyright © 2014 by the American Radio Relay League Inc. For permission to quote or reprint material from *QEX* or any ARRL publication, send a written request including the issue date (or book title), article, page numbers and a description of where you intend to use the reprinted material. Send the request to the office of the Publications Manager (**permission@arrl.org**).

About the Cover

Jacques Audet, VE2AZX, wanted a way to use his Hewlett-Packard Vector Network Analyzer (VNA) at frequencies below 300 kHz, so he built the "Low Frequency Adapter for Your Vector Network Analyzer" shown on the cover. As an added benefit, you can feed the signal from a 1 to 30 MHz signal generator into the Clock Input port of the adapter, and use it as a wideband direct conversion receiver.

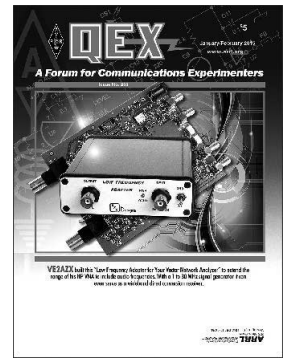

In This Issue

Features

Index of Advertisers

The American Radio Relay League

The American Radio Relay League, Inc, is a noncommercial association of radio amateurs, organized for the promotion of interest in Amateur Radio communication and experimentation, for the establishment of networks to provide communications in the event of disasters or other emergencies, for the advancement of the radio art and of the public welfare, for the representation of the radio amateur in legislative matters, and for the maintenance of fraternalism and a high standard of conduct.

ARRL is an incorporated association without capital stock chartered under the laws of the state of Connecticut, and is an exempt organization under Section 501(c)(3) of the Internal Revenue Code of 1986. Its affairs are governed by a Board of Directors, whose voting members are elected every three years by the general membership. The officers are elected or appointed by the Directors. The League is noncommercial, and no one who could gain financially from the shaping of its affairs is eligible for membership on its Board.

"Of, by, and for the radio amateur," ARRL numbers within its ranks the vast majority of active amateurs in the nation and has a proud history of achievement as the standard-bearer in amateur affairs.

A *bona fide* interest in Amateur Radio is the only essential qualification of membership; an Amateur Radio license is not a prerequisite, although full voting membership is granted only to licensed amateurs in the US.

Membership inquiries and general correspondence should be addressed to the administrative headquarters:

ARRL
225 Main Street
Newington, CT 06111 USA
Telephone: 860-594-0200
FAX: 860-594-0259 (24-hour direct line)

Officers

President: KAY C. CRAIGIE, N3KN
570 Brush Mountain Rd, Blacksburg, VA 24060

Chief Executive Officer: DAVID SUMNER, K1ZZ

The purpose of *QEX* is to:

1) provide a medium for the exchange of ideas and information among Amateur Radio experimenters,

2) document advanced technical work in the Amateur Radio field, and

3) support efforts to advance the state of the Amateur Radio art.

All correspondence concerning *QEX* should be addressed to the American Radio Relay League, 225 Main Street, Newington, CT 06111 USA. Envelopes containing manuscripts and letters for publication in *QEX* should be marked Editor, *QEX*.

Both theoretical and practical technical articles are welcomed. Manuscripts should be submitted in word-processor format, if possible. We can redraw any figures as long as their content is clear. Photos should be glossy, color or black-and-white prints of at least the size they are to appear in *QEX* or high-resolution digital images (300 dots per inch or higher at the printed size). Further information for authors can be found on the Web at **www.arrl.org/qex/** or by e-mail to **qex@arrl.org**.

Any opinions expressed in *QEX* are those of the authors, not necessarily those of the Editor or the League. While we strive to ensure all material is technically correct, authors are expected to defend their own assertions. Products mentioned are included for your information only; no endorsement is implied. Readers are cautioned to verify the availability of products before sending money to vendors.

Larry Wolfgang, WR1B

Empirical Outlook

Looking Forward to the New Year

At the end of each year we take some time to reflect on what has happened over the previous year. We look back at happenings in our lives as well as where our work has taken us. In my case that means thinking about the past 6 issues of *QEX*. I am quite proud of the range and technical content of each issue from 2014! Now, as I write this editorial for the Jan/Feb 2015 issue of *QEX*, it also seems appropriate to consider where we are going over the next 6 issues.

Can 2015 be as incredibly grand as 2014 was? We have moved on from celebrating ARRL's Centennial, with all of the operating activities and events that took place. In 2015 ARRL celebrates the Centennial of *QST*, our Membership Journal. While this means another year-long celebration, most of that activity will focus on our Journal. We have a long way to go before we can celebrate a *QEX* Centennial! (Begun in December 1981 by Paul Rinaldo, W4RI, we just turned 33!)

Looking at the articles I have waiting to be published, and anticipating many more interesting articles to come, I am excited to see that we will continue to provide a wide range of technical articles for you, our readers, to enjoy. There are articles about antenna theory and others about antenna construction, there are some simple construction projects and some more advanced projects. There is an article that involves theory and simulation of oscillators for use in radios, and an IF amplifier project. We have two columnists writing about software defined radio topics, with plans to alternate the SDR: Simplified and Hands On SDR columns with each issue. There are at least a couple of other SDR feature articles in the works.

Our goal is to present a wide range of technical content, so that every reader can find something of interest. Our readers have a wide range of technical backgrounds and expertise, from near beginners excited to learn the finer points of the technical side of our hobby, to life-long electrical engineers with lots of practical design and construction experience. It's a tall order, but we will continue to strive to meet your demands.

Of course the only way we can really meet those demands is to have you write about the topics that interest you, and share projects you have been working on, so that we will continue to have this top-notch technical content.

There are many possibilities, and a whole new year is spread out before us. Where will you help us take *QEX* in 2015?

Robert J. Zavrel, Jr, W7SX, ARRL Technical Advisor

PO Box 91, Elmira, OR 97437; **w7sx@arrl.net**

Bob Zepp: A Low Band, Low Cost, High Performance Antenna — Part 2

This antenna array provides a switchable, 4-direction, vertically polarized, full-azimuth-coverage high gain antenna for 160 meters and a bidirectional horizontal antenna for 40/75/80 meters. Here are the rest of the construction details.

In Part 1, we presented the first two steps in developing the final version of the Bob-Zepp. This began as a simple center fed horizontal wire antenna for 40/80 meters fed with open wire line. By shorting the open wire line at the base, the array becomes a base-fed vertical for 160 meters. Step two involves adding vertical wires to the ends of the horizontal wires; thus the vertical becomes a mini Bobtail curtain. Placing traps on the wires maintains the horizontal configurations on 40 and 80 meters. On 40 meters the antenna is an extended double Zepp, hence the title Bob-Zepp. Furthermore, Part 1 showed how to derive a bidirectional end-fire pattern on 160 meters, thus providing two switchable bidirectional patterns on 160 meters, with both showing considerable gain over a single vertical element.

In Part 2, we begin by showing how the end-fire pattern can become a switchable dual mono-end-fire directional array, thus increasing the gain in these two directions. After Step 3, the final developments are shown to reveal the complete Bob-Zepp.

Step 3

In this end-fire 160 meter configuration, the relative phasing of the currents in the vertical wires can be changed by placing different inductive values where the vertical wires meet the capacitive boots. In effect, by simply changing these inductive values the array can be switched between two *mono-directional* patterns in either end-fire direction, for example, one for "east" and one for "west," while the broadside base-fed curtain remain bidirectional north-south. Figure 9 illustrates the antenna system.

Photo D shows the bottom end of the west leg. You can see the vertical wire coming down to the box, which houses a fixed inductor and remotely operated shorting switch. You can also see the capacitive boot wire, going off to the right. Photo E is a view inside of that box. Photo F is the east leg tuning box, and Photo G shows the tuning circuit inside that box. The variable capacitors are wired in series with the fixed inductor. The motor driven variable capacitors provide for remote tuning of the east or west pattern. The appropriate capacitor is selected with the small relay just below the inductor. Figure 10 gives the schematic diagrams of the west leg circuit and the east leg circuit. We now have three switchable patterns on 160 meters, covering 360° of azimuth direction.

I use a homebuilt 160 meter tuner in the shack. There is a small tuning difference between the east and west patterns, but is easy to tune out with one variable capacitor. Also, DX on 160 meters is almost always worked on nighttime paths, so switching between east and west is not that frequent, especially near local sunrise and sunset. The

Photo D — The west leg of the driven element: the capacitive boot wire runs to the right.

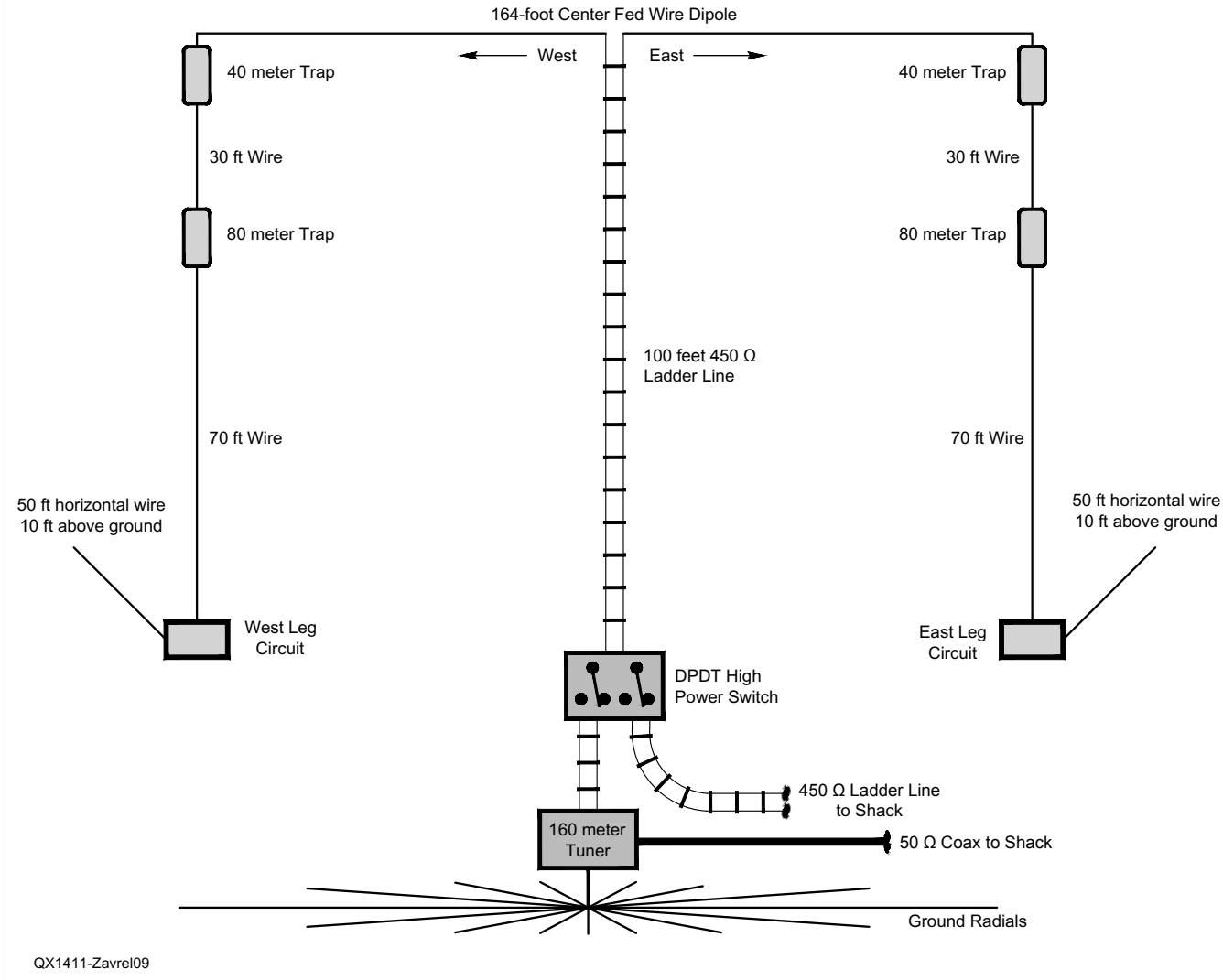

Figure 9 — This diagram illustrates the extended double Zepp antenna on 40 meters, the extended dipole on 75/80 meters and the 160 meter bidirectional north/south curtain plus east and west end-fire antennas.

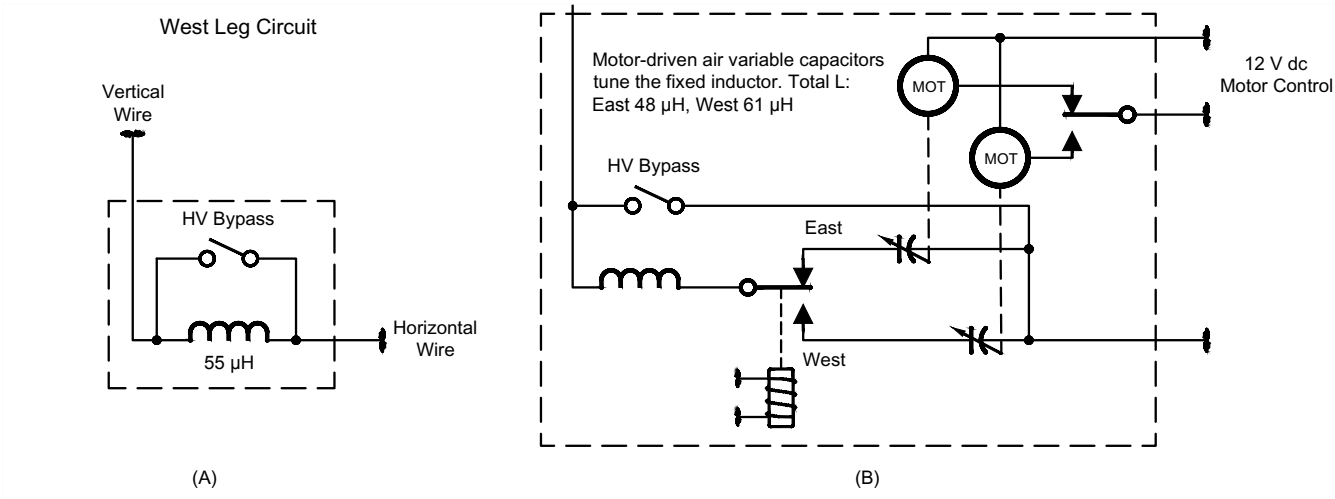

Figure 10 — Here are the schematic diagrams of the tuning circuits at the end of the west and east legs of the antenna. Photo E is the west leg circuit and Photo G is the east leg circuit.

Photo E — The fixed inductor at the west leg. A Russian surplus ceramic switch shorts the inductor out of the circuit when a broadside pattern is desired. The inductor is only used for end-fire patterns.

Photo F — The driven element's east leg tuning box. The heavy cable contains the low-voltage control wires.

same tuner provides complete coverage of the 160 meter band as well, so one tuner in the shack provides full-band coverage *and* tuning out slight differences in the east and west patterns.

The east and west patterns were optimized for forward gain because they are routinely used for transmit only (I have a 4-square receive antenna). By adjusting the inductors, a respectable front to back (F/B) ratio is also possible with some compromise in gain — no surprise there.

To simplify the inductive switching, which creates the directive patterns, a fixed inductor is placed at the base of one end wire while two separate inductive values (through the use of the two series variable capacitors) are available for the respective east and west patterns. This simplification costs only about 0.2 dB gain. The inductors at both driven element legs are completely switched out (shorted) for the north/south curtain pattern, thus only one relay is necessary at the base of the west leg. That also causes the slightly different feed impedances, however.

Step 4

By placing a 1 λ loop reflector in back of the curtain we can create a mono-directional broadside curtain array. In my case, the maximum gain is to the north (actually toward Europe and the Middle East). The actual loop circumference is less than 1 λ, but I can remotely tune the loop from the shack by using another fixed inductor/variable motor driven capacitor from the shack.

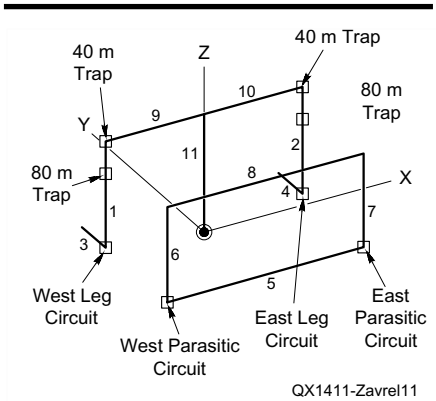

Figure 11 — This drawing is the *EZNEC* model of the complete antenna, including the 1 λ loop reflector.

The following patterns are modeled from *EZNEC* and also bear out through experiment and on-the-air use. All elevation angles were taken at 20° over "average ground." Notice that the gain approaches that of a full-size 4-square.

Figure 11 is an *EZNEC* plot of the antenna, which also shows the relative current values along the various elements. The separation of the loop and the curtain is 90 feet in this generic example. This is for the north pattern. The horizontal sections of the loop are 164 feet, the same over-all width of the driven curtain. The top wire is 90 feet above ground, while the bottom wire is 10 feet above the ground. Fixed loading inductors of 19.5 μH are positioned at the bottoms of both the loop's vertical wires (wires 6 and 7). The tuning and switching takes place at the base of element 7. The inductors needed for the

Photo G — Inside the east leg box: The high voltage switch at the top inside the box shorts the inductor out for broadside patterns. The lower voltage switch selects one of the two variable capacitors. These capacitors are in series with the fixed inductor, which is wound on a PCV pipe section. These capacitors are connected in series with the inductor and provide motor-driven variable tuning for the east and west end-fire patterns. The small relay at the bottom automatically connects the appropriate motor/capacitor for either the east or west pattern. These capacitors must be mounted on insulators. Notice also the nylon insulators connecting to the motors. The motors are 12 V DC, 6 rpm gear motors. The DC control permits easy direction changing when fine tuning the antenna.

Photo H — Here is the parasitic loop tuning box, which is at the base of the east vertical element. This view is looking west down the low horizontal wire of the loop. The horizontal wire is placed about 15 feet high so delivery trucks and other vehicles can pass under it. The horizontal wire is supported by a tree in back of this view, to achieve the desired height clearance. The insulator is visible in the top left corner of the photograph.

end-fire configuration at the bases of wires 1 and 2 are shorted for bobtail configurations.

The plots of Figures 12, and 13 show the outstanding gain for the end-fire east and west patterns, and Figure 14 shows the north pattern using the parasitic loop.

With both loop inductors at 19.5 µH, the array shows maximum gain to the north. By changing either of the loop inductors from 19.5 µH to 4 µH, the loop becomes a director and the pattern is now to the south. Figure 15 shows the switching arrangement to make this change. Figure 16 is the *EZNEC* radiation pattern plot for the pattern to the south.

Building High Power Remote Control Variable Inductors

With three variable, remote control, and high power inductors needed for all the tuning of this array, a simple and far more

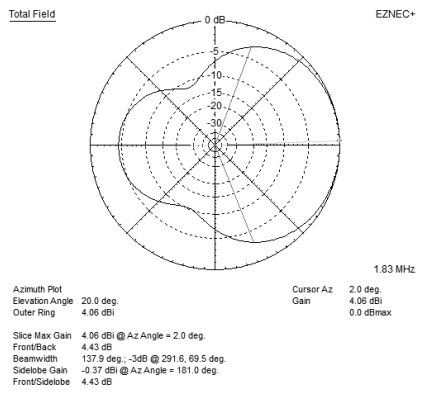

Figure 12 — This *EZNEC* radiation pattern plot shows the end-fire pattern to the east.

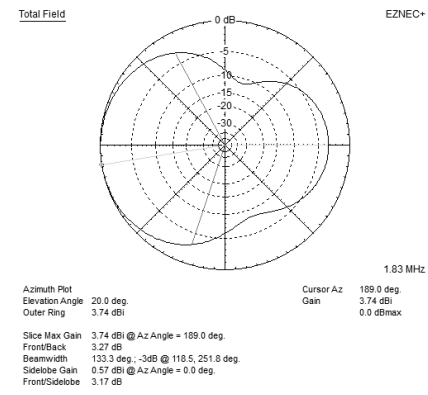

Figure 13 — This *EZNEC* radiation pattern plot shows the end-fire pattern to the west.

Photo I — This is a peek inside the parasitic loop tuning box. The high voltage surplus Russian switch is used to close the loop, thus activating the loop. A remote controlled motor-driven variable capacitor is used in series with the inductor to provide a continuously variable inductance. Thus the array can be adjusted from the shack for maximum forward gain or maximum F/B. A second lower-voltage switch is used to tap the inductor for a director pattern toward New Zealand. The director pattern is a "free feature" but is not very critical, thus fine tuning is not required. The box is an old single-drawer file cabinet with an aluminum sheet access door. The exterior of the box was painted with rust-resistance paint.

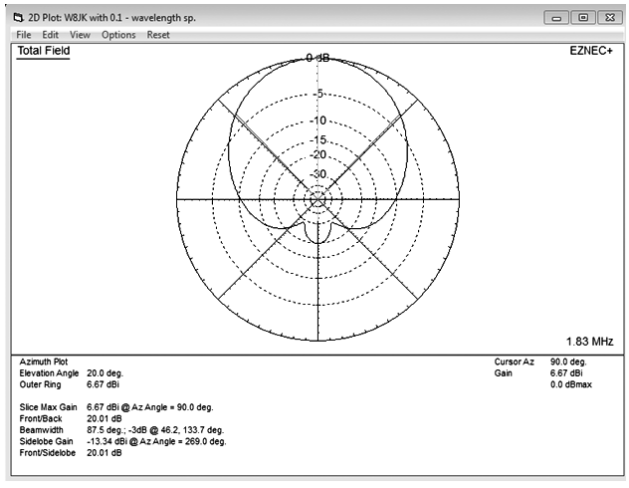

Figure 14 — This *EZNEC* radiation pattern plot shows the pattern to the north, with the loop switched in as a reflector.

economical solution is used rather than very expensive and hard-to-find motor-driven rotary inductors. For the inductive values typically needed for low band tuning, large gauge wire inductors (wound on PVC or ABS conduit) can serve nicely. To make it "variable" simply use a variable capacitor in series with the inductor. Small gear motors are available from numerous surplus supplies (I use **www.surpluscenter.com**). You want one that is geared down to 1 to 2 rpm, and that has a ¼ inch shaft. Low voltage DC control allows for reversing the direction. I even found a small surplus motor speed controller that I use for fine tuning! Then place an *insulated* shaft coupler between the capacitor shaft and the gear motor, since *both* sides of the capacitor are at high RF potential — BE CAREFUL! This is a nice technique to know when any type of remote tuning is needed or desired.

For a series LC circuit, selection of component values to form an equivalent variable inductor is simple. The capacitive and inductive reactances simply cancel. If the capacitive reactance is greater than the inductive reactance (smaller capacitor value), the equivalent is a capacitor, if the capacitive reactance is less than the inductive reactance, the result is an inductor. If they are equal, the result is a short circuit (except for a small resistive value). The vital equations are:

$$X = X_L - X_C \qquad \text{[Eq 1]}$$

and:

$$X_L = \omega L \qquad \text{[Eq 2]}$$

$$X_C = 1/\omega C \qquad \text{[Eq 3]}$$

$$\omega = 2\pi f \qquad \text{[Eq 4]}$$

where:

L is inductance in henrys, C is capacitance in farads, and f is the frequency in hertz.

For example, if we have a 100 µH inductor (about 1131 Ω inductive at 1.8 MHz) and a 78 to 500 pF variable capacitor connected in series, this would provide the equivalent of a 0 to 84 µH variable inductor at 1.8 MHz, where 78 pF is about 1130 Ω capacitive reactance and 500 pF is about 177 Ω capacitive reactance at 1.8 MHz. So, the greater the series capacitance, the greater the equivalent series inductance will be. If we tune the capacitor below 78 µF, the circuit begins to present a capacitive reactance.

Taking Gain Measurements

I developed a simple method of measuring the antenna gain, to make the tuning ad-

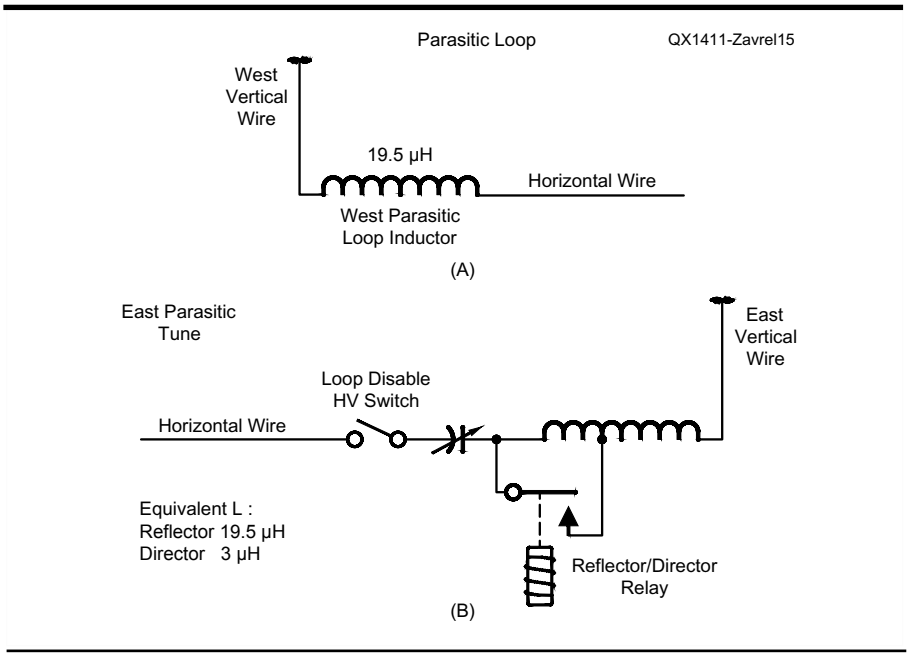

Figure 15 — This drawing shows the switching arrangement to enable or disable the loop, along with the relay to change the inductance value to switch between the loop serving as a reflector and a director for the north and south patterns.

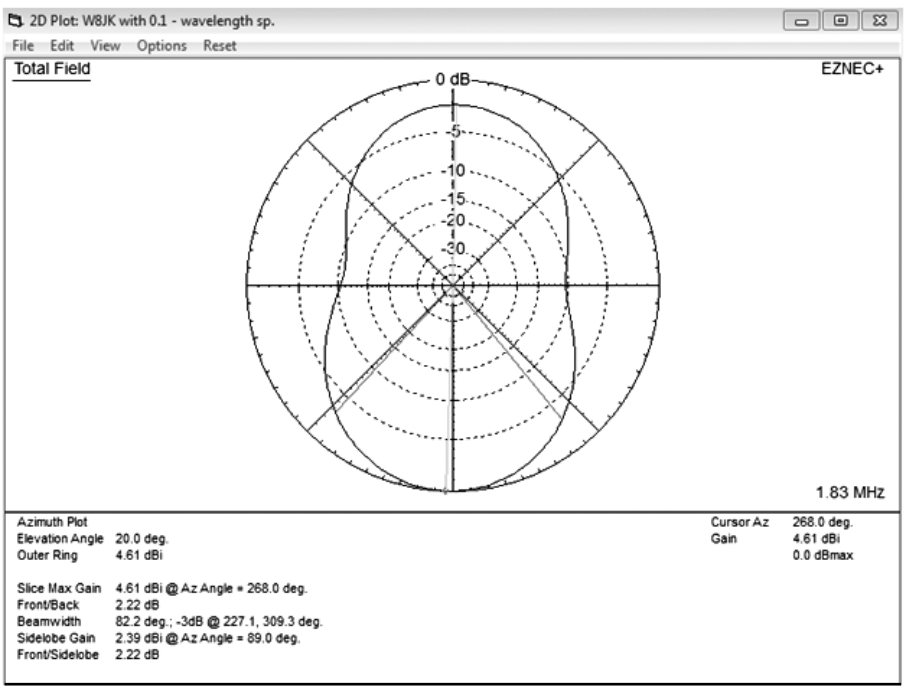

Figure 16 — This *EZNEC* radiation pattern plot shows the pattern to the south, with the loop switched in as a director.

justments on this antenna. I attach an HP AC voltmeter to the speaker output of my Elecraft K3, with the AGC turned off. To create a very simple 160 meter battery operated signal source, I used a common 1.843 MHz digital clock module running on three 1.5 V AA batteries. I mounted the entire assembly in a piece of PVC tubing and added a PVC cap on the bottom end. A four foot wire provides the antenna, and also doubles as a way to hang the signal source from tree branches. To make my gain measurements, I place the signal generator several hundred feet from the array. While tuning the inductors remotely, the AC voltmeter records the response. The HP meter also provides a dB scale, so dB differences can be read directly. If maximum forward gain is desired, the inductances are adjusted for maximum audio output. The signal generator is then moved and the applicable pattern also adjusted, making sure the antenna is properly matched. This makes for a very convenient method of fine tuning the array from the comfort of my shack!

Optimizing Loop Parasitic Elements

Most amateurs are familiar with the Cubical Quad antenna. The quad uses slightly longer or shorter than 1 λ loops for the parasitic elements (reflector and directors), and a resonant 1 λ loop for the driven element. A properly tuned (cut) near-square loop will be equally effective as either a vertical or horizontally polarized parasitic element. For the desired vertical polarization on 160 meters, a simple vertical can be made to provide respectable gain by placing a reflector loop in back of the vertical. Placing a reflector in back of a bidirectional vertical array, such as the Bob-Zepp, outstanding forward gain can be realized. Indeed, over 6 dBi is realized at a 20° take-off angle in the north direction, comparable to a full-size 8-circle array!

Parasitic loops are obviously advantageous for creating substantial gain in low-band systems. Using a fixed loop (nonrotatable array), the loop will always act as a reflector distorting or ruining patterns in other dictions. Also, it can adversely affect receive arrays, like 4-squares or 8-circles operating within several hundred feet of the loop. The solution is to de-tune the loop, effectively taking it out of the "circuit" to avoid the problem, particularly when using a directional receive antenna.

One solution is to break the wire with a switch. Unfortunately, if you place the switch at the wrong location in the loop, it will not eliminate its effect upon the desired pattern. Indeed, it is possible to place a switch at a location where it has no effect whatsoever (at the maximum voltage point). The following two examples show how critical switch placement is. The open switch, by default,

defines a zero-current point (no current is possible across an open circuit). This will also define the high voltage point. As mentioned before, a square loop will affect either a vertically or horizontally polarized signal (unlike a Yagi's parasitic element, which will function on only one polarization effectively). Breaking the loop half way along a vertical section, however, will force the element to be *only* horizontally polarized and visa-versa.

A second effective solution is to break the loop in two locations, but this requires two high voltage switches and considerably more mounting and wiring. Using this solution, make sure the two remaining section lengths are far removed from multiples of ½ λ.

A third solution uses only one switch and provides other advantages as well. A loop at or less than about 0.93 λ total length, open at the *base* of one (single switch) of the vertical elements results in an insignificant parasitic effect with little effect on forward gain compared to a full-sized loop. The addition of two inductors can create either a reflector or a director element, or a north or south pattern. Furthermore, the use of inductors provides "fine tuning" of the parasitic element for maximum gain or F/B. I maximize F/B since this array's gain becomes an outstanding receive antenna in the north direction.

When using odd-shaped loops, the use of two inductors can help "force" the loop to be optimized for vertical polarization. I found it most effective to model the array using *EZNEC*, use the results as a starting point, and then optimize gain or Front to Back Ratio by fine tuning. For the loop dimensions shown, a 0 Ω inductive reactance value at the bottom inductor will result in near-maximum gain to the south. The difference between gains using the loop as a reflector versus as a director is evident in the plots shown in Figures 14 and 16. Using the loop as a director for the south pattern, however, provides an extra 1 dB over the loop "out" configuration, at the expense of a second switch in the loop control box. Now the parasitic element can be switched north, south or "out" for a bidirectional pattern.

As with the east/west pattern tuning, a similar capacitor-inductor combination provides for remote inductive tuning from the shack. Photo H shows the parasitic loop tuning box and Photo I gives us a peek inside the box. Photo J shows the west corner of the parasitic loop.

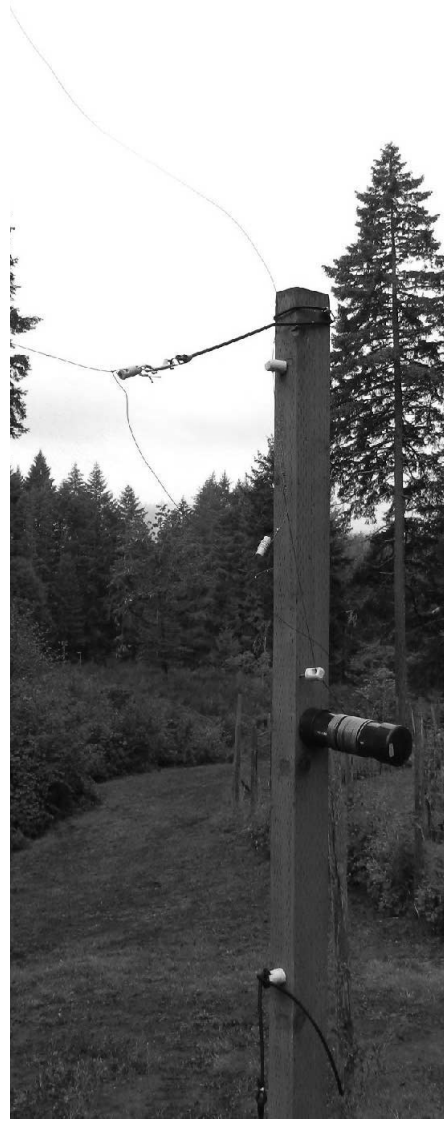

Photo J — Here is the west corner of the parasitic loop: A fixed inductor wound on a 3 inch ABS plastic pipe section with insulated #12 electrical wire solves the problem. ABS end connectors are used to close the pipe and provide a convenient mounting scheme on the post. Note the west anchor for the horizontal wire at the top of the pole using a bungee cord for stress relief. The vertical wire is fed through a ceramic electric fence insulator near the top of the post and with stress relief provided by another bungee cord. My pinot noir vineyard is in the background.

When using low-band parasitic loops, best performance (for a given reduced size <1 λ), can be optimized by making the vertical elements as "vertical" as possible. Inductive loading is placed at the base of the two vertical elements. More important than the different vertical heights, is to keep the horizontal parts of the loop as close to identical in length. This will assure that the current maximums will be placed half way up both vertical elements, and thus provide the best gain and/or F/B ratios possible for the given size. Placement of the loading inductors at the bases of the vertical sections makes them accessible from ground level and prevents additional weight up on the suspended wires.

Results

The gain figures speak for themselves. Running full power, this array can hold its own with full-size 4-square arrays even on the most difficult paths.

Bob Zavrel, W7SX, is an ARRL Life Member, Technical Advisor and Amateur Extra class licensee. He has been licensed since 1966. His primary interest in Amateur Radio is low band DXing and designing and building antennas, tuners, and amplifiers. Bob holds 5BDXCC, 5BWAZ (200), has 334 mixed, and 324 CW entities confirmed. Bob is on the DXCC Honor Roll and the CW DXCC Honor Roll, all using only tree-supported wire antennas. He also hold 9 Band DXCC on 160 through 10 meters. Previous call signs include WN9RAT, WA9RAT, WA9RAT/HR2 and SV1/W7SX.

Bob has a BS in Physics from the University of Oregon and has worked in RF engineering for over 30 years. He has five patents, and has published over 50 papers in professional and Amateur Radio publications, including the first block diagram of an SDR receiver in 1987. He was involved with the first generation of RF integrated circuits for cellular phones, and worked extensively with DDS, WLAN and passive mixer development. Bob is currently an RF Research and Development Engineer for Trimble Navigation with a primary focus on high precision GPS, down to mm accuracy.

Jacques Audet, VE2AZX

7525 Madrid St, Brossard, QC, Canada J4Y 1G3: **jacaudet@videotron.ca**

A Low Frequency Adapter for your Vector Network Analyzer (VNA)

This compact and versatile unit extends low frequency capability down to 20 Hz for your VNA using down/up conversion. It also generates clean signals from audio up to 5 MHz, and provides direct conversion receive capability plus a high impedance input compatible with scope probes to drive 50 Ω loads over a 60 MHz bandwidth.

I always wished my Hewlett-Packard Vector Network Analyzer (VNA) would be capable of going down to frequencies below 300 kHz. I was working on a project that necessitated frequency response tests in the audio range, but it could not be done with my HP machine. So I started designing a low frequency adapter that would retain the accuracy and linearity of my RF VNA. Figure 1 shows the basic diagram of my Low Frequency Adapter (LFA).

System Overview

The VNA generates frequencies from 10 MHz to 15 MHz on its port 1 when set in S_{21} mode. This mode allows measuring attenuation or gain as well as phase shift between ports 1 and 2. The above signal is mixed in a double balanced mixer (DBM), which has its local oscillator (LO) at 10 MHz. The difference signals from 20 Hz to 5 MHz go through a low-pass filter (LPF) and are available at the transmit (TX) output port for frequency response testing. The output of the device under test (DUT) is fed to a high impedance buffer and to a 5 MHz low pass filter before being re-multiplexed in the 10 to 15 MHz range by a second DBM.

The signal at the RF output of this mixer has double sidebands, above and below the 10 MHz LO frequency. The VNA synchronously demodulates the upper sideband and uses this signal to compute the attenuation or gain of the device under test in the S_{21} mode. Both the first and second 5 MHz filters (LPF1 and LPF2) provide attenuation of the 10 MHz LO signal, so it does not go thru the device under test path. These filters also greatly attenuate the sum frequencies in the 20 to 25 MHz range, which could decrease the accuracy if these were present at the second DBM IF input.

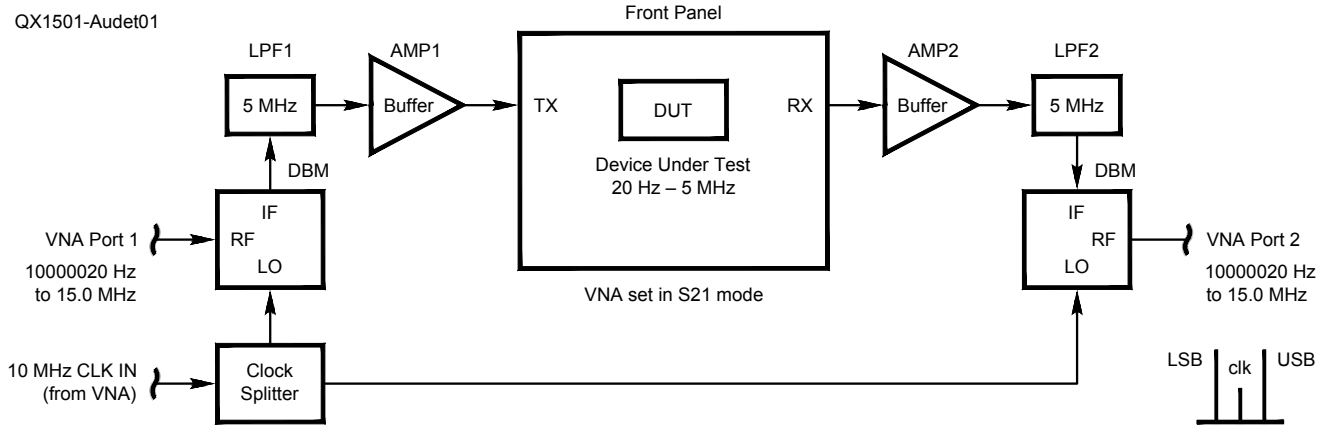

Figure 1 — Basic block diagram of the low frequency adapter (LFA).

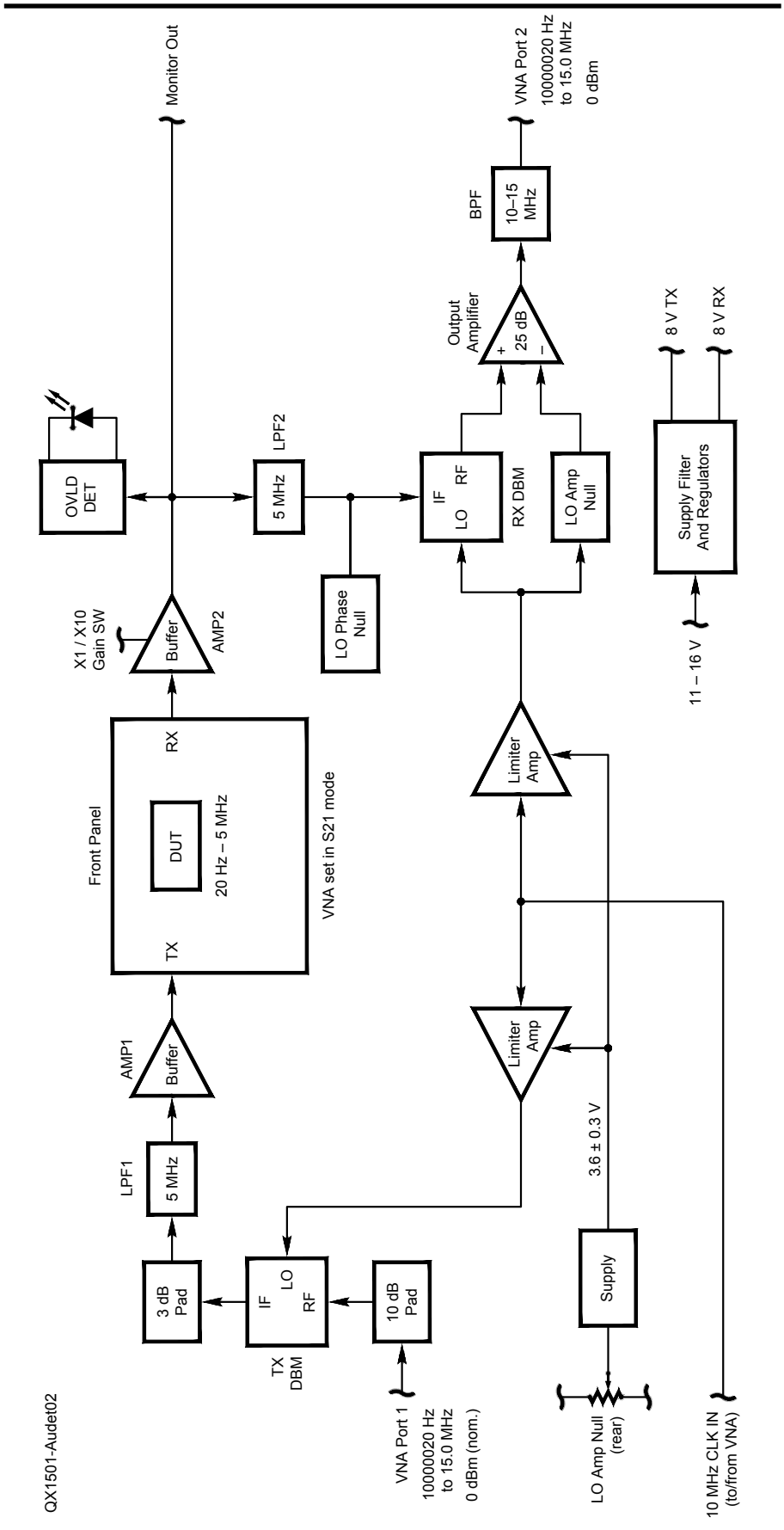

Figure 2 — Detailed block diagram of the low frequency adapter

Since the VNA does coherent detection of the signal (in order to measure the phase), it is necessary to have its internal clock synchronized with the low frequency adapter LO signal. This is normally done by using a common external 10 MHz clock feeding the VNA and the low frequency adapter. This also enables the low frequency adapter to do S_{21} phase measurements from 20 Hz to 5 MHz.

I wanted the low frequency adapter to be as transparent as possible to the VNA. This meant that the low frequency adapter should have unity gain from its input and output. Also the TX output port should have a 50 Ω impedance to be able to drive low impedance loads. On the receive side, the input impedance consists of 1 MΩ in parallel with 8 pF so that it is compatible with oscilloscope probes. An additional capacitor may be added to provide the same input capacitance as your scope input for instance, thus providing a flat frequency response with an external ×10 probe. This high impedance provides much flexibility for the user to terminate the device under test by shunting a parallel termination across the receive (RX) input.

Figure 2 shows a more detailed block diagram of the low frequency adapter.

Detailed Description

The VNA outputs its default-level 0 dBm signal, which is attenuated by 10 dB before reaching the RF port of the TX double balanced mixer. This is done to preserve the linearity at its IF output. The TX output level must track the VNA port 1 level in order to minimize generated distortion on the device under test signals and preserve the VNA capability to perform compression tests. Both double balanced mixers used are of level 7 type, requiring a nominal +7 dBm at the LO port. The 10 MHz clock is sent to a limiter amplifier that drives the two LO ports with a fast square wave, reducing the distortion at high levels and providing a constant LO drive with varying clock input levels. A 3 dB pad at the IF port provides a minimum termination for the TX DBM at both the upper and lower sidebands, helping to minimize distortion. A buffer amplifier (AMP1) provides about 17 dB of gain to compensate for the losses in the pads and the TX DBM, while providing an output level of 225 mV into a high impedance or 112 mV into 50 Ω (–6 dBm).

The RX side provides unity gain from its input to the monitor and VNA outputs. The gain may be increased by 20 dB (×10) using a front switch to improve the system dynamic range. The monitor output has approximately 80 MHz bandwidth in ×1 mode and 60 MHz in ×10 mode. It can be used to monitor the

device under test output with an oscilloscope or to provide a high impedance buffer for the VNA, compatible with oscilloscope probes. An overload detector turns on a red LED when the input exceeds +5 dBm. The same LED is normally green and indicates that the low frequency adapter is powered on. A buffer amplifier (AMP2) also drives a 5 MHz low pass filter, which feeds the IF of the second double balanced mixer. The filter is designed for a 30 Ω load, since this is the impedance that I measured at the IF port when the LO is present.

The signal fed at VNA port 2 consists of the two sidebands and some 10 MHz LO carrier leak.

The second double balanced mixer (RX DBM) must provide a high degree of rejection of the LO signal. This is important at the lowest frequencies, from 20 Hz to 1000 Hz. The LO appears as a spurious signal at the VNA port 2, even more than the undesired LSB signal. For this reason, it is necessary to use the lowest IF bandwidth at the VNA (10 Hz for the HP 8753x). This will require slowing down the sweep speed.

The selected RX DBM provides excellent LO rejection from the LO port to the RF port (typically 70 dB). This was not enough at the lowest frequencies, and limited the dynamic range to 60 to 70 dB, however. The expected dynamic range is 90 dB, which occurs above 2 kHz. With an LO at +7 dBm, and 70 dB of LO-RF isolation, –63 dBm will appear at the RF port. This signal is then amplified by the output amplifier, which has 25 dB of gain. This brings the LO to –38 dBm at the VNA port 2. This high level will reduce the dynamic range at the lowest frequencies. We need to reduce the LO feedthrough below –70 dBm at port 2 to restore the 90 dB dynamic range below 100 Hz.

The external LO nulling circuit uses the LO to feed an adjustable voltage divider connected to the inverting input of the output amplifier. Every double balanced mixer has its own LO to RF phase shift characteristics,

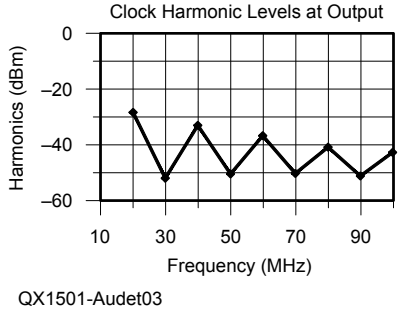

Figure 3 — Measured harmonic Levels of the 10 MHz LO at the output of the RX DBM mixer. Note the strong levels at all even multiples of the LO frequency.

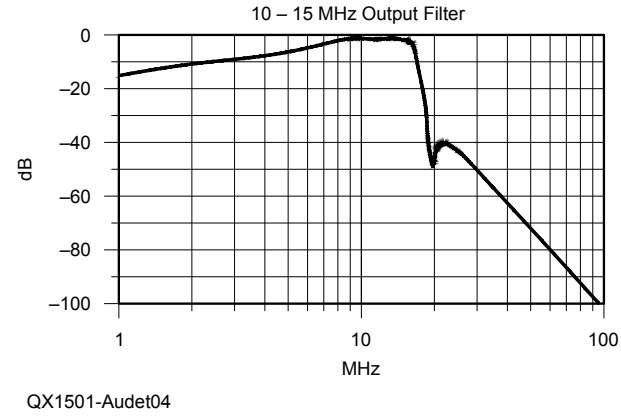

Figure 4 — Band-pass filter frequency response.

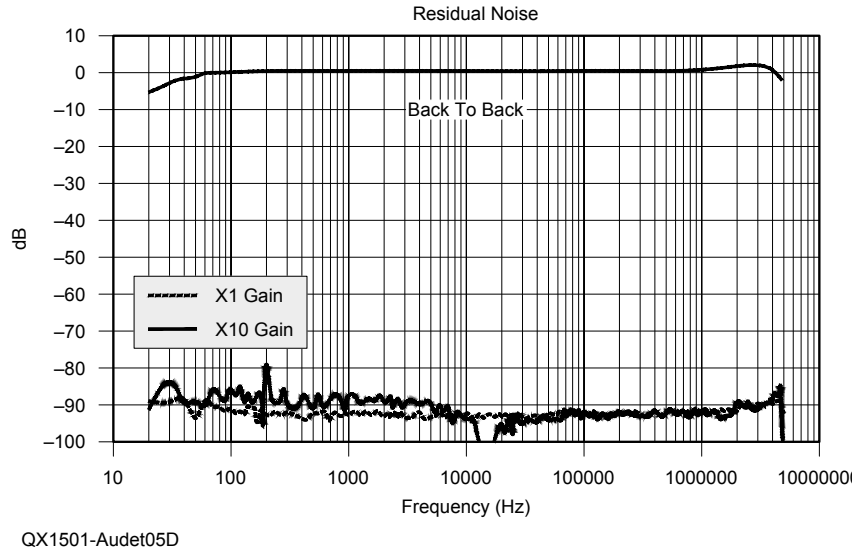

Figure 5 — System measured back-to-back frequency response and residual noise level.

however, so a variable phase shifting circuit is required. I found that adding bias current in the order of a few microamps to the double balanced mixer IF port did shift the phase. A few double balanced mixers, out of the 40 units I tested, had their initial phase too far and could not be used on the RX side. They can be used as a TX double balanced mixers, however.

There are two amplitude nulling adjustments, one located on the circuit board and the other at the rear. The phase adjustment is located at the rear. Doing so allows easy tweaking of LO null before low frequency (below 1 kHz) response tests are done.

During the testing phase, I found that I had some intermodulation problems at the VNA. Looking at the spectrum, I discovered that high levels of harmonics were present at the RX double balanced mixer RF output. See Figure 3.

A band-pass filter was added at the output to clean up these spurs and get rid of all intermodulation problems. Figure 4 shows the filter frequency response.

Figure 5 plots the system back-to-back frequency response and residual noise level, showing a 90 dB and 110 dB dynamic range in the ×1 and ×10 modes respectively.

Figure 6 shows a picture of the completed unit. Part A shows the font panel, while Part B shows the rear panel. Figure 7 is a picture of the assembled circuit board. The detailed circuit schematic for the low frequency adapter is not printed in the article, but can be downloaded from the author's website and the ARRL *QEX* files website.[1, 2] The adapter

[1]Notes appear on page 16.

Figure 6 — The low frequency adapter is built in a standard Hammond extruded aluminum cabinet. The front and rear panels are pictured.

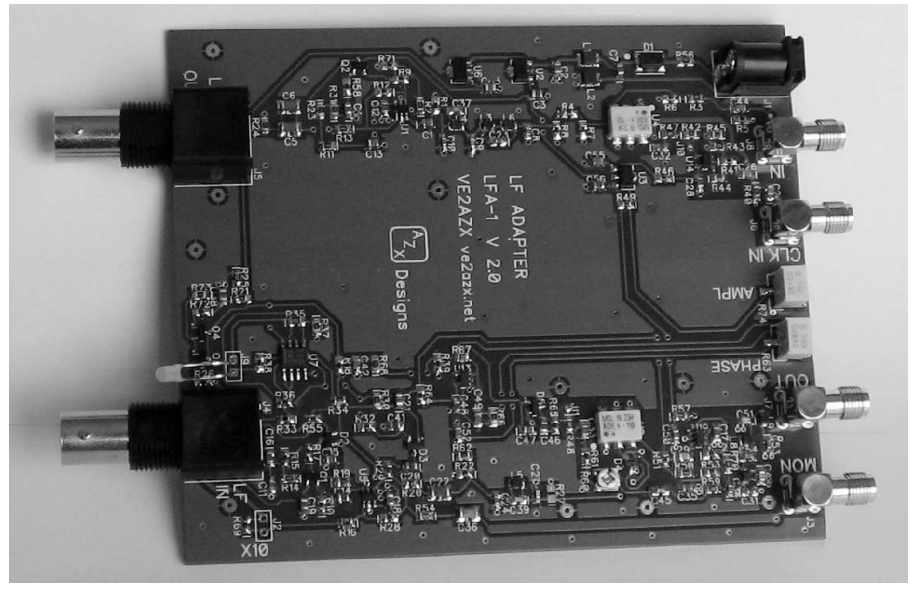

Figure 7 — The assembled circuit board. The R, L and C components are of 0805-size, surface-mounted. Smaller 0603 components will also fit on the pads.

is built on a 3.9 × 4.68 inch (9.9 × 11.89 cm) circuit board, using surface-mounted components on the top surface. It uses a power supply Pi filter and separate regulators for the TX and RX sides, to enhance isolation. The amplifiers used are of the current feedback type, with stable gain that is set by resistors. Two low noise +4 V DC references, consisting of emitter followers, provide a constant output impedance and a flat frequency response. The board may be assembled in approximately five hours.

Low Frequency Adapter Basic Capabilities

All S_{21} measurements are performed within the 10 to 15 MHz frequency range of the VNA. The low frequency measurements include:

- S_{21} magnitude and phase,
- Group Delay,
- Compression point at a single frequency.
- TRU Calibration, with the device under test bypassed with a short circuit, to set a reference amplitude and phase frequency response.

Figure 8 shows the linearity and accuracy in measuring S_{21} magnitude.

Impedance Measurements

The unit as such does not provide for measuring the reflection coefficient S_{11}. The problem of measuring impedances with a return loss bridge is that the accuracy decreases rapidly when the unknown impedance is more than five times above or below the

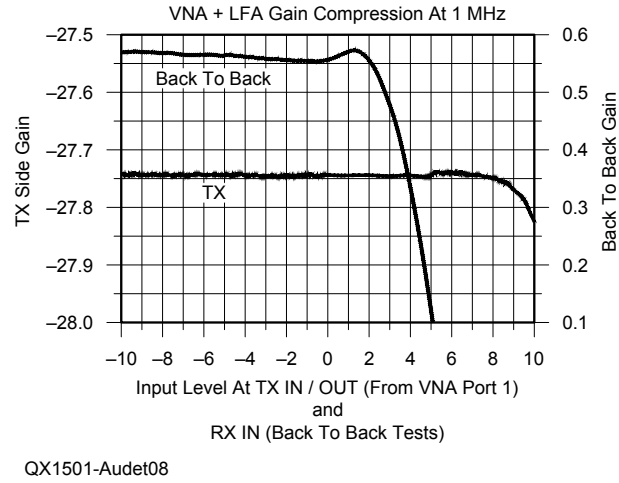

Figure 8 — Linearity / Gain Compression test results. The TX output gain rolls off less than 0.1 dB at +10 dBm, while the RX side gain compression measures ±0.05 dB up to +3 dBm input.

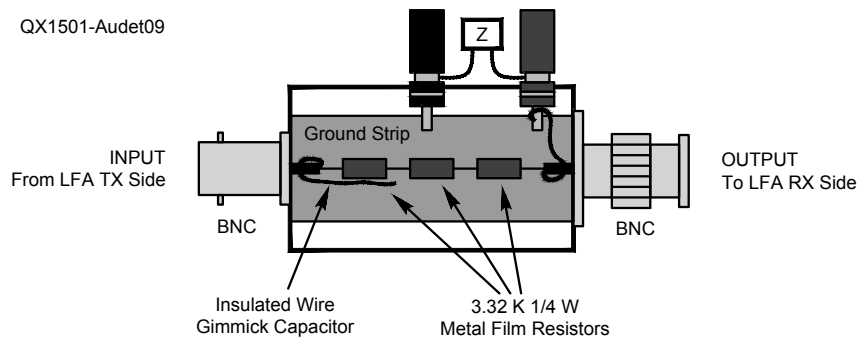

Figure 9 — Here is the shunt impedance adapter physical layout used for impedance measurements. Note the three resistors connected in series to reduce the overall shunt capacitance.

reference impedance. At low frequencies, we are generally interested in measuring a wide range of impedances, from say 0.1 Ω to 1 MΩ. This measurement is best handled by a series or shunt transmission circuit, where S_{21} is measured as a complex value and used to compute the impedance value, including the reactance, inductance, capacitance, and resistance in the series or parallel models. I have created an *Excel* spreadsheet that performs these computations.[3]

Note that the low frequency adapter provides 1 MΩ impedance on the RX side, which gives the user more flexibility in doing shunt impedance measurements. When the device under test cannot be floated, then the shunt configuration must be used. With the normal 50 Ω source and load impedances, the maximum value of shunt impedance that can be measured does not exceed about five times 50 Ω, or 250 Ω. Adding resistors in series with the 50 Ω source (TX) and load (RX) will increase the accuracy in measuring higher impedances at the expense of reducing the dynamic range. For example adding 1000 Ω in series at both the TX and RX sides will give about 32 dB of attenuation when the shunt device under test is unconnected.

With the low frequency adapter, the RX impedance is raised from 50 Ω to 1 M Ω, the attenuation will be about 0 dB with the shunt device under test unconnected, and no reduction in the dynamic range will occur. The *Excel* spreadsheet performs these calculations. Figure 9 shows the layout of the shunt impedance adapter that I used. It provides impedance measurements from < 1 Ω to over 20 kΩ, from 20 Hz to 10 MHz. Photo A shows the completed shunt impedance adapter.

Table 1
Using external probe and attenuator allows large signal capability.

Maximum Input Amplitude	*Setup*
50 mV rms	×10 Gain on LFA, improves dynamic range
500 mV rms	×1 Gain on LFA
5 V rms	×1 Gain + ×10 probe
50V rms	×1 Gain + ×100 attenuator 1 MΩ in/out
500 V rms	×1 Gain + ×100 attenuator + ×10 probe

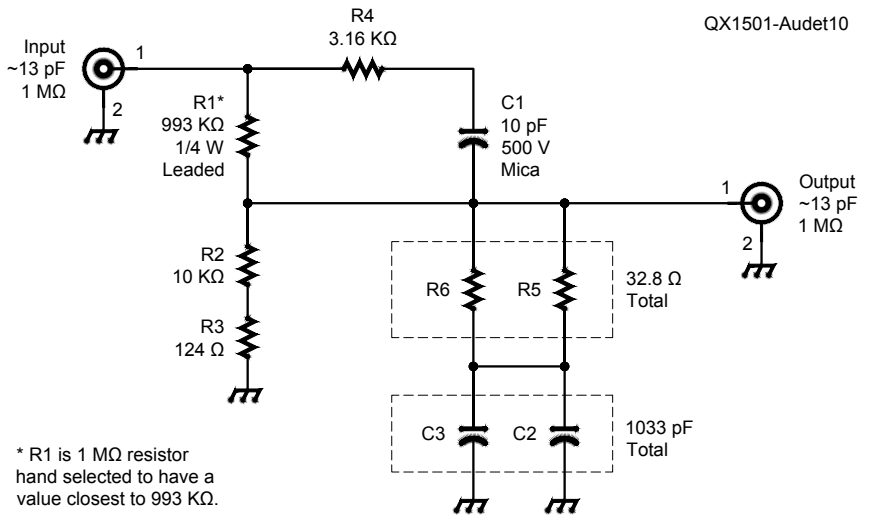

Figure 10 — The schematic diagram for the ×100 divider/attenuator.

Photo A — This photo shows the assembled shunt impedance adapter. The female BNC connector accepts the signal from the low frequency adapter TX connector. The male BNC connector is the output signal, which goes to the low frequency adapter RX connector.

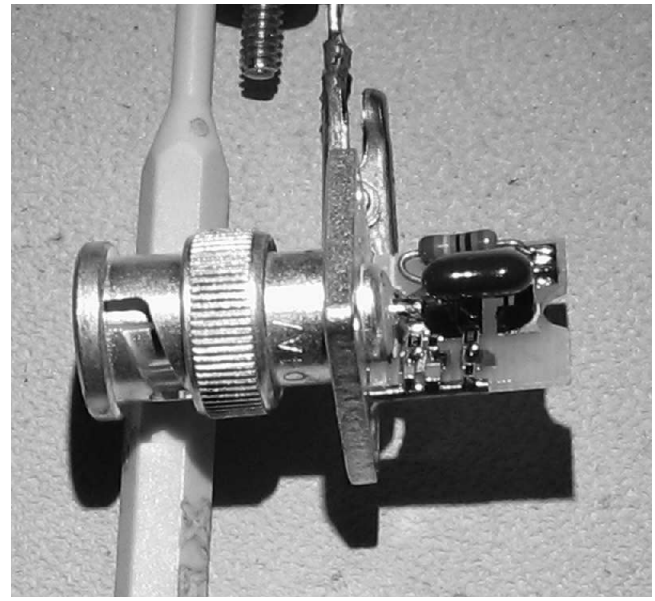

Photo B — Here is the male BNC connector, with the ×100 attenuator circuit board attached. A short wire from the female BNC connector goes to the circuit board pad at the top right corner before placing that end into the square aluminum extrusion.

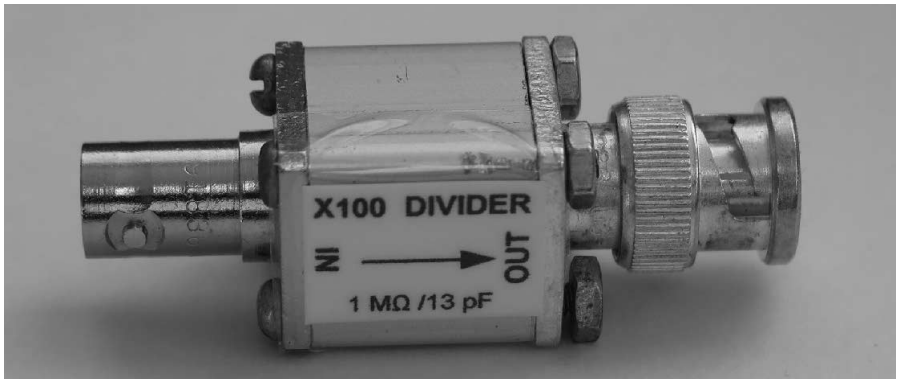

Photo C — This photo shows the completed ×100 attenuator unit.

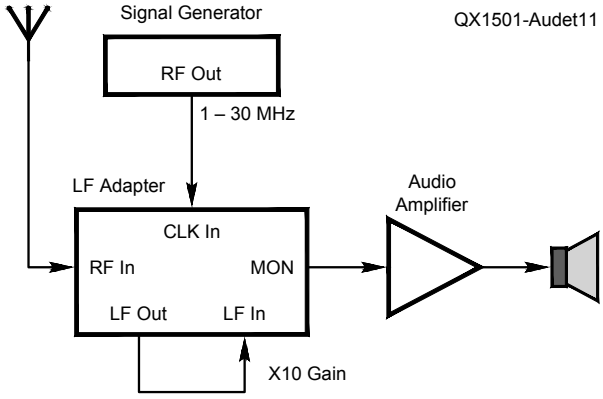

Figure 11 — Setup for an HF direct conversion receiver. The monitor output uses ×10 gain to improve the signal to noise ratio.

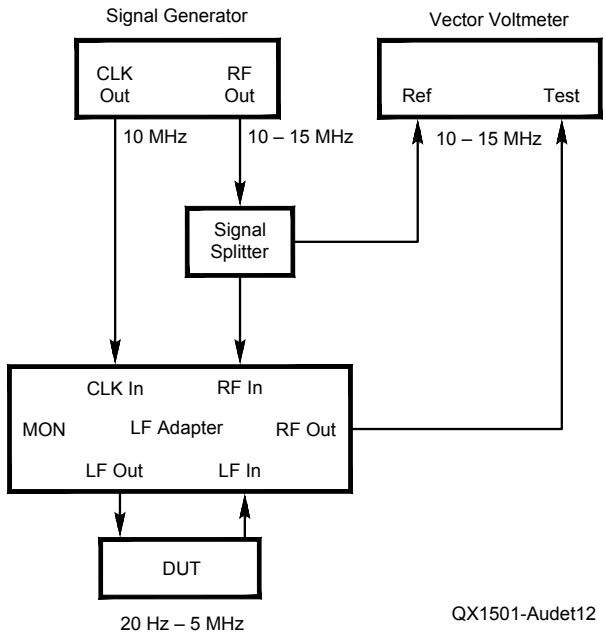

Figure 12 — Setup for using the vector voltmeter at low frequency, using a synthesized RF signal generator. While I have not tried this setup, a very similar arrangement is described in Note 5.

Other Applications of this Low Frequency Adapter

• **Probe Buffer / Amplifier** using the monitor output. It provides an 80 MHz bandwidth in ×1 mode and a 60 MHz bandwidth in ×10 mode.

Using a ×100 attenuator at the low frequency adapter RX input, and/or a ×10 probe provides the ability to handle a very wide range of amplitudes, as shown in Table 1. Figure 10 shows the schematic diagram of the ×100 1 MΩ wideband attenuator that I designed. Photo B is a picture of the circuit board and BNC male connector for the output side of the attenuator. A BNC female connector is used for the input side, and that attaches to the circuit board with a single wire to the circuit board pad between the 933 kΩ and 3.16 kΩ resistors. Photo C is the complete, assembled attenuator. For more details about this ×100 attenuator see the file **Divider-100.pdf** that is part of the **1x15_Audet.zip** file on the ARRL *QEX* files website.[4]

• **Low Frequency Signal Generator**, using your RF signal generator.

The generator clock output provides the clock signal for the low frequency adapter. Its frequency is set from 10.00002 MHz to 15 MHz, to generate an output from 20 Hz to 5 MHz. The low frequency adapter output amplitude tracks the generator output up to +10 dBm.

• **Direct Conversion Receiver**

The low frequency adapter may be used as a simple wideband direct conversion receiver with a well-defined 5 MHz bandwidth. Both sidebands will be detected. Using a low phase noise signal generator allows testing the phase noise of an oscillator using a computer soundcard as a spectrum analyzer. Another possible use is for calibrating the signal generator time base against WWV or CHU, for off the air frequency measurements. Figure 11 illustrates how the low frequency adapter can be connected to an antenna, an RF signal generator and an audio amplifier to create a direct conversion receiver.

• **Vector Voltmeter Operation at Low Frequency**

Figure 12 illustrates the basic operation of the low frequency adapter with a vector voltmeter, for making low frequency measurements. The 10 to 15 MHz signal generator output connects to a signal splitter, so the same signal is going to the RF In port on the low frequency adapter and also to the reference input of the vector voltmeter. Notice that a 10 MHz clock reference signal also connects from the signal generator to the Clock In port on the low frequency adapter. The RF Output, or RX port on the adapter connects to the Test signal input port on the vector voltmeter. The device under test connects to the LF In and LF Out ports on the

front of the low frequency adapter. I have not tried this setup, but a very similar arrangement is described in a Feb 1972 *IEEE Transactions on Instrumentation and Measurements* article.[5]

Conclusion

The Low Frequency Adapter described here adds low frequency capability to a Vector Network Analyzer, as well as adding audio frequency generation, 1 MΩ probe amplified interface, and direct conversion receiver capability. In the VNA application, an IF bandwidth of 10 Hz must be used to extend the lowest frequency down to 20 Hz. The low frequency adapter has allowed me to measure R, L and C components down to 20 Hz, using my Hewlett Packard 8753D VNA. I have also been able to accurately characterize and document the response of many audio type amplifiers that otherwise would have required tedious measurement methods. I wish to acknowledge the help and encouragement of my good friend Bertrand Zauhar, VE2ZAZ, who did the beta testing on this project. Readers seeking more information (component procurement, circuit schematic, updates, and so on) should visit my website at **http://ve2azx.net/technical/LFA/LowFreqAdapter.htm**.

We Design And Manufacture To Meet Your Requirements
***Protoype or Production Quantities**

800-522-2253

This Number May Not Save Your Life...

But it could make it a lot easier! Especially when it comes to ordering non-standard connectors.

RF/MICROWAVE CONNECTORS, CABLES AND ASSEMBLIES

- Specials our specialty. Virtually any SMA, N, TNC, HN, LC, RP, BNC, SMB, or SMC delivered in 2-4 weeks.
- Cross reference library to all major manufacturers.
- Experts in supplying "hard to get" RF connectors.
- Our adapters can satisfy virtually any combination of requirements between series.
- Extensive inventory of passive RF/Microwave components including attenuators, terminations and dividers.
- No minimum order.

NEMAL
Cable & Connectors for the Electronics Industry

NEMAL ELECTRONICS INTERNATIONAL, INC.
12240 N.E. 14TH AVENUE
NORTH MIAMI, FL 33161
TEL: 305-899-0900 • FAX: 305-895-8178
E-MAIL: INFO@NEMAL.COM
BRASIL: (011) 5535-2368

URL: WWW.NEMAL.COM

Jacques Audet, VE2AZX, became interested in radio at the age of 14, after playing with crystal radio sets and repairing old receivers. At age 17, he obtained his first ham license. In 1967 he obtained his BS degree in electrical engineering from Laval University. He then worked in engineering functions at Nortel Networks, where he retired in 2000. He worked mostly in test engineering on a number of products and components operating from dc to light-wave frequencies.

His areas of interest are in RF simulations, filters, duplexers, antennas and using computers to develop new test techniques in measurement and data processing. Jacques is an ARRL Member.

Notes

[1]For the complete circuit schematic, as well as any updated information, see the file named **LFA-V2-Schematic.pdf** on my web site: **ve2azx.net/technical/LFA/LowFreqAdapter.htm**.

[2]The complete circuit schematic, as well as other files associated with this article are available for download from the ARRL *QEX* files website. Go to **www.arrl.org/qexfiles** and look for the file **1x15_Audet.zip**.

[3]The *Excel* spreadsheet that I created to perform these calculations is available for download on my web site: **ve2azx.net/technical/Series_Parallell-Impedance_with_VNA-Re_Im.xls**. This spreadsheet is also included in the **1x15_Audet.zip** file available for download on the ARRL QEX files website.

[4]There is more information about the ×100 1 MΩ wideband attenuator included in the file **Divider-100.pdf**, which is part of the **1x15_Audet.zip** file on *QEX* files website.

[5]R. Lane and J. Butler, "LF Adaptor Extends Vector Voltmeter Magnitude and Phase Measurements down to 10 Hz," *IEEE Transactions on Instrumentation and Measurements*, Feb 1972. A copy of this

Appendix
Low Frequency Adapter Specifications

Supported VNA Mode: S_{21}.

LFA Frequency Range: 20 Hz to 5 MHz.

In the VNA application, an IF bandwidth of 10 Hz must be used to extend the lowest frequency down to 20 Hz.

Clock Input: 10 MHz, 0 to +12 dBm, 50 Ω. Clock must be synchronized to the VNA reference clock.

Input to LFA from VNA Port 1: 10.000 020 MHz to 15.000 MHz, 0 dBm nominal, Max +6 dBm, 50 Ω (at rear).

Output from LFA to VNA Port 2: 10.000 020 MHz to 15.000 MHz, 0 dBm nominal, Max +6 dBm, 50 Ω (at rear).

Low Frequency Output: 20 Hz to 5 MHz, 50 Ω, AC coupled, –6 dBm (112 mV RMS into 50 Ω) or 225 mV nominal into an open circuit.

Return Loss: > 40 dB below 5 MHz.

Harmonics at 1 MHz Out / 0 dBm: –65, –70, –50, –70 dBc for the 2nd, 3rd, 4th,5th harmonics.

Spurs Measured Under No Input From VNA Port 1: – 85, –97, –101, –102, –104 dBm at 10, 30, 50, 70, 90 MHz.

Source Linearity (Up to +9 dBm Out): < 0.05 dB

Low Frequency Input: 20 Hz to 5 MHz, 1 MΩ in parallel with 8 pF, AC coupled, 0 dBm nominal input level (front panel).

Overload Level: ~ +5 dBm, as indicated by a red LED on the front panel.

Damage Level: 20 V RMS.

Loopback of Low Frequency Output to Low Frequency Input: Yields ~ 0 dBm output to VNA port 2 at ×1 Gain.

Frequency Response Uncorrected: –3 db at 35 Hz and 5 MHz, ±1.5 dB from 100 Hz to 4 MHz.

A front panel switch provides ×10 gain to compensate for ×10 scope probe attenuation.

Back-to-back linearity, including HP 8753D VNA: Up to +3 dBm in: < ±0.05 dB.

Two rear adjustments potentiometers allow for tweaking the LO carrier balance to improve dynamic range below 1000 Hz.

Dynamic range: better than 90 dB from 100 Hz to 5 MHz, when used with a VNA having more than 100 dB of dynamic range. Improves by 20 dB at ×10 gain.

Sweep time: For a 170 point log sweep, from 20 Hz to 5 MHz: 50 seconds on the HP 8753D, using 10 Hz IF Bandwidth and LIST frequency mode.

Monitor Output: 50 Ω, AC coupled, open circuit level equals input level ±1 dB.

Frequency response –3 dB into 50 Ω: 200 Hz to > 80 MHz at ×1 and > 60 MHz at ×10 gain.

Maximum Output Level: + 6 dBm into 50 Ω

Power input: +11 V to +16 V DC at < 80 mA (at rear). A balanced Pi filter at the input cleans up the DC source from any switching power supply noise.

Size: 10.5 cm (W) × 15 cm (L) × 3.5 cm (H).

John E. Post, KA5GSQ

Embry-Riddle Aeronautical University, 3700 WIllow Creek Road, Prescott, AX 86301; **john.post@erau.edu**

Optimizing Magnetically Coupled Loop Antennas

Magnetically coupled loop antennas may allow portable medium wave receivers with internal ferrite bar antennas to approach the sensitivity of an expensive communications-grade receiver and large external antenna combination.

Ferrite loop stick antennas, constructed by winding a wire coil around a ferrite bar, permit the construction of very compact, portable medium wave (MW) and AM broadcast band receivers. The tradeoff, however, is a loss of sensitivity due to the limited cross sectional area of the ferrite antenna. Magnetically coupling an external loop antenna to the ferrite loop stick noticeably improves the performance of less sensitive portable MW receivers. This subject is important to anyone operating under portable or emergency conditions that might inhibit the erection of an external antenna, or limit access to a more sensitive receiver.

Under emergency conditions AM broadcast stations may remain on the air even though electric power, telephone, cell-phone and Internet service are not available. During Hurricane Katrina in August 2005, station WWL in New Orleans (AM 870 kHz) was one of the information outlets that remained in service.[1] This station provided information to fringe listeners throughout the Gulf Coast, who otherwise might not have access to any other source of information during that emergency. Additionally, an emerging hobby is "ultralight" broadcast band DXers who chase weak signals using small portable radios combined with external loop antennas.[2]

External loop antennas are readily available for purchase from several manufacturers. For example, the Terk Advantage is an approximately 9 inch diameter loop with the tuning capacitor located at the bottom of the loop. This loop provides for either magnetic coupling or physical connection to a receiver's external antenna jack.[3] Another circular loop is the Select-A-Tenna, which is an approximately 10¾ inch diameter loop with the tuning capacitor located at the center of the loop.[4] One reviewer noted little difference between the performances of these two loop antennas after conducting a head-to-head comparison.[5] A different approach is taken by the Q-Stick+ available at **DXTools.com**. In this case, winding a coil on an oversized ferrite rod produces a magnetically coupled loop with a very small form factor.[6] This approach might be advantageous for some portable applications where space is limited.

Several articles discuss homebrew construction of an external loop antenna. The earliest one I have found discusses improving AM broadcast reception by winding a large loop antenna around nails driven into the wall of a room.[7] The article provides a data table for constructing loops that range in size from 10 turns, with the length of each side given as 24-3/16 inches to 3 turns with the length of each side given as 80-11/16 inches. A second homebrew approach winds 17 turns of wire on an 11 × 14 inch plastic picture frame.[8] Both of these approaches claim to provide great improvement in the performance of ordinary broadcast receivers, even though they seem to occupy opposite corners of the design space.

Reviewing commercial as well as homebrew solutions for the design of external loop antennas raises a number of interesting questions: What geometric relationship couples the maximum amount of signal energy from the external loop antenna into a receiver's ferrite loop stick? What, if any, is the optimum number of turns and area for the loop? What is the performance difference between external loop antennas constructed from different types of conductors such as solid wire, Litz wire, and Litz rope? Is there any theoretical or practical advantage to using an external air core loop compared to an external ferrite core loop? I am not aware of published work on any of these topics so investigation seems appropriate. Although this discussion focuses on the design of an external loop antenna for the AM broadcast band, these concepts apply equally to external loops designed for other frequencies in the medium wave range.

Electromagnetic Considerations

The external loop antenna consists of an air or ferrite-wound coil that resonates with a tuning capacitor to form a resonant or tuned circuit. Faraday's law allows us to determine the open circuit voltage induced in any coil. This law states that the open circuit voltage induced in the coil equals the time rate of change of the magnetic flux through the coil.[9]

$$V_{OC} = -\int \frac{\partial \mathbf{B}}{\partial t} \bullet d\mathbf{S} \qquad \text{[Eq 1]}$$

Consider a circular wire loop with total area A, wound with N turns, with unit normal in the $\boldsymbol{a}_z$ direction. Assume that the loop contains a magnetic flux intensity $\boldsymbol{H} = H_0 \sin(\omega t)\, \boldsymbol{a}_z$ that is constant across the plane of the loop. Applying Faraday's law gives the open circuit voltage at the terminals of the wire loop.

$$V_{OC} = -\int \frac{\partial \mathbf{B}}{\partial t} \bullet d\mathbf{S} = -\int \frac{\partial \mu \mathbf{H}}{\partial t} \bullet d\mathbf{S} = -\omega N \mu H_0 A \cos\left(\omega t\right) \qquad \text{[Eq 2]}$$

[1]Notes appear on page 21.

Then, the peak value of the open circuit voltage across the loop terminals is given by Equation 3.

$$V_{OC\_pk} = \omega N \mu H_0 A \qquad \text{[Eq 3]}$$

Equation 3 demonstrates that the peak value of the open circuit voltage developed across the terminals of a coil increases directly with the radian frequency of operation, ω, the number of turns of the coil, N, the total area of the coil, A, and the magnetic flux density $B_0 = \mu H_0$. Of course, this result assumes that the loop is oriented so that the direction of the magnetic flux is coincident normal (perpendicular) to the plane of the loop.

Figure 1 depicts a cross-sectional view of a coil wound on a ferrite loop stick placed inside an external loop antenna so that both coil axes are coincident along with the axis of the magnetic field. The cross sectional area of the ferrite loop stick is very small compared with the cross sectional area of the external loop, so that the permeability of the external loop is essentially the same as free space. Thus, the peak value of the open circuit voltage developed across the terminals of the external loop antenna is:

$$V_{p\_pk} = \omega N_p \mu_0 H_0 A_p \qquad \text{[Eq 4]}$$

where N_p and A_p are the number of turns and cross-sectional area, respectively of the external loop antenna.

The peak value of the open circuit voltage developed across the terminals of the ferrite loop stick coil is given by Equation 5.

$$V_{s\_pk} = \omega N_s \mu_{r\_eff} \mu_0 H_0 A_s \qquad \text{[Eq 5]}$$

where N_s and A_s are the number of turns and cross-sectional area, respectively of the coil on the ferrite loop stick, while μ_{r_eff} is the increase in inductance when the ferrite rod is inserted into the coil.[10]

Because the dimension of the coils and the distances between them are much smaller than the wavelength of an electromagnetic wave at MW frequencies, magnetostatic approximations of Maxwell's equations are valid. This consideration leads to an equivalent circuit model of the magnetic coupling between the two coils in terms of their mutual inductance.[11] This quantity determines how much signal energy couples from the external loop antenna into the receiver's ferrite loop stick.

Appendix 1 demonstrates that the mutual inductance between the external loop antenna and the coil wound on the ferrite loop stick is:

$$M = \frac{\mu N_s N_p A_s}{2a} \qquad \text{[Eq A-6]}$$

This result demonstrates that the mutual inductance between the two coils is a function of:

1) the number of turns on each of the coils, N_s and N_p,
2) the permeability of the ferrite loop stick, μ,
3) the area of the ferrite loop stick A_s in meters squared, and
4) the radius of the external loop antenna, a, in meters.

Circuit Considerations

From a circuit perspective, connecting individual variable capacitors to the terminals of each inductor forms a doubled-tuned resonant transformer. The goal is to design the external loop antenna in order to maximize the current in the secondary (ferrite loop stick) of the double-tuned transformer. Appendix 2 demonstrates that the current in the secondary at resonance is given by Equation A-9.

$$\overline{I_s} = \frac{j\overline{V_p}}{\frac{r_p r_s}{\omega M} + \omega M} = \frac{j\omega M \overline{V_p}}{r_p r_s + (\omega M)^2} \qquad \text{[Eq A-9]}$$

If it were possible to construct one or both of the loops such that $r_p = 0\ \Omega$ and/or $r_s = 0\ \Omega$, perhaps through use of superconducting windings, the current in the secondary would become

$$\overline{I_s} = \frac{j\overline{V_p}}{\omega M} \qquad \text{[Eq 6]}$$

Substituting in the open-circuit voltage V_p, Equation 4, and the mutual inductance M, and Equation A-6 from the Appendices into Equation A-9 gives Equation 7.

$$\overline{I_s} = \frac{jV_p}{\omega M} = \frac{j\omega N_p \mu_0 H_0 A_p}{\omega \frac{\mu N_s N_p A_s}{2a}} = \frac{2jaH_0 A_p}{\mu_{r\_eff} N_s A_s} \qquad \text{[Eq 7]}$$

For this special (and impractical) case, current in the secondary is maximized by increasing the external loop radius, a, and area, A_p, while still maintaining a resonant condition. Increasing the area of the external loop "captures" more signal energy in the transformer primary to couple into the transformer secondary. Thus, the optimum external loop under this constraint consists of a single turn of wire resonated to the desired frequency with the receiver located in the center of the loop.

For the practical case of a lossy loop antenna and ferrite loop stick neither r_p nor r_s are zero. Appendix 2 demonstrates that in this case there is an optimum value of mutual inductance that will maximize the current in the coil on the ferrite bar, given by Equation A-13.

$$M_{opt} = \frac{\sqrt{L_p L_s}}{\sqrt{Q_p Q_s}} \qquad \text{[Eq A-13]}$$

The optimum mutual inductance found by Equation A-13 is equal to the geometric mean of the inductances of the loop antenna and ferrite loop stick, divided by the geometric mean of the quality factors of the loop antenna and ferrite loop stick. Before applying Equation A-13, it is necessary to further explore the relationship between inductance and quality factor for the inductor formed by the external loop antenna. This is the subject of the next section.

External Loop Antenna Considerations

The inductance of the external loop antenna resonates with a tuning capacitor to form a resonant or tuned circuit. In the case of a large diameter air-wound coil attaining a given inductance will require an additional length of conductor compared with a coil wound on a high-permeability core. Because of this consideration, the air-wound coil will contain relatively fewer turns with a relatively larger equivalent distributed capacitance C_d.[12]

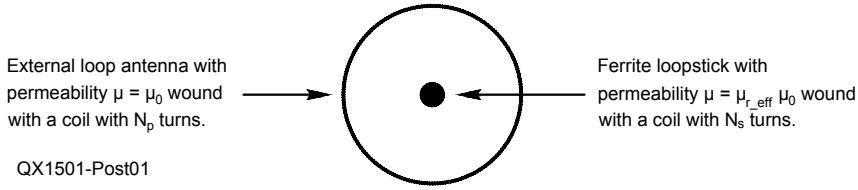

Figure 1 — Cross-sectional view of a ferrite loop stick wound with a coil that is placed inside an external loop antenna so that both loop axes are coincident along with the axis of the magnetic field. The two coils form a magnetically-coupled circuit.

Appendix 3 investigates this situation and demonstrates that one consequence of a large distributed capacitance in the loop's windings is a limitation in the maximum allowable inductance in order to cover the entire AM broadcast band using a typical variable capacitor. For example, a common value of inductance for a ferrite loop stick antenna is 688 μH, which implies an equivalent distributed capacitance of only a few picofarads according to Figure A-6. Conversely, Figure A-6 demonstrates that the inductance of an air-wound coil with an equivalent distributed capacitance of 20 pF is limited to approximately 250 μH in order to cover the entire AM broadcast band within the range of a typical 20 to 365 pF variable capacitor.

Even more important, increasing the equivalent distributed capacitance decreases the inductor's self-resonant frequency. Equation A-23 shows that this causes a concomitant reduction in the quality factor of the inductor as the operating frequency increases. Decreasing the quality factor of the external loop increases the optimum mutual inductance, M_{opt}, given by Equation A-13. This will require a reduction in the radius of the external loop antenna a, (see Equation A-6), since any increase in the number of turns N_p in order to maintain M_{opt} would only further increase the inductor's distributed capacitance and lower the inductor's self-resonant frequency.

The optimum external loop antenna is constructed in a way that balances these two effects. A small diameter external loop contains a relatively large number of turns of relatively small radius in order to achieve a given inductance. This construction reduces the distributed capacitance; increasing the loop Q so that the actual value of mutual coupling is larger than the optimum value of mutual coupling. Hence, the loop is smaller than the optimum size. Conversely, a large diameter external loop requires a relatively small number of turns of relatively large radius to achieve a given inductance. This construction increases the distributed capacitance; reducing the quality factor of the loop so that the actual value of mutual coupling is smaller than the optimum value of mutual coupling. Hence, the loop is larger than optimum size. Thus, the optimum size external loop antenna is obtained when the *actual* value of mutual coupling (Equation A-6) equals the *optimum* value of mutual coupling (Equation A-13).

Experimental Procedure

In an attempt to partially span the design space, nine loop antennas were constructed on heavy cardboard tubes with diameters 4-5/16 inches, 7-13/16 inches, and 12-7/8 inches. See Figure 2. Loops were wound on the tubes using either #22 American Wire Gauge (AWG) solid hookup wire, Litz wire consisting of 175 strands of #46 AWG solid copper wire, or Litz rope consisting of 660 strands of #46 AWG solid copper wire. The length of conductor in each case was approximately 70 feet. The procedure described in Appendix 4 was applied in order to determine the inductance and distributed capacitance for each of the nine loop antennas. The procedure described in Appendix 5 was applied to determine the quality factor (Q) of each loop antenna over a range of frequencies that include the AM broadcast band. Figures A-8 through A-10 along with Table A-1, Appendix 6, summarizes the results of these procedures for the nine loop antennas.

Again using the procedures described in Appendix 4 and Appendix 5, three ferrite loop sticks were characterized in order to determine their inductance and distributed capacitance as well as the Q of each ferrite loop stick over a range of frequencies that include the AM broadcast band. Figure A-11, along with Table A-2, in Appendix 6, summarizes the results of these procedures for the three ferrite loop sticks.

As an example of the analysis procedure, Figure 3 plots the individual Q measurements for the 12-7/8 inch diameter loop antenna constructed with Litz rope across the AM broadcast band frequencies, as well as the best fit quadratic curve. Figure 3 also plots the individual Q measurements for the ferrite loop stick #2 across the AM broadcast band frequencies, as well as the best fit quadratic curve. It is important to recognize that the Q of the ferrite loop stick is reduced because of loading by the receiver circuitry. In order to approximate this effect, the lower curve depicts the Q of the ferrite loop stick divided by two, to account for loading. The final curve depicts the geometric mean of the quality factors of the two inductors, which varies from almost 140 at the low-frequency end of the band to nearly 80 at the high-frequency end of the band.

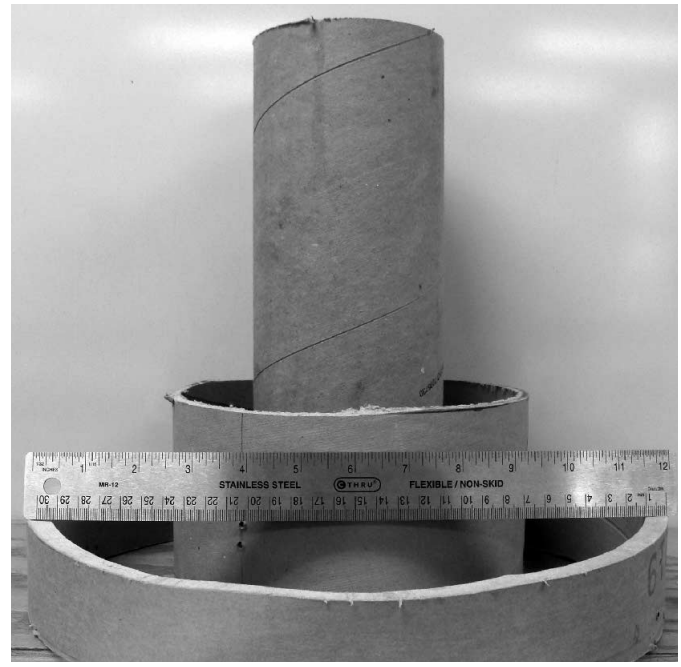

Figure 2 — Photograph of cardboard tubes used as forms for constructing loop antennas.

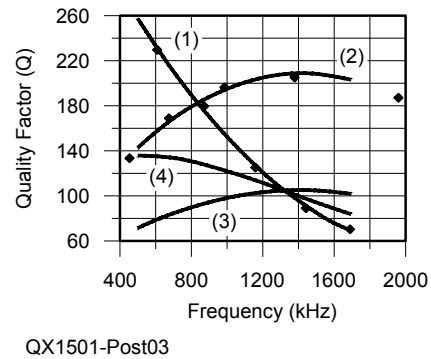

Figure 3 — Measured quality factor values (diamond symbols) for the 12-7/8 inch diameter loop antenna constructed with Litz wire and ferrite loop stick 2 across the AM broadcast band frequencies, along with best fit quadratic curves for each case (curves 1 and 2). The quality factor of the ferrite loop stick is reduced by a factor of two to account for loading by the receiver (curve 3). The geometric mean of the loop antenna quality factor and loaded ferrite loop stick quality factor (curve 4) decreases from about 130 to about 70 across the AM band.

The calculated mutual inductance between the 12-7/8 inch diameter loop antenna constructed with Litz wire and ferrite loop stick #2 is 5.0 μH. This is found by application of Equation A-6 along with $\mu_0 = 4\pi \times 10^{-7}$, $\mu_{r\_eff} = 11.53$(from Table A-2), $N_p = 21$ (from Table A-1), $N_s = 90$ (from Table A-2), $A_s = 5$ mm × 12 mm = 60 μm^2, and a = 12-7/8 inches × 0.0254 in/cm / 2 = 0.1635 m. Now it is possible to solve Equation A-13 in order to determine the ideal geometric mean of the quality factors. The measured inductance for the 12-7/8 inch diameter loop antenna constructed with Litz rope is 273.5 μH, (Table A-1). The measured inductance for ferrite loop stick

#2 is 522.5 μH, (Table A-2).

Applying both these values along with a desired mutual inductance of 5.0 μH results in a geometric mean of the quality factors of 75.6. Figure 3 shows that the 12-7/8 inch diameter loop antenna is near this value at the high end of the AM broadcast band, so the design of the loop antenna is optimized near that frequency.

Increasing the loop antenna diameter should optimize the design at a slightly lower frequency. This is because increasing the diameter also increases the distributed capacitance, which would lower the loop antenna quality factor compared with Figure 3 (curve #1), as well as the geometric mean of the quality factor Figure 3 (curve #4).

In order to apply this insight, a final loop antenna was constructed from a 6 inch length of 15 inch outer diameter cast acrylic tubing with a 0.125 inch wall thickness.[13] This loop antenna was constructed of approximately 70 feet of Litz wire, which formed a coil with 18 turns. See Figure 4. A standard 20 to 365 pF broadcast band capacitor tunes the loop antenna, as shown in Figure 5. Figure 6 shows the result of applying the procedure described in Appendix 5 to determine the *Q* of this loop antenna over a range of frequencies that include the AM broadcast band. The procedure described in Appendix 4 was applied in order to obtain the measured inductance and distributed capacitance for this loop antenna, shown in Figure 6. The measured inductance of 308.9 μH is very close to the calculated value of 307.7 μH obtained from Wheeler's equation, Equation A-26.

Comparison of the 15 inch loop constructed of Litz wire, Figure 2, with the 12-7/8 inch loop constructed of Litz wire, Figure A-11, reveals several counter-intuitive results. First, the distributed capacitance of the 15 inch loop antenna is 2.1 pF less than that of the smaller loop antenna, even though the 15 inch loop has three fewer turns than the smaller loop antenna. Second, the maximum quality factor of the 15 inch loop antenna is about 50% greater than that of the smaller loop antenna, and the maximum quality factor occurs at about a 50% higher frequency than the smaller loop. This result demonstrates the superior material properties of acrylic tubing compared with cardboard, which results in a reduction of the distributed capacitance as well as the dissipative loss, both serving to substantially increase the overall quality factor of the 15 inch loop antenna.

Figure 7 plots the individual quality factor measurements for the 15 inch diameter loop antenna constructed with Litz wire across

Figure 4 — Photo of 15 inch diameter cast acrylic tubing wound with 18 turns of 175/46 Litz wire.

Figure 5 — External loop antenna constructed from approximately 70 feet of Litz wire wound on a 6 inch length of 15 inch outer diameter cast acrylic tubing with a 0.125 inch wall thickness. A standard 20 to 365 pF broadcast band capacitor (hidden from view here) resonates the loop antenna.

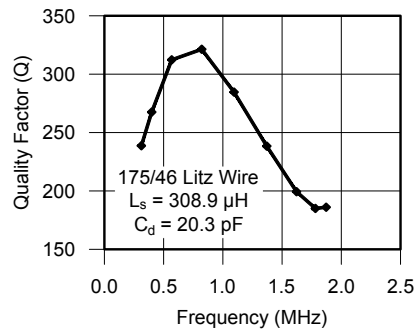

Figure 6 — Measured quality factor (*Q*) as a function of frequency along with measured values of inductance and distributed capacitance for a 15 inch diameter loop constructed from 175/46 Litz wire on a cast acrylic form.

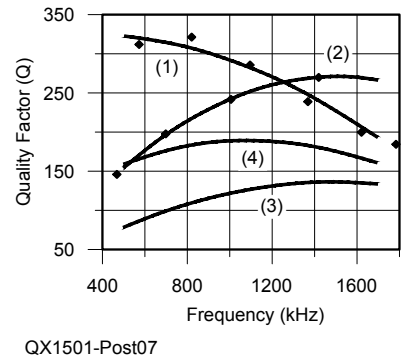

Figure 7 — Measured quality factor values (diamond symbol) for the 15 inch diameter loop antenna constructed on a cast acrylic form with Litz wire and ferrite loop stick 2 across the AM broadcast band frequencies along with best fit quadratic curves for each case (curves 1 and 2). The quality factor (*Q*) of the ferrite loop stick is reduced by a factor of two to account for loading by the receiver (curve 3). The geometric mean of the loop antenna quality factor and loaded ferrite loop stick quality factor (curve 4) is approximately 175 across the band.

the AM broadcast band frequencies (curve 1), as well as the best fit quadratic curve (curve 2). Figure 7 also plots the individual quality factor measurements for ferrite loop stick #2 across the AM broadcast band frequencies (curve 3), as well as the best fit quadratic curve (curve 4). Again, it is necessary to reduce the quality factor of the ferrite loop stick by half in order to approximate the loading effect of the receiver circuitry as depicted by curve 3. Curve 4 depicts the geometric mean of the quality factors of the two inductors, which is approximately 175 across the AM band. This is a substantial increase in overall Q when compared with the 12-7/8 inch loop antenna, as shown in Figure 3.

The calculated mutual inductance between the 15 inch diameter loop antenna constructed with Litz wire and ferrite loop stick #2 is 3.7 μH. This is found by application of Equation 6 along with $\mu_0 = 4\pi \times 10^{-7}$, $\mu_{r\_eff} = 11.53$, (Table A-2), $N_p = 18$, $N_s = 90$ (Table A-2), $A_s = 5$ mm × 12 mm = 60 μm^2, and $a = 15$ inches × 0.0254 inches/cm / 2 = 0.1635 m. Next, applying Equation A-13 using the approximate geometric mean of the quality factors along with the measured inductance for the 15 inch diameter loop antenna of 308.9 μH and the measured inductance for ferrite loop stick #2 of 522.5 μH (Table A-2), gives an optimum mutual inductance of 2.3 μH. Thus, the 15 inch loop antenna is slightly undersized compared with the optimum value. Practically speaking, however, the performance difference is probably not discernable.

Examples of Improved AM Broadcast Band Reception

The external loop antenna provides a small, but noticeable improvement in the reception of fringe stations with a portable AM receiver from my home in northern Arizona. Figure 8 is a photo of the portable receiver placed in an external loop. For example, KFNN broadcasting from Tempe, Arizona at 1510 kHz with a transmitter power of 22 kW is normally barely audible during daylight hours. Combining the receiver with the external loop antenna frequently improves reception so that the station is plainly audible. Another, example is KKOB broadcasting from Albuquerque, New Mexico at 770 kHz with a transmitter power of 50 kW. Late in the afternoon the signal is barely discernable in the receiver's noise floor. Addition of the external loop antenna frequently results in noticeably improved reception of this station.

Conclusion

In most cases the sensitivity of portable medium wave (MW) and AM broadcast band receivers is limited by the internal ferrite loop stick antenna. It is possible to combine a portable receiver with an external loop antenna in order to reclaim some of this sensitivity. The improvement is not dramatic, but it is noticeable and in many cases sufficient to provide adequate reception of fringe stations that might otherwise be buried in the noise floor of the receiver. External loop antennas constructed for the AM broadcast band are relatively compact in size, which makes them quick and easy to employ under portable or emergency conditions.

Analysis of a circuit model of an external loop antenna inductively coupled to a ferrite loop stick demonstrates that increasing the radius of the loop to capture more signal power becomes counterproductive above a certain size. This is because the distributed capacitance between windings increases rapidly as the number of turns is reduced at larger diameters. As the distributed capacitance increases, the quality factor (Q) of the external loop antenna decreases even more rapidly. The increase in distributed capacitance with larger loops also dramatically reduces the improvement in Q normally obtained by winding the coil with Litz wire or Litz rope instead of a solid or stranded conductor.

Additional work is possible in this area by performing a theoretical analysis of external loop antennas constructed from ferrite rods. Additional investigation of the performance improvement possible with external loop antennas constructed for MW frequencies either below or above the AM broadcast band might also prove interesting.

Figure 8 — Example of an external loop antenna combined with a portable medium wave (MW) receiver in order to improve reception of fringe stations.

John E. Post is an associate professor of electrical and computer engineering with Embry-Riddle Aeronautical University in Prescott, AZ. He holds an Amateur Extra class license, KA5GSQ, and has BS, MS, and PhD degrees in electrical engineering.

Notes

[1]"WWL (AM)", *Wikipeida. The Free Encyclopedia.* Wikimedia Foundation, Inc. 7 Apr 2012. Web. 15 Feb 2014, **http:// en.wikipedia.org/wiki/WWL_(AM)**.
[2]Bruce A. Conti, "The modern AM Broadcast Band DXer Defined: The Joy of Going 'Ultralight,'" *Popular Communications*, July 2012.
[3]**www.terk.com/radio-antennas/**
[4]**www.ccrane.com/instruction-manuals/select-a-tenna.pdf**
[5]**radiojayallen.com/select-a-tenna-vs-terk-am-advantage/**
[6]**www.dxtools.com/QStick.htm**
[7]Douglas Kohl, "Low-Cost Loop Antenna Extends AM Radio Reception," *Popular Electronics*, July, 1978.
[8]**www.hard-core-dx.com/nordicdx/antenna/loop/inducloop.html**
[9]Stuart M. Wentworth, *Fundamentals of Electromagnetics with Engineering Applications,* John Wiley & Sons, Inc., Hoboken, NJ, 2005.
[10]Jack R. Smith, K8ZOA, "Observations on Ferrite Rod Antennas," *QEX*, Jul/Aug 2008, pp 22–35.
[11]Umar Azad, Hengzhen Crystal Jing, and Yuanxun Ethan Wang, "Link Budget and Capacity Performance of Inductively Coupled Resonant Loops," *IEEE Transactions on Antennas and Propagation*, Vol. 60, No. 5, May 2012.
[12] Gabriele Grandi, Marian K. Kazimierczuk, Mario Massarini, and Ugo Reggiani, "Stray Capacitances of Single-Layer Solenoid Air-Core Inductors", *IEEE Transactions on Industry Applications*, Vol. 35, No. 5, September/October 1999.
[13]**www.eplastics.com/Plexiglass-Cast-Acrylic-Tubing**
[14]J.E. Post, KA5GSQ, "Optimizing the Design of Spiral Inductors on Silicon," *IEEE Trans. On Circuits and Systems—II: Analog and Digital Signal Processing*, Vol. 47, No. 1, Jan 2000, pp 15–17.
[15]H. A. Wheeler, "Inductance Formulas for Circular and Square Coils," *Proceedings of the IEEE*, Vol. 70, No. 12, Dec, 1982.

Appendix 1

Figure A-1 depicts the geometry of a single-turn circular loop with radius *a* meters lying in the *x-y* axis driven by a current of *i* amperes. The magnetic field intensity at the center of the loop is given by Equation A-1. See Note 9.

$$\mathbf{H} = \frac{i}{2a}\mathbf{a_z} \qquad \text{[Eq A-1]}$$

If the loop contains N_p tightly wound turns, the total magnetic field intensity at the center of the loop becomes:

$$\mathbf{H} = \frac{N_p i}{2a}\mathbf{a_z} \qquad \text{[Eq A-2]}$$

Now, place a small ferrite bar with permeability μ at the center of the loop so that the long axis of the bar coincides with the z-axis. Then, the magnetic flux density inside the bar is:

$$\mathbf{B} = \mu\mathbf{H} = \frac{\mu N_p i}{2a}\mathbf{a_z} \qquad \text{[Eq A-3]}$$

Assuming the cross-section of the ferrite bar is small so that the flux density is essentially constant inside the bar, the flux linkage between the circular loop and a single turn on the ferrite bar is:

$$\Phi = \int \mathbf{B} \bullet d\mathbf{S} = BA_s = \frac{\mu N_p i A_s}{2a} \qquad \text{[Eq A-4]}$$

where A_s is the cross-sectional area of the ferrite bar in m^2. Then if a coil with N_s turns is placed around the ferrite bar, the total flux linkage, λ, between the two coils is found by multiplying by the number of turns in the second coil, or:

$$\lambda = \Phi N_s = \frac{\mu N_s N_p i A_s}{2a} \qquad \text{[Eq A-5]}$$

By definition, dividing the total flux by the driving current gives the mutual inductance, *M*, between the circular loop and the coil on the ferrite bar:

$$M = \frac{\lambda}{i} = \frac{\mu N_s N_p A_s}{2a} \qquad \text{[Eq A-6]}$$

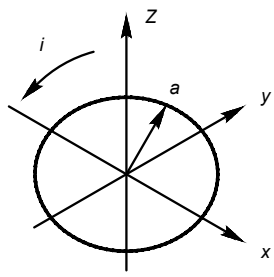

QX1501-PostA01

Figure A-1 — Geometry of circular loop with radius *a* and current *i* with the plane of the loop lying along the x-y axis.

Appendix 2

Connecting a variable capacitor, C_s, to the terminals of the coil on the ferrite loop stick and another variable capacitor, C_p, to the terminals of the external loop antenna forms a magnetically coupled double-tuned resonant transformer, as shown in Figure A-2. In this circuit the loop antenna serves as the primary while the ferrite loop stick serves as the secondary of the transformer. Loses in the transformer primary are modeled by the series resistor, r_s, while losses in the secondary of the transformer are modeled by the series resistor, r_p. It is important to note that there are two possible polarities for the secondary voltage, $\overline{V_s}$, depending upon the orientation of the winding direction of the two coils as shown in the figure. Applying the pi-model equivalent circuit for the coupled inductors, and establishing mesh currents gives an equivalent circuit, as shown in Figure A-3, which is straightforward to analyze.

Applying KVL in each mesh and writing the result in matrix form gives:

$$\begin{bmatrix} \frac{1}{j\omega C_p} + r_p + j\omega L_p & -j\omega M \\ -j\omega M & \frac{1}{j\omega C_s} + r_s + j\omega L_s \end{bmatrix} \bullet \begin{bmatrix} \overline{I_p} \\ \overline{I_s} \end{bmatrix} = \begin{bmatrix} \overline{V_p} \\ \pm\overline{V_s} \end{bmatrix} \qquad \text{[Eq A-7]}$$

Then, application of Cramer's rule to solve for the secondary current gives:

$$\overline{I_s} = \frac{\begin{vmatrix} \frac{1}{j\omega C_p} + r_p + j\omega L_p & \overline{V_p} \\ -j\omega M & \pm\overline{V_s} \end{vmatrix}}{\begin{vmatrix} \frac{1}{j\omega C_p} + r_p + j\omega L_p & -j\omega M \\ -j\omega M & \frac{1}{j\omega C_s} + r_s + j\omega L_s \end{vmatrix}} = \frac{\pm\left(\frac{1}{j\omega C_p} + r_p + j\omega L_p\right)\overline{V_s} + j\omega M\overline{V_p}}{\left(\frac{1}{j\omega C_p} + r_p + j\omega L_p\right)\left(\frac{1}{j\omega C_s} + r_s + j\omega L_s\right) + (\omega M)^2} \qquad \text{[Eq A-8]}$$

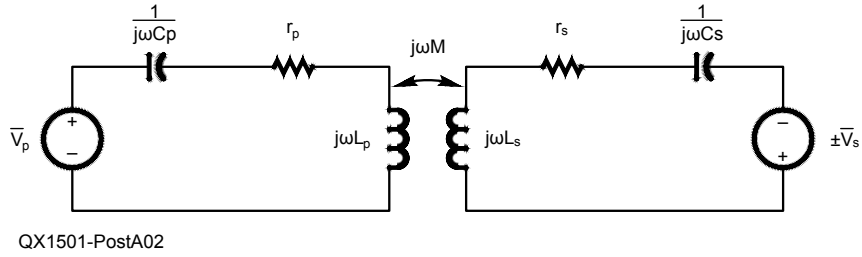

Figure A-2 — Doubled-tuned resonant circuit formed by mutual inductance between the external loop antenna and ferrite loop stick. In this schematic, the subscript "p" indicates components in the primary circuit while the subscript "s" indicates components in the secondary circuit.

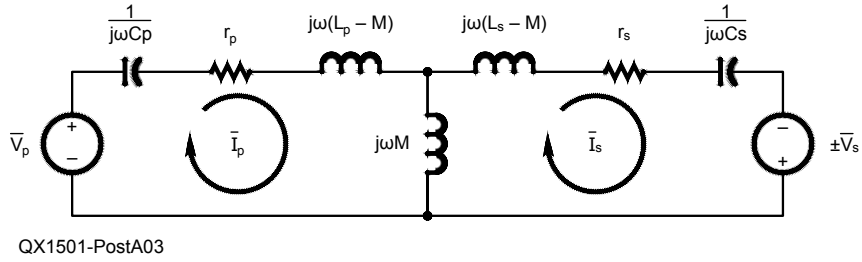

Figure A-3 — Equivalent circuit of the doubled-tuned resonant circuit shown in Figure A-2, obtained after applying the pi-model equivalent circuit for the coupled inductors and establishing mesh currents.

or

$$\overline{I_s} = \frac{\pm\left(j\left(\omega L_p - \frac{1}{\omega C_p}\right) + r_p\right)\overline{V_s} + j\omega M\overline{V_p}}{\left(j\left(\omega L_p - \frac{1}{\omega C_p}\right) + r_p\right)\left(j\left(\omega L_s - \frac{1}{\omega C_s}\right) + r_s\right) + (\omega M)^2}$$

Tuning both the primary and the secondary to resonance causes the imaginary portion of the denominator terms to vanish, so that the secondary current becomes:

$$\overline{I_s} = \frac{\pm r_p\overline{V_s} + j\omega M\overline{V_p}}{r_p r_s + (\omega M)^2} = \frac{\pm\frac{r_p}{\omega M}\overline{V_s} + j\overline{V_p}}{\frac{r_p r_s}{\omega M} + \omega M} \approx \frac{j\overline{V_p}}{\frac{r_p r_s}{\omega M} + \omega M} \qquad \text{[Eq A-9]}$$

The final approximation in Equation A-9 results from comparing the relative sizes of the primary and secondary voltage sources for practical problems. Differentiating the approximate result in Equation A-9 with respect to the mutual inductance, *M*, setting the result equal to 0, and solving the resulting expression demonstrates that the current in the secondary is maximized under the condition that

$$\omega M = \sqrt{r_p r_s} \qquad \text{[Eq A-10]}$$

or

$$M = \frac{\sqrt{r_p r_s}}{\omega}$$

The value of mutual inductance predicted by Equation A-10 occurs when the two inductors are placed in such physical proximity that they are critical coupled, so that

$$M_{opt} = k_c\sqrt{L_p L_s} = \frac{\sqrt{r_p r_s}}{\omega} \qquad \text{[Eq A-11]}$$

which yields a value of critical coupling:

$$k_c = \sqrt{\frac{r_p r_s}{\omega^2 L_p L_s}} = \frac{1}{\sqrt{Q_p Q_s}} \qquad \text{[Eq A-12]}$$

Equation A-12 follows after applying the definition of quality factor for series resonant circuits, $Q = \omega L / r$. Then, eliminating k_c from Equations A-11 and A-12 yields an expression for the optimum value of mutual inductance, M_{opt}, between the loop antenna and the ferrite loop stick.

$$M_{opt} = \frac{\sqrt{L_p L_s}}{\sqrt{Q_p Q_s}} \qquad \text{[Eq A-13]}$$

Appendix 3

Figure A-4 depicts a lossy inductor with equivalent series inductance, L_s, with a finite self-resonant frequency. The equivalent series resistance, r_s, models resistive losses primarily due to skin effect and proximity effects. The capacitor, C_d, accounts for the distributed capacitance between the turns of the coil. Equation A-14 gives the equivalent impedance at the terminals of the inductor.

$$Z_{eq} = r_{eq} + j\omega L_{eq} = \frac{1}{j\omega C_d + \frac{1}{j\omega L_s + r_s}} = \frac{j\omega L_s + r_s}{j\omega C_d \left(j\omega L_s + r_s\right) + 1} \qquad \text{[Eq A-14]}$$

Then, it is possible to separate the real and imaginary portions of Equation A-14 to find the frequency dependent equivalent series resistance, r_{eq}, and equivalent series inductance, L_{eq}.

$$r_{eq} = \frac{r_s}{\left(1-\omega^2 L_s C_d\right)^2 + \left(\omega r_s C_d\right)^2} \approx \frac{r_s}{\left(1-\omega^2 L_s C_d\right)^2} \qquad \text{[Eq A-15]}$$

and

$$L_{eq} = L_s \frac{\left(1-\omega^2 L_s C_d - \frac{r_s^2 C_d}{L_s}\right)}{\left(1-\omega^2 L_s C_d\right)^2 + \left(\omega r_s C_d\right)^2} \approx \frac{L_s}{\left(1-\omega^2 L_s C_d\right)^2} \qquad \text{[Eq A-16]}$$

Equations A-15 and A-16 demonstrate that the equivalent series resistance and inductance both increase dramatically as the frequency, ω, approaches the self-resonant frequency of the inductor, $\omega_s = 1 / \sqrt{L_s C_d}$.

Connecting a tuning capacitor, C_t, to the terminals shown in Figure A-4B forms a series tuned circuit with resonant frequency:

$$\omega_0 = \frac{1}{\sqrt{L_{eq} C_t}} = \sqrt{\frac{\left(1-\omega_0^2 L_s C_d\right)}{L_s C_t}}$$

or,

$$\omega_0 = \frac{1}{\sqrt{L_s \left(C_t + C_d\right)}} \qquad \text{[Eq A-17]}$$

Then, applying Equation A-17 to find the low resonant frequency corresponding to a tuning capacitance, C_{tmax}, is

$$f_{low} = \frac{1}{2\pi\sqrt{L_s \left(C_{t\max} + C_d\right)}} \qquad \text{[Eq A-18]}$$

while the high resonant frequency corresponding to a tuning capacitance C_{tmin} is

$$f_{high} = \frac{1}{2\pi\sqrt{L_s \left(C_{t\min} + C_d\right)}} \qquad \text{[Eq A-19]}$$

The tuning ratio is found from the ratio of the high and low frequencies:

$$\text{Tuning Ratio} = \frac{f_{high}}{f_{low}} = \sqrt{\frac{C_{t\max} + C_d}{C_{t\min} + C_d}} \qquad \text{[Eq A-20]}$$

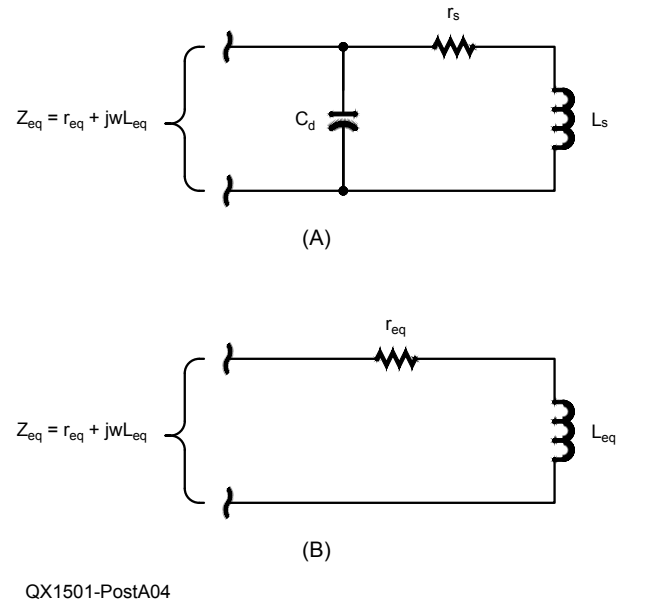

Figure A-4 — Circuit model of lossy inductor with finite self-resonant frequency, with frequency independent values shown at A, and equivalent circuit of lossy inductor with finite self-resonant frequency with frequency dependent values shown at B.

For the AM broadcast band, the tuning ratio is (1700 / 540) = 3.15, which implies a ratio of maximum to minimum tuning capacitance of 9.91 if $C_d = 0$. In order to maintain the tuning ratio for non-zero values of C_d, either C_{tmax} must increase or C_{tmin} must decrease. Usually, it is not practical to decrease C_{tmin} below some minimum value, so the only alternative is to increase C_{tmax}. Figure A-5 plots C_{tmax} derived from Equation A-20 in order to illustrate this situation. The plot was generated assuming $0 \leq C_d \leq 25$ pF, and $C_{tmin} = 15$ pF. As shown in Figure A-5, $C_{tmax} = 150$ pF when $C_d = 0$ pF but approaches 375 pF when $C_d = 25$ pF.

The inductance, L_s, required to achieve resonance is obtained from the product of the low and high resonant frequencies, Equation A-18 and Equation A-19.

$$L_s = \frac{1}{2\pi f_{high} \cdot 2\pi f_{low}} \bullet \frac{1}{\sqrt{\left(C_{t\min} + C_d\right)\left(C_{t\max} + C_d\right)}} \qquad \text{[Eq A-21]}$$

Applying the tuning ratio for the AM broadcast band of 3.15 along with Equation A-20 in Equation A-21 gives:

$$L_s = \frac{1}{2\pi f_{high} \cdot 2\pi f_{low}} \bullet \frac{1}{3.15\left(C_{t\min} + C_d\right)} \qquad \text{[Eq A-22]}$$

Equation A-22 specifies the required inductance, L_s, to tune the AM broadcast band given the upper and lower resonant frequencies, minimum tuning capacitance, and equivalent distributed capacitance. Examination of this equation shows that the inductance required to resonate a tank circuit must decrease as the equivalent distributed capacitance increases. Figure A-6 shows this relationship graphically by plotting Equation A-22 assuming $0 \leq C_d \leq 25$ pF, a tuning ratio of 3.15, and $C_{tmin} = 15$ pF. The figure shows that the required inductance, L_s, declines precipitously with increases in the equivalent distributed capacitance, C_d.

The quality factor, Q, of the resulting resonant circuit (assuming the capacitor is lossless) is found from substituting Equations A-15 and A-16 into the definition of quality factor for a series circuit.

$$Q = \frac{\omega_0 L_{eq}}{r_{eq}} = \frac{\omega_0 L_s}{r_s}\left(1 - \omega_0^2 L_s C_d\right) = \frac{\omega_0 L_s}{r_s}\left(1 - \left(\frac{\omega_0}{\omega_s}\right)^2\right) \qquad \text{[Eq A-23]}$$

The first factor in the last term of Equation A-23 models the intrinsic quality factor of the overall resonant circuit, while the second term models the self-resonance loss caused by the distributed capacitance C_d.[14] Equation A-23 demonstrates that the quality factor vanishes as the resonant frequency, ω_0, approaches the inductor's self-resonant frequency, $\omega_s = 1 / \sqrt{L_S C_d}$. This result illustrates the deleterious effect that the distributed capacitance, C_d, has on the circuit's quality factor, because it decreases the inductor's self-resonant frequency, ω_s.

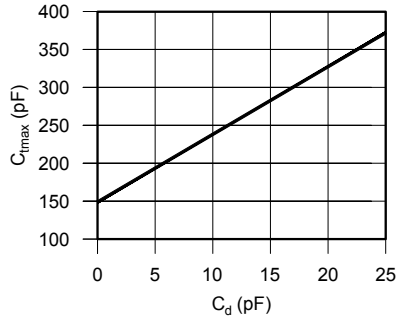

Figure A-5 — Relationship between distributed capacitance, C_d and maximum required tuning capacitance, C_{tmax}, assuming C_{tmin} = 15 pF and a tuning ratio of 3.15. The plot demonstrates how relatively small increases in distributed capacitance, C_d require relatively large increases in maximum tuning capacitance, C_{tmax}, in order to tune a band of frequencies.

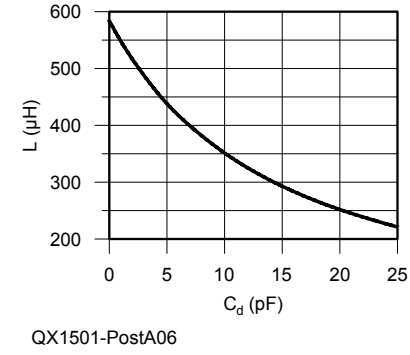

Figure A-6 — Inductance, L_s, required in order to tune the AM broadcast band for values of distributed capacitance between 0 and 25 pF.

Appendix 4

The resonant frequency for the series tuned circuit, Equation A-17, in terms of cyclic frequency is:

$$f_0 = \frac{1}{2\pi\sqrt{L_s\left(C_d + C_t\right)}} \qquad \text{[Eq A-24]}$$

Rearranging this equation to solve for the tuning capacitance, C_t, results in:

$$C_t = \frac{1}{\left(2\pi f_0\right)^2 L_s} - C_d \qquad \text{[Eq A-25]}$$

Equation A-25 is in the form of the equation of a line, $y = mx + b$, with a y-intercept of $b = -C_d$ and slope $m = 1 / L_s$. In order to obtain the inductance, L_s, and distributed capacitance, C_d, a network analyzer first determines the resonant frequency, f_0, resulting from known values of tuning capacitance, C_t. Then it is possible to plot each pair of points on a scaled axis with ordinate, C_t and abscissa, $1 / (2\pi f_0)^2$. Finally, linear regression analysis of the measured data gives the slope, m, and y-intercept, b, of the best-fit regression line resulting in the distributed capacitance, $C_d = -b$ and inductance, $L = 1 / m$.

For example, Figure A-7 depicts the result of regression analysis on a loop antenna constructed from 34 turns of 660/46 Litz rope wound on a 7-13/16 inch cardboard form. Tuning capacitance values (C_t) that range from 807 pF to 2.3 pF produced resonant frequencies that range from 318.5 kHz to 2.133 MHz, resulting in the data points marked with a "*" on the plot. The reciprocal of the slope, m, of the regression line results in an inductance of 303.6 μH, while the negative of the y-intercept results in a distributed capacitance of C_t = 15.47 pF.

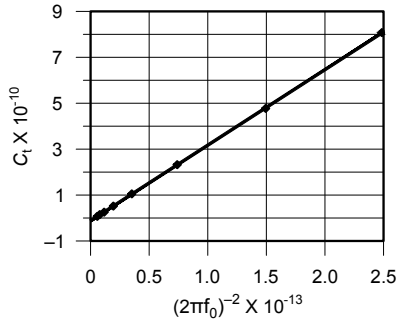

QX1501-PostA07

Figure A-7 — Linear regression analysis of measurements of a loop antenna constructed from 34 turns of 660/46 Litz rope wound on a 7-13/16 inch cardboard form. The inductance of the loop is L_s = 303.6 μH and the distributed capacitance of the loop is C_d = 15.47 pF.

Appendix 5

In addition to determining the resonant frequency of the loop antenna, the equivalent circuit function of the network analyzer provides values for the equivalent series resistance, r_s, the equivalent series inductance, L_s, and the series capacitance, C_s, of the characterized circuit at each resonant frequency. Then, given these values, it is possible to compute the measured quality factor, Q, of the resonant circuit at each frequency.

$$Q = \frac{\omega_0 L_s}{r_s} = \frac{1}{r_s}\sqrt{\frac{L_s}{C_s}} \qquad \text{[Eq A-26]}$$

Figure A-8 depicts the result of regression analysis and Q determination for the three 4-5/16 inch coils constructed using Litz rope, Litz wire, and #22 AWG solid wire listed in Table A-1. It is notable that the maximum Q of the loop antenna constructed from Litz rope is about two and one-half times that of the loop antenna constructed from solid wire, while the maximum Q of the loop antenna constructed from Litz wire falls roughly midway between the other two. Above approximately 1 MHz, the Q of the loop antenna constructed from Litz wire falls below the Q of the loop antenna constructed from solid wire. Additionally, the Litz wire coil is the smallest diameter resulting in a coil with the least axial length and the maximum inductance. The Litz rope is the largest diameter, resulting in a coil with the most axial length and the minimum inductance. The diameter of the solid wire is intermediate to the other conductors, which results in a value of inductance in between the other two inductance values. Finally, the distributed capacitances of the three loop antennas are the same to within about 1 pF.

Figure A-9 depicts the result of regression analysis and Q determination for the three 7-13/16 inch coils constructed using Litz rope, Litz wire, and #22 AWG solid wire listed in Table A-1. In this case the maximum Q of the loop antenna constructed from Litz wire and solid wire is about the same as in Figure A-9, while the maximum Q of the loop antenna constructed from Litz rope is only about two-thirds of its value in Figure A-9 because of a disproportionate increase in distributed capacitance. The distributed capacitance shown in Figure A-10 has roughly doubled compared with the distributed capacitance shown in Figure A-8. Above 1 MHz there is only a small difference between the Q of the three loop antennas shown in Figure A-9.

Figure A-10 depicts the result of regression analysis and Q determination for the three 12-7/8 inch coils constructed using Litz rope, Litz wire, and #22 AWG solid wire listed in Table A-1. In this example the Q of the loop antenna constructed from Litz rope is only about 50% greater than that of the loop antenna constructed from solid wire, while the maximum Q of the loop antenna constructed from Litz wire falls roughly midway between the other two. The distributed capacitance shown in Figure A-10 has roughly doubled again compared with the distributed capacitance shown in Figure A-9. Above about 800 kHz the Q of the loop antenna constructed from Litz wire is about the same as the Q of the loop antenna constructed from solid wire. Less than a 50% improvement is noted in the Q of the loop antenna constructed from Litz rope compared with the other two cases.

Figure A-11 depicts the result of regression analysis and Q determination on ferrite loop sticks 1, 2, and 3 listed in Table A-2. The Q of loop sticks 1 and 2 is about the same for low frequencies, but loop stick 1 achieves about 25% higher Q above 1.5 MHz. The large inductance and relatively large distributed capacitance cause the Q of loop stick 3 to decline rapidly at frequencies above about 750 kHz. Because the Q of loop stick 1 is roughly intermediate between loop sticks 1 and 3, it was selected as representative for this analysis.

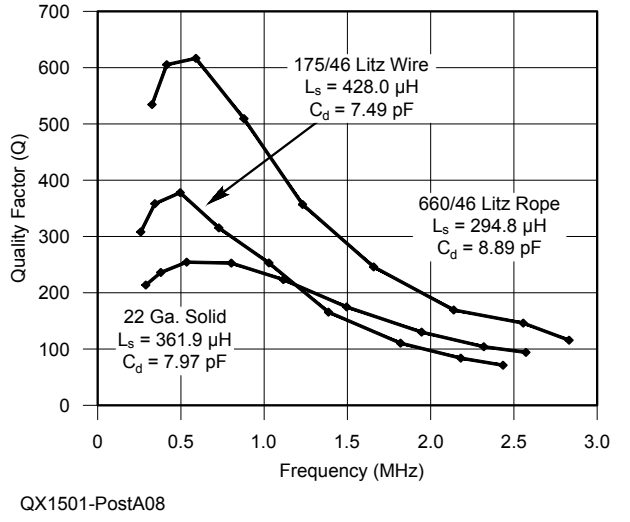

Figure A-8 — Measured quality factor as a function of frequency, along with measured values of inductance and distributed capacitance for 4-5/16 inch diameter loops constructed from 660/46 Litz rope, 175/46 Litz wire, and #22 AWG solid wire.

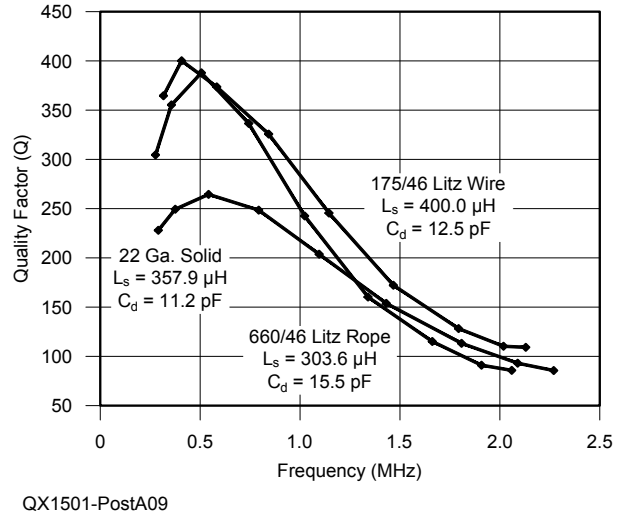

Figure A-9 — Measured quality factor as a function of frequency, along with measured values of inductance and distributed capacitance for 7-13/16 inch diameter loops constructed from 660/46 Litz rope, 175/46 Litz wire, and #22 AWG solid wire.

Table A-1

Measured and Calculated Inductances for Nine Loop Antennas

Conductor	*Diameter (Inches)*	*No. Turns*	$L_{measured}$ *(μH)*	$L_{calculated}$ *(μH)*	*% Error (M-C) / C %*
#22 AWG Solid	4-5/16	61	361.9	366.2	1.17
#22 AWG Solid	7-13/16	34	357.9	357.6	–0.08
#22 AWG Solid	12-7/8	21	301.4	310.4	2.90
175/46 Litz Wire	4-5/16	61	428.0	418.8	–2.20
175/46 Litz Wire	7-13/16	34	400.0	391.0	–2.30
175/46 Litz Wire	12-7/8	21	323.6	332.1	2.56
660/46 Litz Rope	4-5/16	61	294.8	282.6	–4.32
660/46 Litz Rope	7-13/16	34	303.6	301.6	–0.66
660/46 Litz Rope	12-7/8	21	273.5	273.5	0.00

Measured and calculated inductances for nine loop antennas wound on cardboard forms with diameters of 4-5/16 inches, 7-13/16 inches, and 12-7/8 inches, each constructed using #22 AWG solid hookup wire, Litz wire consisting of 175 strands of #46 AWG solid wire, and Litz rope consisting of 660 strands of #46 AWG solid wire. The length of conductor in each case was approximately 70 feet.

Table A-2

Inductances and Distributed Capacitances for Three Ferrite Loop Sticks

Ferrite Loop	*No. Turns*	$L_{ferrite}$ *(μH)*	L_{air} *(μH)*	μ_{r_eff}	$C_{d\_ferrite}$ *(pF)*	C_{d_air} *(pF)*
1	90	502.0	50.58	9.925	1.81	1.46
2	90	522.5	45.33	11.53	2.5	1.45
3	120	1036	75.77	13.67	2.95	1.26

Inductances and distributed capacitances for three ferrite loop sticks measured with the ferrite in place (ferrite) and with the ferrite removed (air). Loop sticks 1 and 2 are flat ferrite bars with cross sections approximately ½ inch × 3/16 inch and 2–3/8 inches in length. Loop stick 3 is a round ferrite bar 3/8 inches in diameter and 2–3/8 inches in length.

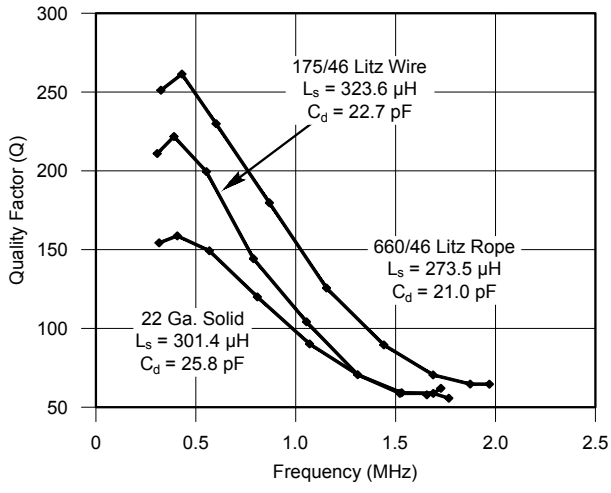

Figure A-10 — Measured quality factor as a function of frequency along with measured values of inductance and distributed capacitance for 12-7/8 inch diameter loops constructed from 660/46 Litz rope, 175/46 Litz wire, and #22 AWG solid wire.

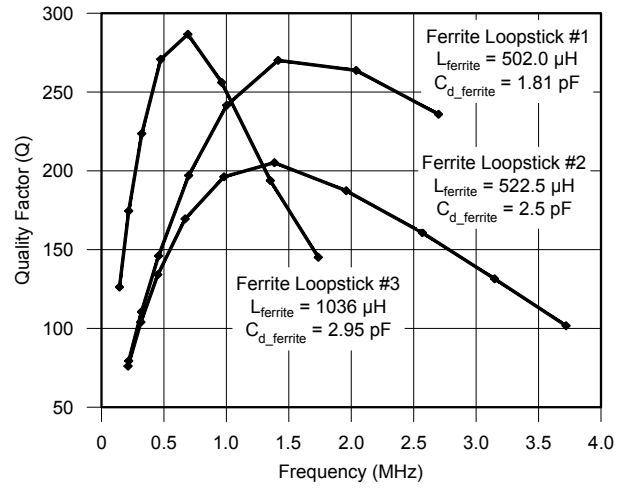

Figure A-11 — Measured quality factor as a function of frequency, along with measured values of inductance, L_s, and distributed capacitance, C_d, for ferrite loop sticks 1, 2, and 3.

Appendix 6

Table A-1 depicts the measured and calculated inductances for the nine loop antennas wound on cardboard forms with diameters of 4-5/16 inches, 7-13/16 inches, and 12-7/8 inches, each constructed using #22 AWG solid copper hookup wire, Litz wire consisting of 175 strands of #46 AWG solid copper wire, and Litz rope consisting of 660 strands of #46 AWG solid copper wire respectively. The measured inductances were obtained by applying the linear regression technique described in Appendix 4, for each loop antenna.

In order to provide additional confirmation of the measured results, calculated inductance values were obtained by applying Wheeler's formula for a circular coil,

$$L = \mu_0 n^2 a \left[0.48 \ln\left(1 + \pi \frac{a}{b}\right) + 0.52 a \sinh\left(\pi \frac{a}{b}\right) \right] \qquad \text{[Eq A-27]}$$

where μ_0 is the permeability of free space, n is the number of turns in the coil, a is the coil radius in meters, and b is the axial length of the coil in meters.[15] Table A-1 shows that error between the measured values obtained by regression analysis and the values calculated by applying Wheeler's formula for a circular coil is no more than a few percent. The inductances obtained for the Litz rope are generally smaller than the other conductors because the larger diameter of the Litz rope increases the axial length of the coil for a given number of turns compared with the coil length obtained with either the solid wire or Litz wire.

Table A-2 depicts the inductances and distributed capacitances for three ferrite loop sticks measured with the ferrite in place (ferrite) and with the ferrite removed (air) obtained by applying the linear regression technique, Appendix 4, for each ferrite loop stick. The value for μ_{r_eff} shown in the table was found by taking the ratio of the inductance measured with ferrite in place to the inductance measured with ferrite removed (air).

HPSDR is an open source hardware and software project intended to be a "next generation" Software Defined Radio (SDR). It is being designed and developed by a group of enthusiasts with representation from interested experimenters worldwide. The group hosts a web page, e-mail reflector, and a comprehensive Wiki. Visit www.openhpsdr.org for more information.

TAPR is a non-profit amateur radio organization that develops new communications technology, provides useful/affordable hardware, and promotes the advancement of the amateur art through publications, meetings, and standards. Membership includes an e-subscription to the *TAPR Packet Status Register* quarterly newsletter, which provides up-to-date news and user/technical information. Annual membership costs $25 worldwide. Visit www.tapr.org for more information.

NEW!

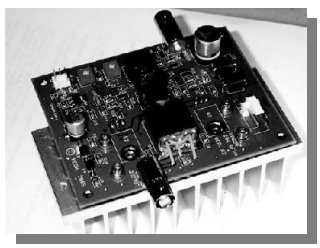

PENNYWHISTLE
20W HF/6M POWER AMPLIFIER KIT

TAPR is proud to support the HPSDR project. TAPR offers five HPSDR kits and three fully assembled HPSDR boards. The assembled boards use SMT and are manufactured in quantity by machine. They are individually tested by TAPR volunteers to keep costs as low as possible. A completely assembled and tested board from TAPR costs about the same as what a kit of parts and a bare board would cost in single unit quantities.

HPSDR Kits and Boards

- **ATLAS** Backplane kit
- **LPU** Power supply kit
- **MAGISTER** USB 2.0 interface
- **JANUS** A/D - D/A converter
- **MERCURY** Direct sampling receiver
- **PENNYWHISTLE** 20W HF/6M PA kit
- **EXCALIBUR** Frequency reference kit
- **PANDORA** HPSDR enclosure

TAPR

PO BOX 852754 • Richardson, Texas • 75085-2754
Office: (972) 671-8277 • e-mail: taproffice@tapr.org
Internet: www.tapr.org • Non-Profit Research and Development Corporation

Sivan Toledo, 4X6IZ

School of Computer Science, Tel-Aviv University, Tel-Aviv 69978, Israel: **stoledo@tau.ac.il**

A Selective Robust Weak-Signal UHF Front End

The author presents a 431 to 435 MHz external front end for a USRP N200 Ettus Research transceiver.

Quite a few modern wideband receivers do not have a selective front-end that can receive weak signals while rejecting strong out-of-band signals. This article explains the issues involved in the design of external front ends for such receivers and describes a concrete front-end unit and its performance. The unit we describe was designed for a Universal Software Radio Peripheral (USRP) N200 radio with a WBX RF daughter card and for 431 to 435 MHz signals, but the design can be easily adapted to other bands and radios.

The WBX is a direct-conversion IQ transceiver that feeds the IQ analog-to-digital (ADC) and digital-to-analog (DAC) converters on the USRP motherboard. The ADCs and DACs are controlled by a field programmable gate array (FPGA) that performs some digital signal processing (up/down sampling and the required anti-aliasing filtering) and sends/receives samples from a computer. Demodulation and other processing tasks are typically done by the computer.

Figure 1 shows a simplified block diagram of the receive chain of the WBX, which covers 50 to 2200 MHz. The receiver response is essentially flat across this frequency range; any signal in this range that is present at the antenna connector of the WBX reaches the mixer. In theory, the mixer translates signals near the frequency of the local oscillator (LO) to frequencies near DC, which the post-mixer anti-aliasing filters pass to the ADCs. Signals far away from the LO are translated to high frequencies that the anti-aliasing filters block. But in practice, strong out-of-band signals generate intermodulation products in the mixer or in the amplifiers that precede it. Some of these spurious signals are often within the passband of the anti-aliasing filters, so they generate interference at the ADC, possibly even causing saturation. This implies that the WBX and similar radios require a selective external front end if they are used to receive weak signals in the presence of strong signals.[1] In many areas, simply connecting the radio to an external antenna guarantees reception of strong signals (cellular base stations, broadcast radio and television, and so on).

A selective front-end can also help the WBX cope with out-of-band signals whose frequency is close enough to that of signals of interest to pass the analog post-mixer anti-aliasing filter (say 15 MHz away). Such signals can saturate in the ADCs even if they are not strong enough to cause intermodulation. A saturated ADC produces no useful data. AGC action can reduce the gain of the WBX to prevent saturation, but this gain reduction also reduces the dynamic range available for weak signals of interest (effectively, the ADC represents them using fewer bits per sample).

[1]Notes appear on page 36.

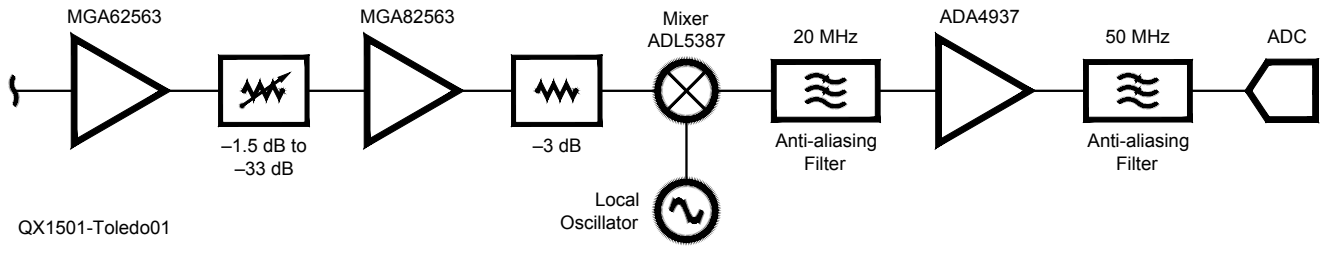

Figure 1 — A highly simplified block diagram of the receive chain of the Ettus WBX RF daughter board (and the ADC, which completes the analog chain and is part of the USRP motherboard). The diagram omits the antenna selection and transmit/receive switches. The signal chain that follows the mixer is complex (separate I and Q channels). The MGA82563 and the mixer are protected from high input power, but this is not shown on the published schematics of the WBX; see text for details.

Selectivity is not the only property that a weak-signal front end for the WBX should have. The WBX has a lot of gain and a fairly good noise figure (5 dB), but for signals near or below the thermal noise floor, more gain and a lower noise figure are helpful. This brings us to the second requirement for our front-end unit: low-noise amplification. As in any front end design, the low-noise amplifier (LNA) can also eliminate the noise-figure degradation that might be caused by the antenna-to-receiver cable and by selective filters.

The requirements so far, selectivity and low-noise amplification, are not new and many existing front-end designs satisfy them to some extent. Currently available and well-documented examples include Sam Jewell's VLNA series, which offers low noise, high gain, but little filtering , LNAs from Down East Microwave (single stage with less gain than the VLNA but somewhat more filtering), the EXTRA series by Gyula Nagy (single stage with a output helical filter, providing more selectivity than the previous two).[2, 3, 4] All of these LNAs have a noise figure of less than 1 dB.

Unfortunately, none of the available units offers narrow filering. I tried to use a chain of two Down East Microwave LNAs with a connctorized ready-made bandpass filter from Cross Country Wireless between them, but the radio still suffered from periods of strong out-of-band interference.[5] Increasing the attenuation in the variable attentuator between the MGA62563 and the MGA82563 using an AGC algorithm prevented saturation, but it also resulted in loss of weak-signal reception. This filter is fairly expensive (over $90) and I was not able to find alternative connectorized filters with more selectivity at a similar or lower cost.

All the available LNAs that I could find had another problem: they can usually destroy the WBX and similar radios if a strong signal is present at their input. Some similar radios are prone to self-destruction even without an LNA (the WBX is apparently not prone to such self destruction; see below). The next section analyzes this issue.

Safe Power Limits in Receive Chains

Receiver front-ends are optimized for weak signals coming from the antenna, but in certain situations they can be subject to relatively powerful signals. Strong signals can appear at the front-end, either due to a powerful nearby transmitter (including out-of-band broadcast transmitters) or due to leakage from our own transmitter. High-enough power will destroy the front-end of any receiver, but some receivers can withstand more input power than others, making them more robust. For example, the Icom IC-R9500 receiver is specified to withstand 5 W of RF input, which is very robust, whereas the Agilent N9000A spectrum analyzer can only withstand –10 dBm in some configurations when the preamplifier is on, and with no input attenuation.[6] Unfortunately, the safe input level of most receivers, including the WBX, is not specified by the manufacturers.

To understand the potential for physical damage by strong signals, let us consider the first few stages of the signal chain of the WBX, including an external LNA mounted near the antenna, such as the DEM 432LNA. Table 1 shows the maximum input power each stage is rated for, the output power at 1 dB compression, which is a lower bound on the maximum power the stage can generate, and the gain for each of the four stages. A device specified with a P1 dB output (output

Table 1
Safe Input Levels

	DEM 432LNA	*MGA62563*	*MGA82563*	*ADL5387*
P_{in} maximum	22.4 dBm	21 dBm	13 dBm	15 dBm
P_{out} at 1dB compression	19 dBm	18 dBm	17.4 dBm	12.7 dBm
Gain	17 dB	22 dB	14.7 dB	4.4 dBm

Note: Possible high output levels (P1 dB), and gain of an external LNA and the first three active stages in the WBX. The data for the MGA62563, MGA82563, and the ADL5387 are from the manufacturers' data sheets.

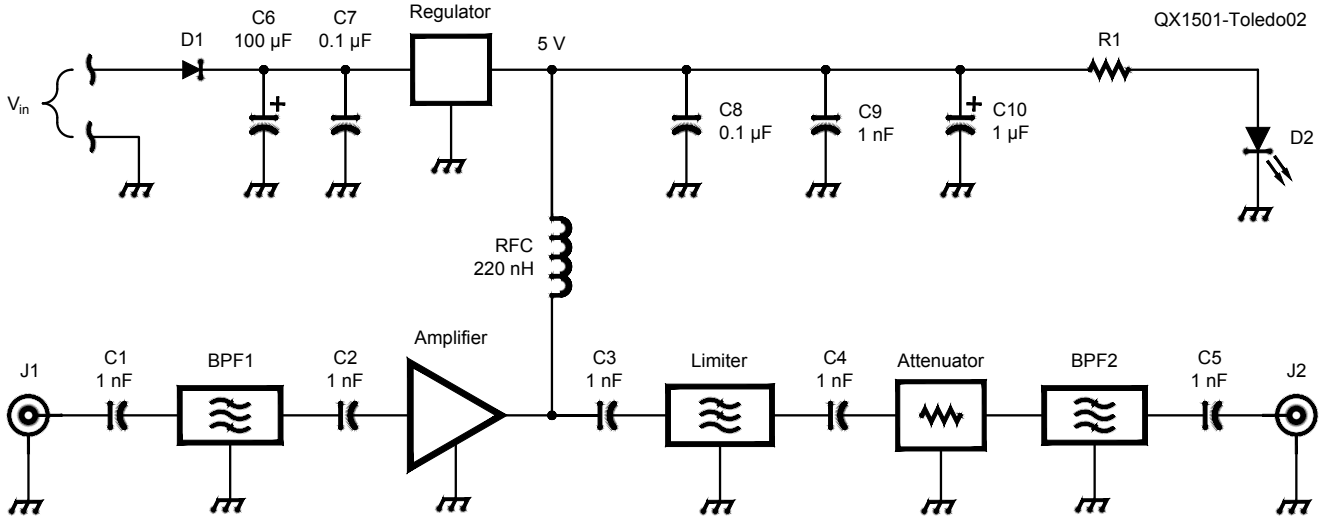

Figure 2 — Schematic of the front end. Table 2 presents the part list for the unit.

power at 1 dB compression) of 18 dBm, for example, can certainly generate 18 dBm of RF power at its output. At this output level the device is already somewhat non-linear, but it is usually not yet saturated. The non-linearity increases at higher power, so typical devices can generate a bit more power than their P1 dB specification, but not much more; 2 to 3 dB is a reasonable estimate. The receive chain also contains switches (omitted from Figure 1), attenuators, and other passive components, but these can tolerate higher power levels than active components so we ignore them here (they do need to be included in a formal anlysis).

The data for the DEM 432LNA are from the DEM data sheet for the LNA, except for the maximum input power, which is taken from the data sheet of the active device in the amplifier, the FPD750SOT89.The data in the table shows that each one of these stages is probably capable of destroying the next. For example, if the MGA62563 is presented with –3 dBm at its input, it will amplify it by 21 dB to 18 dBm (22 minus the 1 dB compression). If the variable attenuator is set to –1.5 dB, the MGA82563 sees 16.5 dBm at its input, which exceeds its limit by 3.5 dB.

A somewhat optimistic estimate of the maximum safe input power level of the WBX (for the components up to the mixer) is 15 dBm + 3 – 14.7 + 1.5 – 22 = –17.2 dBm. If we include a 19 dB LNA, the safe input level drops to around –36.2 dBm. The estimate is optimistic in the sense that we assume that amplifiers do not generate more power than their P1 dB specification, so a conservative estimate might be 3 dB or so lower, to cover the possibility that the last amplifier in the chain is saturated. The safe power level varies with frequency, because of filtering (here only in the external LNA if one is used) and because the gain of the amplifiers varies a bit with frequency (the gains cited above for 432 MHz or so).

If we can ensure that there are no signals stronger than about –40 dBm at the input of the external LNA, we are all set; we won't destroy the LNA or the WBX. But if we want to ensure that the receiver won't be damaged by higher power levels, we need to improve the design of the front end.

There are two complementary ways to make the front-end more robust. One is to add *limiters* that limit the power at certain points in the receive chain, and the other is to add filters. A limiter is an RF circuit that behaves like a very mild attenuator at low power levels but reflects most of the input power back at high power levels (the device becomes an RF short when input power is high), thereby protecting sensitive devices that follow it in the receive chain. Limiters are typically implemented using PIN diodes and they usually limit at 0 to 14 dBm output or so.[7]

Matt Ettus of Ettus Research told me that the WBX includes protection for the MGA82563 and the mixer, so we only need to ensure that we do not destroy the MGA62563.[8]

Filters help protect receivers by preventing strong out-of-band signals from reaching the receiver, potentially damaging it. When used in front of a limiter, as in the design described here, they reduce the likelihood that a strong out-of-band signal will trigger any limiting action that would distort weak in-band signals.

Design

Figure 2 shows the schematic of the UHF front-end that I designed to improve the performance of the WBX. The front end is intended to follow a mast-top DEM 432LNA, but it can also be fed directly from the antenna. The signal chain starts with a helical filter, followed by an internally matched PGA-103+ amplifier with a gain of about 22 dB, a noise figure of about 0.5 dB, and P1 dB of about 21.5 dB (all specified at 400 MHz). The amplifier is followed by an RLM-33+ limiter, which limits power at about 12 dBm (at 400 to 500 MHz; it can output slightly more power at higher frequencies; its input 1 dB compression point is 5 dBm), a 3 dB attenuator, and a SAW filter. All the components are internally matched to 50 Ω.

The limiter-attenuator combination ensures that the 10 dBm input-power limit of the SAW filter is never exceeded. A 5 dB attenuator would provide wider margins and

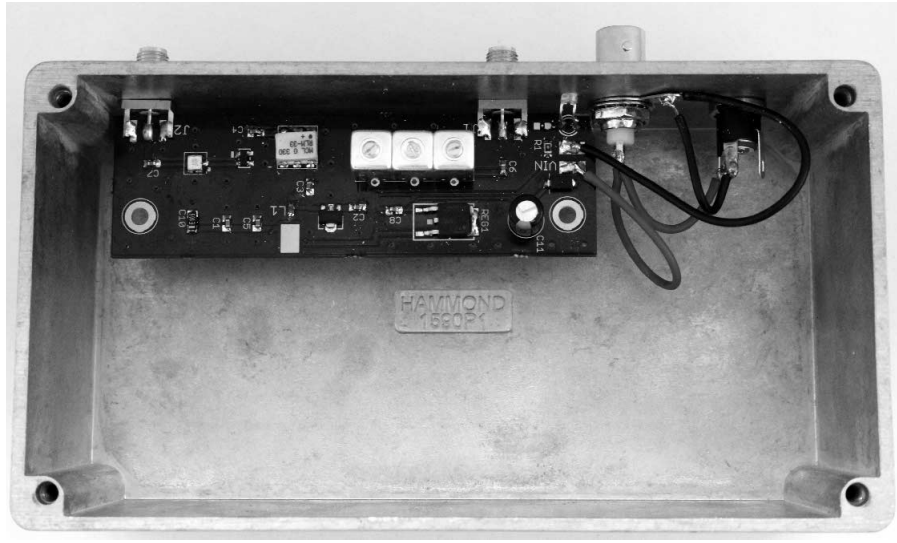

Figure 3 — The interior of the finished front-end in an aluminum box. The DC connector is for input power, and the BNC connector powers the mast-top LNA.

Figure 4 — The finished front-end unit.

is probably preferable. The insertion loss of the SAW filter is about 2 dB, so the WBX should see no more than 7 dBm at its input, which is safe. The limiter itself is rated at 33 dBm (2 W), which is more than the PGA-103+ can generate, so it cannot be destroyed in this circuit either. The PGA-103+ can withstand a 21 dBm input, and because the insertion loss of the helical filter is 3 dB, the overall front-end unit can tolerate up to 24 dBm at its input (The helical filter can withstand a 1 W input, so it does not limit the safe input level). This implies that it can be used safely when connected to a mast-top 432LNA, which is unlikely to produce more than 24 dBm. The run of coax between the mast-top LNA and the front-end unit provides an additional margin of protection.

The SAW filter is very sharp and provides excellent selectivity. The helical filter does not provide much additional selectivity, but as explained above, it reduces the likelihood that out-of-band signals will trigger limiting action that distorts in-band signals. I included the helical filter in the design for another reason. I was worried that the narrow SAW filter will have wide variations in group delay (the time a signal is delayed in the filter) within its passband. This is harmless for narrow-band applications, but troublesome in applications that need to accurately estimate the arrival time of signals. The inclusion of the helical filter, whose group delay is much flatter, allows the unit to achieve reasonable selectivity even if the SAW filter is not used. As you will see in the measurements section below, within the center of the passband of the SAW filter its group delay is fairly constant, so this turned out not to be an important issue. On the other hand, the helical filter is the most expensive component in the front-end unit, so dropping it from the design is not unreasonable. Of the other components, the most expensive are the limiter and the SMA connectors.

The power supply section is straightforward. It can use either a standard linear regulator (78M05, the one that is also used in the 432LNA), or a low-dropout (LDO) replacement, TL720M05. The LDO requires a higher-value output capacitor for stability, but otherwise the two regulators are similar, except that the LDO can function down to 5.5 V, whereas the 78M05 requires a 7.5 V input.

The PGA-103+ is rated from 50 to 4000 MHz (with somewhat degraded performance at the high end) and the limiter is rated for 30 to 3000 MHz, so the unit can be easily adapted to other bands. Helical filters with the same circuit board layout are available for other bands (center frequencies of 146 MHz and 1270 MHz); finding a suitable SAW filter for other bands may be more of a challenge. The values of blocking capacitors and of the choke may need to be adapted to other bands.

Construction

I built the first unit on a piece of double-sided copper-clad board in which I cut out some of the copper by hand, in order to quickly test the design. For the next version I designed a circuit board and had a few made by a low-cost US-based manufacturer (OSH Park, which charged about $20 for 3 identical boards). The schematic and circuit board design files are available for download from the ARRL *QEX* files website.[9]

Making the first board by hand was not trivial, so in hindsight, I should have started off with a manufactured circuit board. Readers interested in the hand-made technique, which does produce good UHF circuits even with tiny components (the SAW filter is 3 mm × 3 mm with 0.38 mm separation between pads), can read about it in my blog.[10]

The circuit board uses mostly surface-mount devices. Capacitors and the choke are in 0603 packages. There's generous space around components, making the board easy to assemble. I probably could have shrunk the layout quite a bit without hurting ease-of-assembly much.

Performance

I measured the performance of the front-end unit using a calibrated Agilent E5061B Vector Network Analyzer. Figure 5 shows the magnitude response between 375 MHz and 500 MHz, and Figure 6 shows the response around the passband. The unit has 15 dB of gain (with a –3 dB attenuator) with –3 dB points near 429 and 438 MHz. The gain between 430.4 and 436.6 MHz is quite flat and varies by less than 0.5 dB. The stopband attenuation is high, reaching about –60 dB at 375 and 500 MHz. The input return loss in the passband is 12.8 dB or better and the output return loss is 13.65 dB or better. Output to input isolation is 32 dB or better.

The selectivity of the unit is provided mostly by the SAW filter BPF2. The 3 dB bandwidth of the input helical filter BPF1 is specified to be about 34 MHz, so its response contributes little to the selectivity of the overall unit. It does provide some measure of

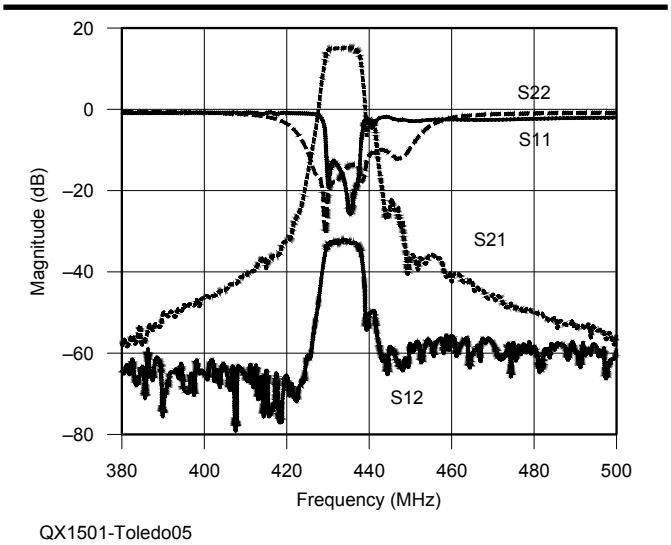

Figure 5 — Scattering parameters of the front end: gain (S_{21}), isolation (S_{12}), input return loss (S_{11}), and output return loss (S_{22}).

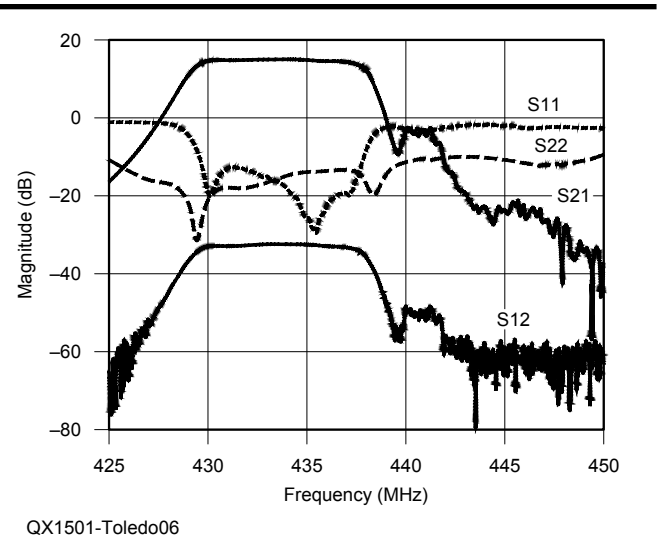

Figure 6 — A close-up of the scattering parameters near the pass band of the front end.

protection to the amplifier from strong way-out-of-band signals.

Figure 7 shows the magnitude response of the SAW filter alone. We can see that it is the main determinant of the response of the entire unit. The two responses are similar not only in terms of the bandwidth, but also in terms of details like the smooth rolloff toward lower frequencies and the two "shoulders" in the rolloff toward higher frequencies.

Figure 8 shows the group delay of the unit. The input-to-output delay in the front end is high, up to 283 ns (at 437.7 MHz). Within the center of the passband, between 431 and 435 MHz, the delay is smaller, around 150 ns. The VNA output indicates that the group delay is noisy (variation of about 50 ns between 431 and 435 MHz), but at least some of this is probably due to noise in the measurement of the phase response of the unit and in the numerical differentiation that computes the delay from phase measurements. The high delay is a result of the relatively narrow and sharp filter, so it is not unexpected.

I also measured the 1 dB compression point and the 3rd order intercept point of the unit. The measurements were done using an Agilent N9010A signal analyzer (used as a spectrum analyzer), an Agilent N5171B signal generator, and a Mini-Circuits ZFSC-2-4-S+ splitter-combiner. For two-tone measurements, the second signal generator consisted of a VWNA 3E network analyzer used as a signal generator together with a DEM 432MHz LNA. The results of the measurements (shown in Figure 9) show that the gain of the unit under test was 14.6 dB, that the input-referenced 1 dB compression point is –11 dBm (output referenced 2.6 dBm), and that the output-referenced 3rd order intercept point is 19.25 dBm (input referenced 4.66 dBm). The intercept and compression points of the units are determined primarily by the limiter, not by the PGA-103+ amplifier. The PGA-103+ output 1 dB compression point is 21.5 dB, whereas the limiter input 1 dB compression point is much lower, at 5 dBm.

Conclusions

Highly-integrated receivers and transceivers with wide frequency coverage are available for VHF, UHF and above. They are available in a wide range of prices and performance levels, ranging from sub-$20 USB-dongle receivers to transceivers costing hundreds or thousands of dollars (obviously at much higher levels of performance).[11]

In spite of the high level of integration, most of these receivers and transceivers lack a high-performance front-end. Designing a

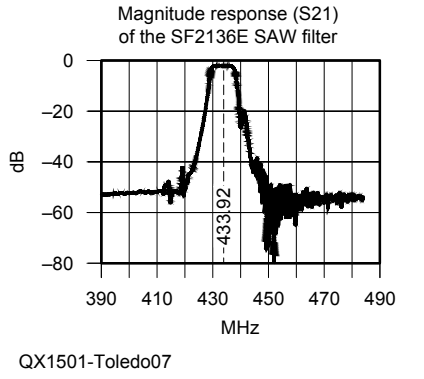

Figure 7 — The magnitude response of the SAW filter, taken from the manufacturer's data sheet dated 2/10/2011.

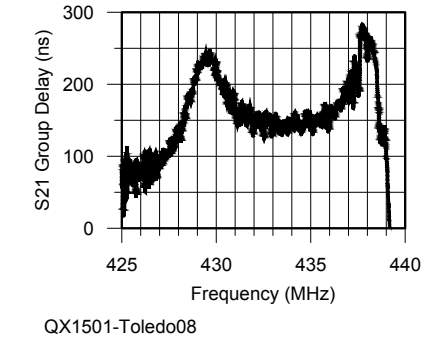

Figure 8 — Input-to-output delay in the front end.

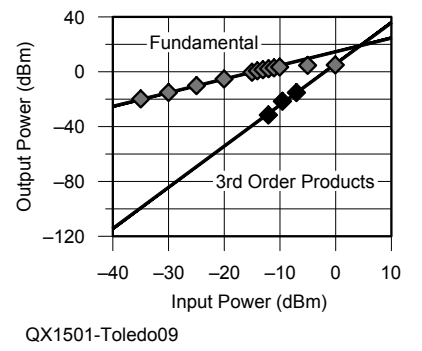

Figure 9 — Gain measurements used for estimating intercept and compression points.

Table 2
Parts List for the Front-End Unit

Designator	*Manufacturer*	*Part Number*	*Price*
BPF1	Temwell	TT67295B-435M	$18
BPF2	RF Monolithics	SF2136E	$0.75
Amplifier	Mini-Circuits	PGA-103+	$2
Limiter	Mini-Circuits	RLM-33+	$10
Attenuator	Mini-Circuits	LAT-5+ or LAT-3+	$2
Regulator	Texas Instruments	TL720M05 or 78M05	$1.23
RFC — 220 nH 0606	TE Connectivity	9-1624112-0	$0.47
C1, 2, 3, 4, 5, 9	Kemet or others	1 nF 0603	$0.02
C7, 8	Kemet or others	0.1 μF 0603	$0.02
C6	Panasonic or others	100 μF 35 V electrolytic	$0.78
C10	Nichicon or others	1 μF 10 V for 78M05 or 47 μF 10 V for TL720M05 tantalum	$1
D1	Diodes Inc or others	Schottky 40 V 1 A	$0.45
D2	Kingbright or others	3 mm green LED	$0.13
R1	Any	180 Ω 0805 or adjust for LED	$0.02
J1, 2	Molex or others	SMA card-edge jack with nut	$6.70

Prices are approximate and reflect the pricing for the small quantities required for one unit. Temwell and Mini-Circuits have minimum-order requirements; all the other parts are available from Digi-Key and other distributors in small quantities.

low-noise amplifier is not hard (especially given the availability of low-cost, low-noise internally-matched integrated amplifiers). Ready-made filters are somewhat harder to find, because they are frequency and bandwidth specific, but for some frequency-bandwidth combinations, commercially-available SAW filters can give excellent results at low cost. Ensuring that the external front-end does not damage the receiver is more challenging, however, and this topic has not received much attention. Hopefully this article will result in safer high-performance front ends.

It is also worth noting that the unit is designed for weak signals and that it does not cope well with strong in-band signals, especially when it is coupled with a mast-mounted LNA. Strong in-band signals amplified by the amplifier or amplifiers that precede the limiter and the receiver can cause severe intermodulation. Far out-of-band signals are less of an issue because they are attenuated by the two filters in this unit (and by band-pass filters in the mast-mounted LNA).

The research reported in this article was supported by the Minerva Center for Movement Ecology. Sivan Toledo, 4X6IZ, is Professor of Computer Science at Tel-Aviv University. He holds BS and MS degrees from Tel-Aviv University and a PHD from the Massachusetts Institute of Technology, where he was also Visiting Associate Professor in 2007 – 2009. He was first licensed in 1982.

Notes

[1]The vendor of the USRP and WBX, Ettus Research, also produces similar RF daughter boards for higher frequencies (SBX and CBX). More generally, many modern receivers and transceivers with a similarly-wide frequency coverage usually have little or no front-end selectivity because of the difficulty of producing tunable band-pass filters.

[2]Sam Jewell, "VLNA: A Very Low Noise (Pre)-Amplifier for the UHF 70 cm to 9 cm Bands," *Version E1*, 2013. PDF documentation at **http://www.g4ddk.com/**.

[3]A variety of low noise amplifiers, including the one used in this design, are available from Down East Microwave; **www.downeastmicrowave.com/PDF/l-lna.PDF**.

[4]More information about the Extra series of preamplifiers by Gyula Nagy, HA8ET, is available on his website: **www.ha8et.hu/**.

[5]For more information about the Cross Country Wireless band-pass filters, go to: **www.crosscountrywireless.net/filter.htm**.

[6]It would be much better if the manufacturers would do the testing to determine the maximum safe input level than to have users discover that level accidentally.

[7]For a technical background on PIN-diode limiters, see Skyworks Application Note "PIN Limiter Diodes in Receiver Protectors," at: **www.skyworksinc.com/uploads/documents/200480C.pdf**, 2004. Originally published as "PIN-LImiter Diodes Effectively Protect Receivers," *EDN*, Dec 17, 2004, pp 50 – 64.

[8]The limiter is not shown in the schematics of the WBX; In personal correspondence with Mat Ettus, the designer of the WBX, he told me that it is there.

[9]The schematic and circuit board design files for this project are available for download from the ARRL QEX files website. Go to **www.arrl.org/qexfiles** and look for the file **1x15_Toledo.zip**.

[10]Read the author's technical Blog at: **http://sivantoledotech.wordpress.com/**.

[11]Current examples include USRP receivers and transceivers from Ettus Research starting at $775, BladeRF from Nuand starting at $420, the FUNcube-dongle receivers at about $200, and sub-$20 DVB-T dongles that can be used as general-purpose sampling receivers.

M² ANTENNA SYSTEMS, INC.

Bring Your Ideas to Us

M² brings your antenna designs to life!

WORLD CLASS PRODUCTS

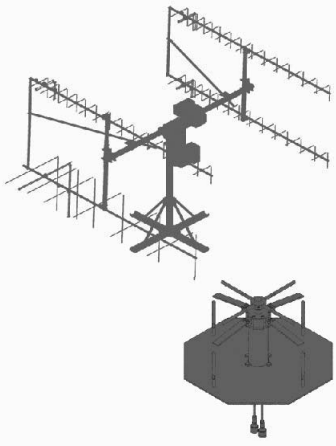

M² makes more than just high quality off-the-shelf products. We also build custom antenna systems using innovative designs to meet our customers' demanding specifications.

Our high-performing products cover high frequency, VHF, UHF and microwave.
Ask us about our custom dish feeds.

From simple amateur radio installations to complete government and commercial projects, we have solutions for nearly every budget.

Directional HF and small satellite tracking stations are our specialties.

Contact us today to find out how we can build a complete antenna system to meet your needs!

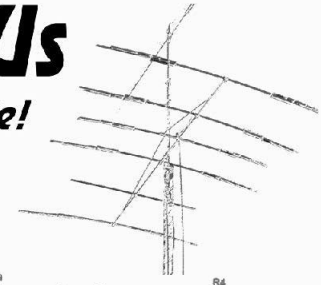

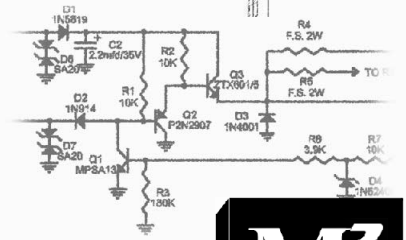

M² ANTENNA SYSTEMS, INC.

M² offers a complete line of top quality amateur, commercial and military grade antennas, positioners and accessories. We produce the finest off-the-shelf and custom radio frequency products available.

For high frequency, VHF, UHF and microwave, we are your source for high performance RF needs. M² also offers a diverse range of heavy duty, high accuracy antenna positioning systems.

For communications across town, around the world or beyond, M² has World Class Products *and Engineering Services* to suit your application.

M² products are proudly 'Made in the USA'

4402 N. Selland Ave.
Fresno, CA 93722
Phone (559) 432-8873
http://www.m2inc.com
sales@m2inc.com

ANTENNAS POSITIONERS ACCESSORIES

Ray Mack, W5IFS

17060 Conway Springs, Austin, TX 78717; **w5ifs@arrl.net**

SDR: Simplified

Columns rebooted — A look at angle modulation and decoding in an SDR.

An Update

I spent most of the past year on another writing project that I finished this spring. It is good to be back writing this column for *QEX* readers! You will have noticed that we now have two SDR columns in *QEX*. Scotty Cowling, WA2DFI, with his "Hand On SDR" column, is going to be focusing on helping you integrate software and off-the-shelf hardware into usable SDR radios you can put on the air. I will continue to focus on something more akin to laboratory experiments to show what goes on under the covers in SDR software and hardware. Some of our experiments will also be usable on the air, but they will be very much "do it yourself" endeavors.

We started out using the Analog Devices Blackfin Stamp board. I will be going back to that platform from time to time for projects that require significant horsepower. The simple projects will use the eZDSP-5535 from TI. The Stamp is still available from Digi-Key for $220. The eZDSP-5535 is available for around $100 from Digi-Key or Mouser. We will also look at using FPGA devices from Altera. Scotty mentioned to me that the BeMicroCV-A9 should be available soon and hopefully, with reasonably priced development tools. It is amazing how capable inexpensive FPGA devices have become.

We will look at leveraging the FPGA work done in the high performance software designed radio (HPSDR) project from the HPSDR group and TAPR. Those boards are still available if you want to work with them instead, but we will look at porting that work into our own projects. Some of our projects will go into the control of an SDR. If the development tools for the BeMicroCV-A9 are affordable, I believe that the board will satisfy most of the needs for a full SDR transceiver. We will still need something such as a Beagle Bone Black plus LCD (approximately $100) to make an entire radio. The Beagle Bone Black is based on a TI Sitarra processor, which is a continuation of the OMAP media processing family. I want to work over the coming year to bring you enough hardware and software to build a self-contained radio for 160 m through 40 m, with the antenna essentially connected directly to the ADC for receive and to the DAC for transmit. We might even be able to extend the range up to 6 m and still stay within a reasonable budget!

Angle Modulation

We looked briefly at angle modulation several years ago but did not do a demodulation implementation.[1] The two types of angle modulation are frequency modulation (FM) and phase modulation (PM). The equations for the modulated signals are:

FM → $V = \sin(2\pi f_C t + \Sigma(f_{SIGNAL}(t)\,\Delta\theta))$

PM → $V = \sin((2\pi\ f_C\ t + f_{SIGNAL}(t))$

where:

$f_{SIGNAL}(t)$ is a time varying signal containing information to be transmitted and is scaled to provide the appropriate amount of phase or frequency deviation. f_C is the carrier frequency in Hz. $\Delta\theta$ is the incremental change in phase of the carrier waveform.

The PM equation is straightforward. The instantaneous angle is an offset from the angle of the carrier waveform. The phase difference ($f_{SIGNAL}(t)$) is scaled so that the change in angle for positive and negative excursions is less than 90° so there is no rollover in phase. Typically, the phase

[1]Notes appear on page 40.

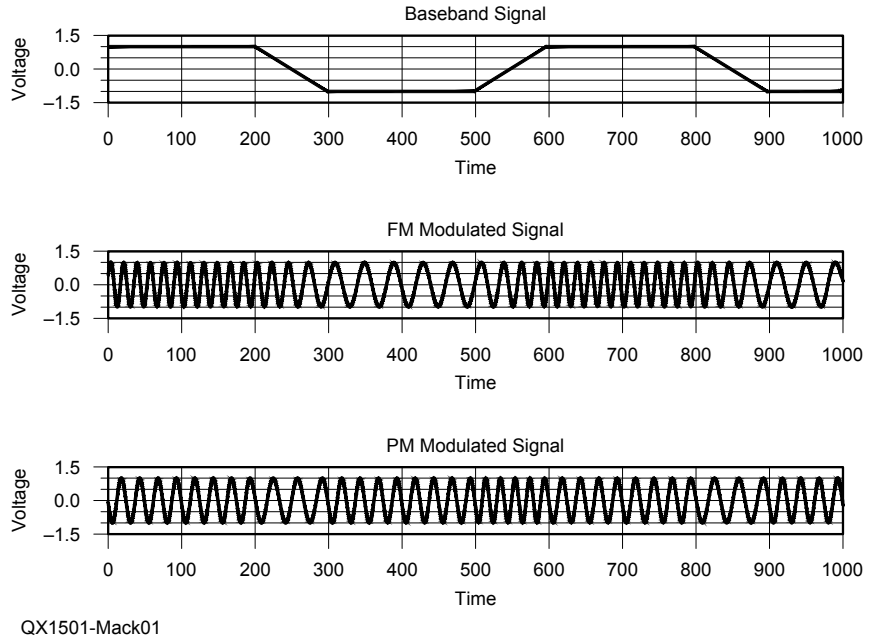

Figure 1 — The top waveform shows a digital modulating waveform. The middle waveform is an FM transmitter modulated with the digital signal. The bottom waveform is a PM transmitter modulated with the digital signal.

change is limited to much less than 90°. The FM equation is complicated because it is a function of the sum of all of the angles before it plus the current offset angle. In math, the sum is replaced with a definite integral from time equal zero to the present time. Its evaluation can be pretty messy. Figure 1 gives a clear picture of the difference between PM and FM. The modulating signal is a digital signal that has a smooth transition between the positive and negative values. Notice that the PM signal only changes from the carrier frequency during the transitions between stable values, and the FM signal is essentially never the same as the carrier frequency.

PM Demodulation

An ordinary balanced modulator is an excellent phase detector and is a classic method used in phase locked loops (PLL). An extraction of the original modulating signal occurs when we multiply the modulated signal with a sine wave that is 90° out of phase from the original carrier:

$V_O = \sin(2\pi f_C t + f_{SIGNAL}(t)) \times \cos(2\pi f_C t)$

$V_O = \frac{1}{2} \sin(2\pi f_C t + f_{SIGNAL}(t) + 2\pi f_C t) - \frac{1}{2} \sin(2\pi f_C t + f_{SIGNAL}(t) - 2\pi f_C t)$

$V_O = \frac{1}{2} \sin(4\pi f_C t + f_{SIGNAL}(t)) - \frac{1}{2} \sin(f_{SIGNAL}(t))$

The output of the modulator is the sum of a double frequency signal and the baseband signal. We recover the baseband signal by passing the multiplier output through a low pass filter to eliminate the double frequency signal. The modulation process and demodulation are linear if the phase change is very small. For very small angles, $\sin(x)$ is the same as x (when x is in radians), so the low frequency signal is the same as the original modulating signal. Figure 2 shows a modulating waveform, the modulated signal, and the output of the demodulator. The demodulator oscillator can be adjusted so that its phase is correct, just as it is in a PLL.

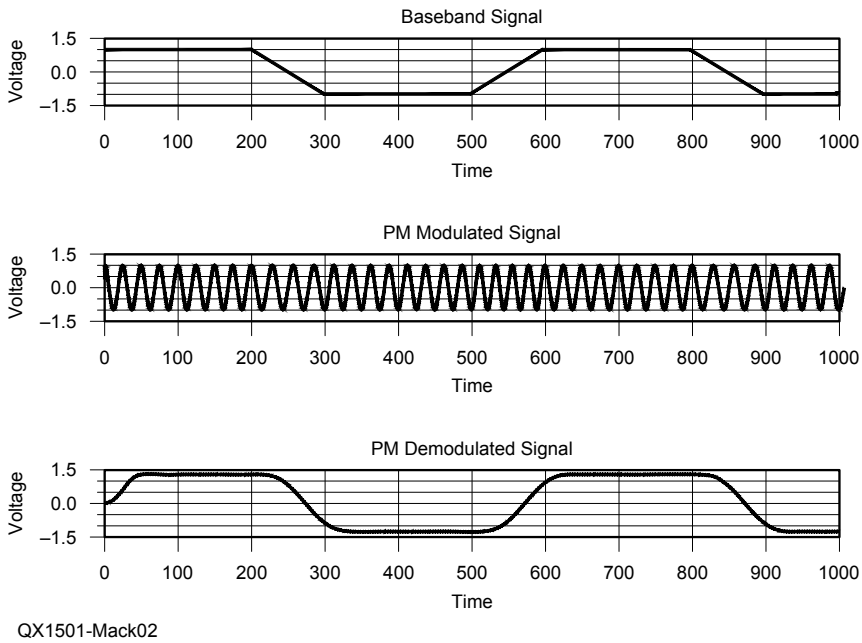

Figure 2 — The top waveform is the original modulating signal, the middle waveform is a PM modulated signal, and the bottom waveform is the output of the demodulator.

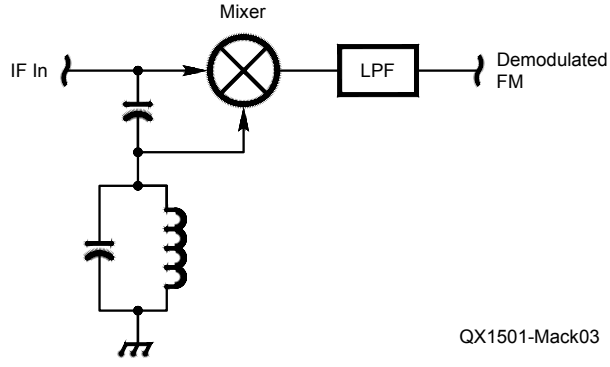

Figure 3 — This is the schematic of an analog quadrature FM demodulator.

FM Demodulation

FM demodulation is more problematic. The change in angle from the unmodulated carrier is constantly increasing or decreasing and exceeds ±90° as a normal part of operation. For that reason, a simple phase comparator using the recovered carrier will not demodulate FM. In PM demodulation, the phase comparison is an absolute comparison against the carrier phase. FM requires that we measure the *rate of change of phase* and sum those incremental phase changes.

It turns out we can use the same balanced modulator with some minor changes to implement the rate of change/accumulate operation. The quadrature demodulator performs exactly the operation we wish to accomplish. The analog circuit in Figure 3 operates by delaying the modulated signal by approximately 90° through the series capacitor. The tuned circuit tends to follow the last cycle of the delayed incoming signal. The result is that the "demodulating oscillator" tracks the incoming signal and performs the same phase detection we saw for PM. If the frequency is increasing rapidly, the phase difference will be positive and increasing even during a single cycle, and result in a steadily increasing voltage. Of course, the reverse holds when the frequency is decreasing.

The analog circuit has a double effect because the phase change across the capacitor will be different as the frequency changes. The change in phase shift will be much smaller than the incremental phase change of the signal, so it still works. In an SDR, we don't have to worry about the variable phase shift because we can set the delay to a fixed value. The analog circuit is almost always set to a fairly large frequency, such as 10.7 MHz, so there is little chance that a single cycle can increase or decrease in phase by more than 90° from the previous cycle. The danger in an SDR is that we set the filter and center frequency so low that the phase change from cycle to cycle can be more than 90°.

As a practical matter, the phase change from cycle to cycle needs to be less than about 10° so that the approximation "sin(x)

= x" is valid. Figure 4 shows the results of an SDR experiment done entirely on a computer. A hardware PLL works in exactly the same fashion as the quadrature demodulator plus low pass filter. The PLL oscillator is adjusted more or less on a cycle by cycle basis to force it to track the changes in the incoming signal. The result is that the measured phase difference is relative to a fairly recent phase of the incoming signal rather than the phase of the carrier. A PLL will automatically track the incoming carrier frequency to null any dc offset. The FM detection code for the HPSDR project was written by Bob McGwier, N4HY, and Frank Brickle, AB2KT. This code implements a PLL in software and an FPGA.

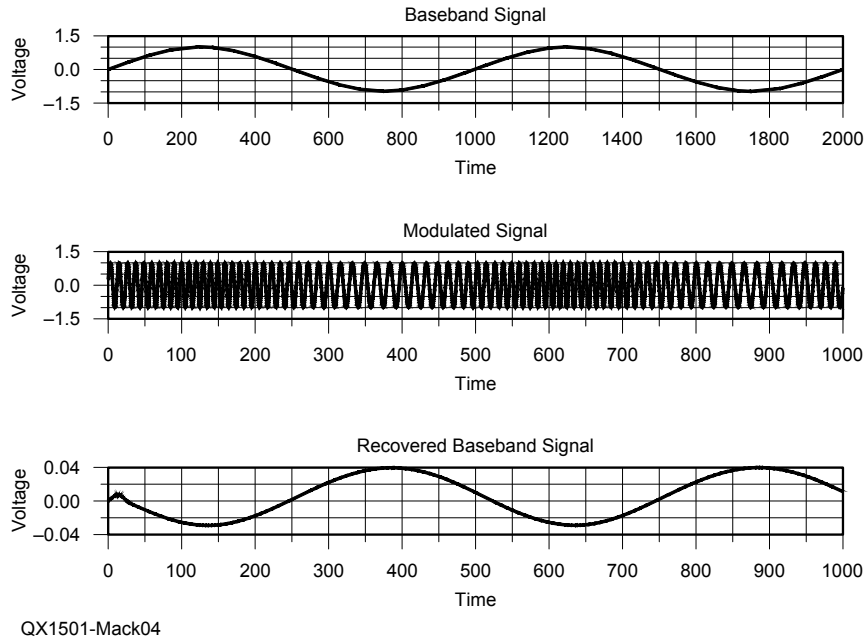

Figure 4 — The top waveform is the original modulating signal, the middle waveform is a FM modulated signal, and the bottom waveform is the output of the software quadrature demodulator.

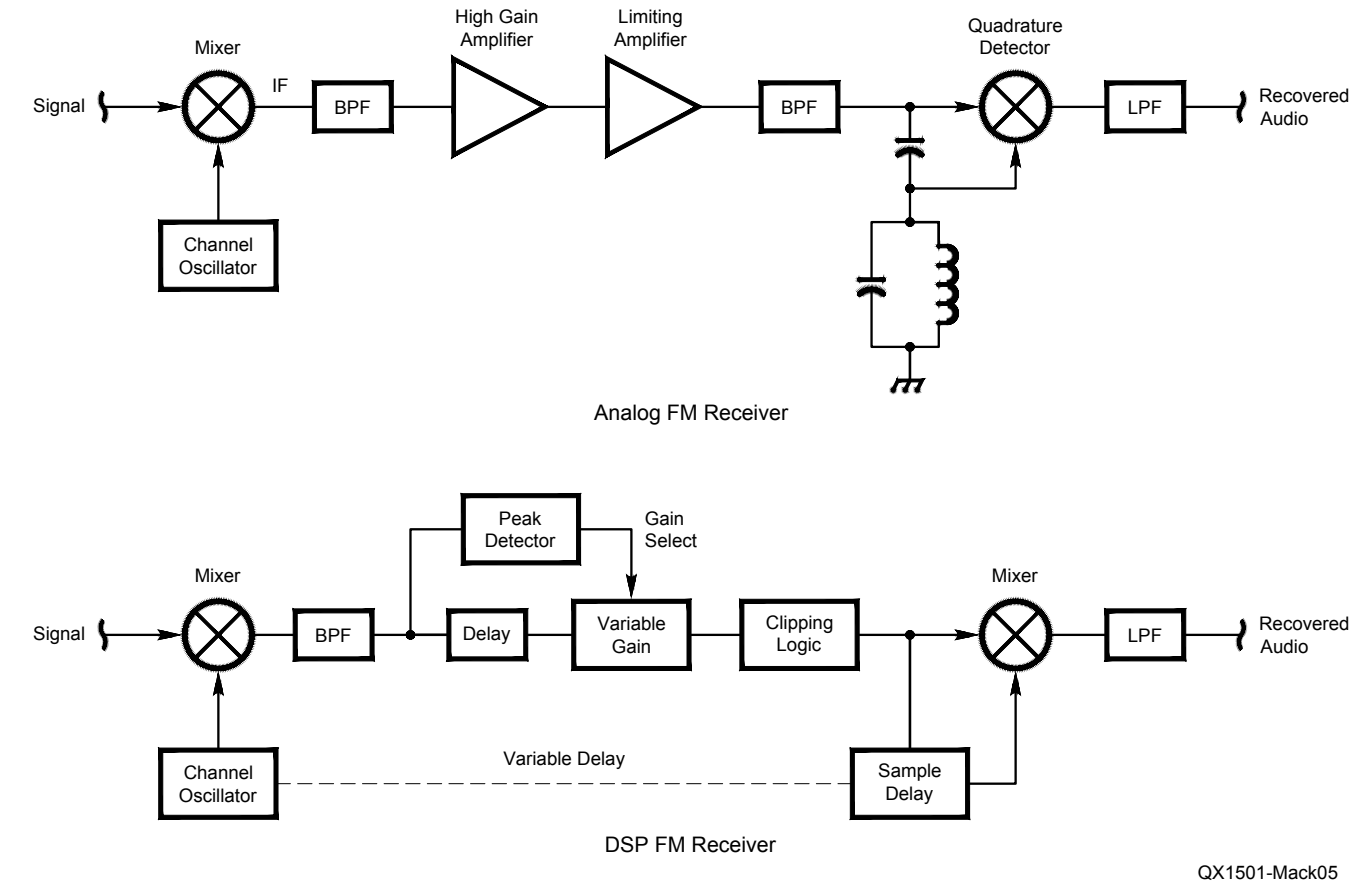

Figure 5 — The top schematic is that of an analog FM receiver. The block diagram on the bottom is the equivalent done in software for and SDR.

DSP Implementation

Listing 1 shows the PM receiver function that we can use to implement its operations. Optimum modulation recovery requires that the reference phase for the phase detector is as close to 90° as possible. That requires both automatic frequency control and automatic phase control. In order to satisfy both requirements, it is also necessary for the modulated signal to have a long term average of zero phase shift. In digital modes, we start with a preamble that has a known bit sequence in order to allow the receiver to zero in on both the phase and frequency. Once the receiver has locked its phase and frequency, the data is also required to maintain an average of zero phase shift. That is accomplished by "bit stuffing" so that on average there are as many ones as zeroes in the modulated stream. In general the "stuffed bits" are different from "normal bits" so that we know not to count them. These concepts are used by satellite TV and satellite radio for transmission.

An SDR implementation of an FM receiver looks just like an analog FM receiver as shown in Figure 5. Once the signal has been translated to the "IF" it must be band pass filtered to eliminate all but the desired signal. Next it is amplified and clipped to set the amplitude to a constant value. Lastly, the signal is passed to the quadrature detector and low pass filter. The clipping amplifier in the SDR is also similar to the analog implementation. We can use a peak detector to decide how much gain to apply before we clip the signal. The previous examples used sine wave signals as inputs to the multiplier, but the circuits will work just as well with clipped versions. Listing 2 shows the main FM receiver function that we can use to implement the various operations. All of the source code is available for download from the ARRL *QEX* files website.[2] Listing 3 contains the functions that are shared between the FM and PM demodulators.

The first step in designing the FM SDR is to make sure we cover all of the constraints. The phase change from cycle to cycle must be less than 10° in order for the demodulation to be linear. There is a three way constraint between sample rate (needed to be able to get 90° phase delay), carrier frequency (ability to filter out 2× content), and deviation (10° maximum change). Amateur narrow band FM has 5 kHz deviation, with a maximum modulation frequency of 3 kHz. A rough calculation (far from scientific) sets our minimum intermediate frequency to 100 kHz — ((360° / 10°) × 3 kHz). The rate of change of phase (and carrier frequency change) is proportional to the modulating frequency rather than the deviation. The ratio of 3 kHz baseband to 200 kHz double frequency makes the final low pass filter constraint easy to accomplish. Our final constraint requires that we are able to approximate a 90° difference at the quadrature detector. The minimum sample frequency is four times the intermediate frequency. We will have more freedom to set the time delay and the intermediate frequency if we increase the sample frequency to 800 kHz, 1000 kHz, or 1200 kHz.

Of course, we now have another limitation to overcome. The Blackfin Stamp processor runs at 500 MIPS (Million Instructions Per Second), so we will have only 500 instructions to execute per sample if we choose 1000 kHz. This is a good example of where using an FPGA to help the processor makes sense. The small number of available instructions argues for not using many function calls. A reasonable design will use a 16 bit ADC running at 1 MSPS.

Next, we design the peak detector and limiter. The peak detector will encounter approximately 10 samples per cycle. This is a small number so the samples will, in general, not contain the peak value for the cycle. We can approximate the peak value by choosing the high value for each half cycle and performing a running average. We limit the value out of the clipping to 250. We want to adjust the gain so that the peak value before clipping is approximately 4000. If the amplitude is greater than 4000 without gain, we simply pass the samples directly to the clipper.

The time delay for exactly 90° delay in the quadrature detector is 2.5 samples with 1000 kHz sampling and 100 kHz IF. We have to choose either two or three samples for the delay. It turns out that either value will accomplish the required delay. The slight error will result in a small dc offset to the recovered audio, which will be removed with the normal high pass filtering. The offset will not cause distortion. It makes sense to choose a two sample delay if we will use an IF between 100 kHz and 200 kHz.

Notes

[1]Raymond Mack, W5IFS, "SDR:Simplified," *QEX*, Nov/Dec 2011, p 33–36.

[2]The program listings and source code files are available for download from the ARRL *QEX* files website. Go to **www.arrl.org/qex-files/** and look for the file **1x15_Mack_SDR.zip**.

Listing 1

```
/************************
Description: This function implements a continuous loop for a
             Phase Modulation Receiver.
Parameters:  frequency -- the center frequency of the IF (in Hz)
         bandwidth - the IF bandwidth (in Hz)
Inputs:      one sample per loop from the input sampling process
Outputs:     one sample per loop to the output process
Returns:     nothing
Notes:          this function assumes that a multi-tasking kernel allows
          this function to operate as a task that cooperates with the
          input sampling task and the output presentation task. This function waits
          for the sampling process to give it a single sample at the beginning
             of each sample period.  This function processes the samples and decodes
             them into a baseband signal that is sent out one sample per sample period.
************************/
void PM_receiver(int frequency, int bandwidth)
{
int input_sample, output_sample;
int phase_detector_sample;

  // set up the IF bandpass filter for the center frequency, bandwidth, and 27 filter taps
  setup_IF_bandpass_filter(frequency, bandwidth, 27);
  // set up the baseband bandpass filter for 300 Hz low frequency, 3000 Hz high frequency,
  // and 27 filter taps
  setup_baseband_filter(300, 3000, 27);
  // initialize the peak detector moving average
  last_peak = 0;
  average_index = 0;
  // the main loop for the demodulator
  do
  {
    input_sample = wait_for_sample();
    // we re-use the input sample variable because it is already in a register
    input_sample = IF_filter(input_sample);
    // perform the function to adjust the phase detector reference
    phase_detector_sample = PM_lock_phase();
    // Clip the IF signal
    input_sample = angle_modulation_clipper(input_sample);
    // do the demodulation
    output_sample = input_sample * phase_detector_sample;
    // filter the baseband
    output_sample = baseband_filter(output_sample);
    // send the output sample to the consuming task
    send_output_sample(output_sample);
  } while (PM_active());
}
```

Listing 2

```
/************************
Description:      This function implements a continuous loop for a
Frequency Modulation Receiver.
Parameters:frequency -- the center frequency of the IF (in Hz)
           Bandwidth – the IF bandwidth (in Hz)
Inputs:    one sample per loop from the input sampling process
Outputs:   one sample per loop to the output process
Returns: nothing
Notes:            this function assumes that a multi-tasking kernel allows
           this function to operate as a task that cooperates with the
           input sampling task and the output presentation task. This function waits
           for the sampling process to give it a single sample at the beginning of each sample
           period.  This function processes the samples and decodes them into a baseband
           signal that is sent out one sample per sample period.
************************/
Void FM_demodulator(int frequency, int bandwidth)
{
int input_sample, output_sample;
int n_minus_2, n_minus_1;

  // set up the IF bandpass filter for the center frequency, bandwidth, and 27 filter taps
  setup_IF_bandpass_filter(frequency, bandwidth, 27);
  // set up the baseband bandpass filter for 300 Hz low frequency, 3000 Hz high frequency,
  // and 27 filter taps
  setup_baseband_filter(300, 3000, 27);
  // the main loop for the demodulator
  do
  {
    input_sample = wait_for_sample();
    // we re-use the input sample variable because it is already in a register
    input_sample = IF_filter(input_sample);
    // Clip the IF signal
    input_sample = angle_modulation_clipper(input_sample);
    // do the demodulation
    output_sample = input_sample * n_minus_2;
    n_minus_2 = n_minus_1;
    n_minus_1 = input_sample;
    // filter the baseband
    output_sample = baseband_filter(output_sample);
    // send the output sample to the consuming task
    send_output_sample(output_sample);
  } while (FM_active());
}
```

Listing 3

```
/************************
Description:      This function implements the limiter function that is
                 common to PM and FM demodulation
Parameters:input_sample -- the current IF signal sample
Inputs:    running average of previous peak samples
Outputs:   Updated running average of peak samples
Returns:        clipped IF sample
Notes:            this function is different from most in that the variables
           have static allocation. This is necessary to hold the
           history of the incoming samples.

************************/
int angle_modulation_clipper(int input_sample)
{
static int last_peak, moving_average[8], average_index, this_peak_candidate, average_peak;

    average_index &= 7; // this is never initialized so this keeps it in range
    this_peak_candidate = abs(input_sample);
    if (this_peak_candidate < last_peak)
    {
      // store this peak in the moving average
      moving_average[average_index] = last_peak;
      average_index++;
      // Reset the peak detector
      last_peak = 0;
      // wrap the average array index
      average_index &= 7;
      average_peak = moving_average[0] + moving_average[1] + moving_average[2] +
                     moving_average[3] + moving_average[4] + moving_average[5] +
                     moving_average[6] + moving_average[7];
      // divide the accumulated value by 8
      average_peak >>= 3;
    }
    else
    {
      last_peak = this_peak_candidate;
    }
    // apply the gain
    if (average_peak > 1024)
    {
       input_sample *= 4;
    }
    if (average_peak > 512)
    {
       input_sample *= 8;
    }
    // clip the waveform
    if (input_sample > 250)
    {
       input_sample = 250;
    }
    if (input_sample < -250)
    {
       input_sample = -250;
    }
    return (input_sample);
}
```

Letters to the Editor

QEX Editing Errors

Hello Larry,

I lived in Singapore for four years but I am now back in my home state of Michigan. I have started taking *QEX* and have noticed some mistakes in editing that I would like to point out.

In the Jan/Feb 2013 issue, in the article by Ulrich Rohde, N1UL, and Rucha Lakhe, "Mathematical Stability Problems in Modern Nonlinear Simulation Programs," I believe there is an error on page 20, in the right hand column, under the line "**VERBOSE *n***," the text says, "where 0 $n \leq 4$." This should probably be "where $0 \leq n \leq 4$."

In the same issue, in the article by Jeremy Clark, VE3PKC, "Build Amateur Radio Systems Using Scicoslab/Modnum," there is an error on page 40, in the middle of the last column. The sentence that says, "Finally, Figure 10G shows the recovered 1 kHz tone versus the original transmit tone of 1 kHz." There is no Figure 10G included with the article, but Figure 10F looks like the graph described here.

In the Mar/Apr 2014 issue, in the article by Barry Boothe, W9UCW, there are several mistakes that I noticed. On page 21, in the left column, under the subheading "Series 2 Conclusions," on the 3rd line, the text says "the field intensity of a coil loaded." I think this should be "the field intensity of a loaded coil." This probably isn't a major problem, but might make readers pause and say, "What?"

On page 24, Figure 29, "Photo B" is actually Photo C and "Photo C" is actually Photo B. This could also be a bit confusing.

In Robert Zavrel's (W7SX) article, "Radiation Resistance, Feed Point Impedance and Mythology," in the middle column of page 32, in the last sentence of the 2nd paragraph, the text says, "The methods and definitions in this paper, however, can for a basic understanding…" Huh? I think this should be "The methods and definitions in this paper, however, can be used for a basic understanding…"

In the May/Jun 2014 issue, in Pete Horowitz's article, "RF Power Amplification Using a High Voltage, High Current IGBT," in the 3rd paragraph on page 20, under Notes, Note 4 has been cut off.

I found several typographical errors in the article by Paul Wade, W1GHZ, "Locked VCXOs for Stable Microwave Local Oscillators with Low Phase Noise."

On page 24, in the right hand column, under the subheading "VCXO Examples" under "80 MHz," the 2nd line "80 MHz VXCO…" should be "80 MHz VCXO…"

Under "96 MHz," in the 1st paragraph, on the 18th line, the text says "sections of the 74CH390 divide…" should be "sections of the 74HC390 divide…" In the 2nd paragraph under this same subheading, on the 3rd line, "right side or the board" should be "right side of the board."

On page 28, in the left hand column, in the 4th line, the text says "capacitors on the bottom side to for better…" Huh? That probably should say "capacitors on the bottom side for better…." In the right hand column, in the 3rd full paragraph, the 6th line says, "may be useful since crystals do tend drift…" should be "may be useful since crystals do tend to drift…."

In the Nov/Dec 2014 issue, in the article by Colin Brackney, KR4HO, "A Receiving Converter for Two-Meter Radios," throughout the text, reference designators SO1, SO2, and SO3 are used, but the schematic diagram of Figure 3 on pages 16 and 17 has J1, J2, and J3 (which is what they should be).

Also in the text, reference designator SW3 is used, but the schematic diagram of Figure 3 has S3 (which is what it should be).

On page 15, in the middle column, the 2nd line up from Figure 2 says, "and FM activity should not found on these…" should be "and FM activity should not be found on these…"

These are just some glaring faux pas that I noticed.

— 73, Larry Joy, 9V1MI/WN8P, 8440 Marilla Rd, Copemish, MI, 4962; **wn8p@arrl.net**

Hi Larry,

Thank you for your comments and detailed review of these recent issues of *QEX*. It is great to know that readers are paying attention. Anyone who knows me, knows that I strive to produce an error-free issue of *QEX* every time! In fact, probably the most common criticism I receive from my boss and my wife is that I am too much of a perfectionist. Of course I am far from perfect, but I do strive to eliminate every grammar and style error from the articles I prepare for publication. Still, you found several mistakes in every issue for the past year. I will try to do better. I do like to receive feedback from our readers. During my Scouting Wood Badge Training course, I heard the phrase "Feedback is a gift!" over and over. I absolutely agree. Without feedback and someone pointing out our errors, how can we get better? How can we create a better magazine, which readers can enjoy without tripping over typos and other mistakes, unless someone points them out and makes us strive to be better? Please don't hesitate to send notes about errors that you find. I am always pleased to hear from *QEX* readers with questions, comments and even complaints.

One of the problems you pointed out was a Note that was cut off in Pete Horowitz's article, "RF Power Amplification Using a High Voltage, High Current IGBT" in the May/Jun 2014 issue. It looks like the end of that Note was chopped off "behind" the white space at the bottom of the page. Here is the complete text for Note 4.

[4]This description perhaps oversimplifies the situation to some extent. For example, the 4062 manifests somewhat more complicated behavior, as can be also seen in general from transient thermal impedance models among the members of this group.

I apologize for not noticing this missing text on the final page layout of the article.

— 73, Larry Wolfgang, WR1B, QEX Editor; **lwolfgang@arrl.org**

2014 *QEX* Index

Features

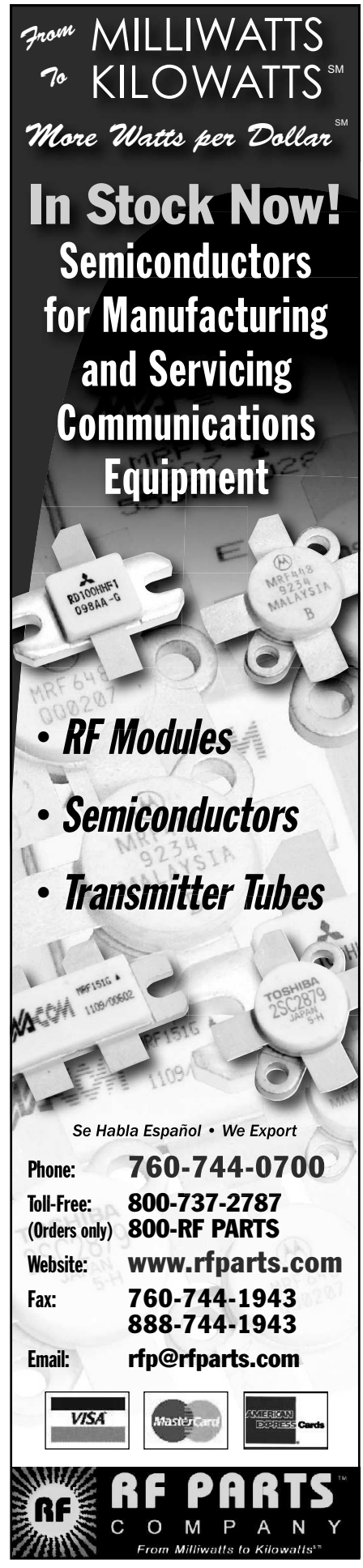

Down East Microwave Inc.

We are your #1 source for 50MHz to 10GHz components, kits and assemblies for all your amateur radio and Satellite projects.

Transverters & Down Converters, Linear power amplifiers, Low Noise preamps, coaxial components, hybrid power modules, relays, GaAsFET, PHEMT's, & FET's, MMIC's, mixers, chip components, and other hard to find items for small signal and low noise applications.

We can interface our transverters with most radios.

Please call, write or see our web site **www.downeastmicrowave.com** for our Catalog, detailed Product descriptions and interfacing details.

Down East Microwave Inc.
19519 78th Terrace
Live Oak, FL 32060 USA
Tel. (386) 364-5529

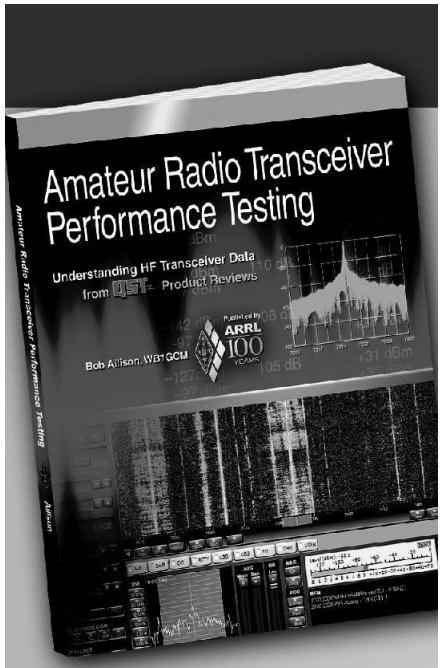

Amateur Radio Transceiver Performance Testing

Understanding HF Transceiver Data from QST *Product Reviews*

By Bob Allison, WB1GCM

QST's monthly "Product Review" column has long been the most-read section of the magazine. That's not surprising, as most radio amateurs are interested in reading about the latest station equipment, and product review testing helps operators make informed decisions based on their needs.

Amateur Radio Transceiver Performance Testing explains in detail the performance data tables from *QST* Product Reviews, providing a valuable resource for Amateur Radio operators who are looking to purchase a transceiver. It discusses how published laboratory data relates to actual performance, how each major test is performed, the significance of each test, and what the numbers mean. You'll gain a better understanding of the extensive testing ARRL performs, technical terms and parameters presented in Product Review, and develop the capability to reach your own conclusion about which HF transceiver is best for you.

Amateur Radio Transceiver Performance Testing
ARRL Order No. 0086
Special ARRL Member Price!
Only $19.95* (retail $22.95)
*plus shipping and handling

ARRL *The national association for AMATEUR RADIO®*
SHOP DIRECT *or call for a dealer near you.*
ONLINE WWW.ARRL.ORG/SHOP
ORDER TOLL-FREE 888/277-5289 (US)

QEX 01/2015

Arduino for Ham Radio

A Radio Amateur's Guide to Open Source Electronics and Microcontroller Projects

By Glen Popiel, KW5GP

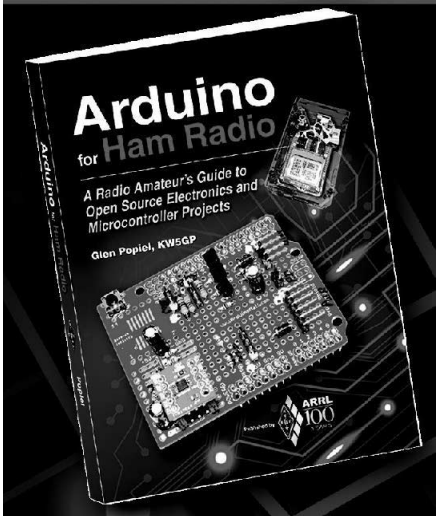

The Arduino has become widely popular among hobbyists and ham radio operators. Hams are exploring these powerful, inexpensive microcontrollers, creating new projects and amateur station gear. With its Open Source model, the Arduino community freely shares software and hardware designs, making projects easier to build and modify.

Arduino for Ham Radio introduces you to the exciting world of microcontrollers and Open Source hardware and software. It starts by building a solid foundation through descriptions of various Arduino boards and add-on components, followed by a collection of ham radio-related practical projects. Beginning with simple designs and concepts and gradually increasing in complexity and functionality, there is something here for everyone. Projects can be built quickly and used as-is, or they can be expanded and enhanced with your own personal touches.

Projects Include:
- Random Code Practice Generator
- CW Beacon and Foxhunt Keyer
- Fan Speed Controller
- Digital Compass
- Weather Station
- RF Probe with LED Bar Graph
- Solar Battery Charge Monitor
- On-Air Indicator
- Talking GPS/UTC Time/Grid Square
- Iambic Keyer
- Waveform Generator
- PS/2 CW keyboard

...and more.

Arduino for Ham Radio
ARRL Order No. 0161
Special Member Price!
Only $29.95* (retail $34.95)

ARRL *The national association for AMATEUR RADIO®*
SHOP DIRECT or call for a dealer near you.
ONLINE WWW.ARRL.ORG/SHOP
ORDER TOLL-FREE 1-888-277-5289 (US)

QEX 01/2015

From MILLIWATTS *To* KILOWATTS

More Watts per Dollar

Transmitting & Audio Tubes

Eimac® RF Taylor® TUBES

COMMUNICATIONS
BROADCAST
INDUSTRY
AMATEUR

Immediate Shipment from Stock

3CPX800A7	4CX1000A	810
3CPX1500A7	4CX1500B	811A
3CX400A7	4CX3500A	812A
3CX800A7	4CX5000A	833A
3CX1200A7	4CX7500A	833C
3CX1200D7	4CX10000A	845
3CX1200Z7	4CX15000A	6146B
3CX1500A7	4CX20000B	3-500ZG
3CX3000A7	4CX20000C	3-1000Z
3CX6000A7	4CX20000D	4-400A
3CX10000A7	4X150A	4-1000A
3CX15000A7	572B	4PR400A
3CX20000A7	805	4PR1000A
4CX250B	807	...and more!

Se Habla Español • We Export

Phone: 760-744-0700
Toll-Free: 800-737-2787
(Orders only) RF PARTS
Website: www.rfparts.com
Fax: 760-744-1943
888-744-1943
Email: rfp@rfparts.com

VISA MasterCard American Express Cards

RF PARTS COMPANY

The ARRL HANDBOOK for Radio Communications

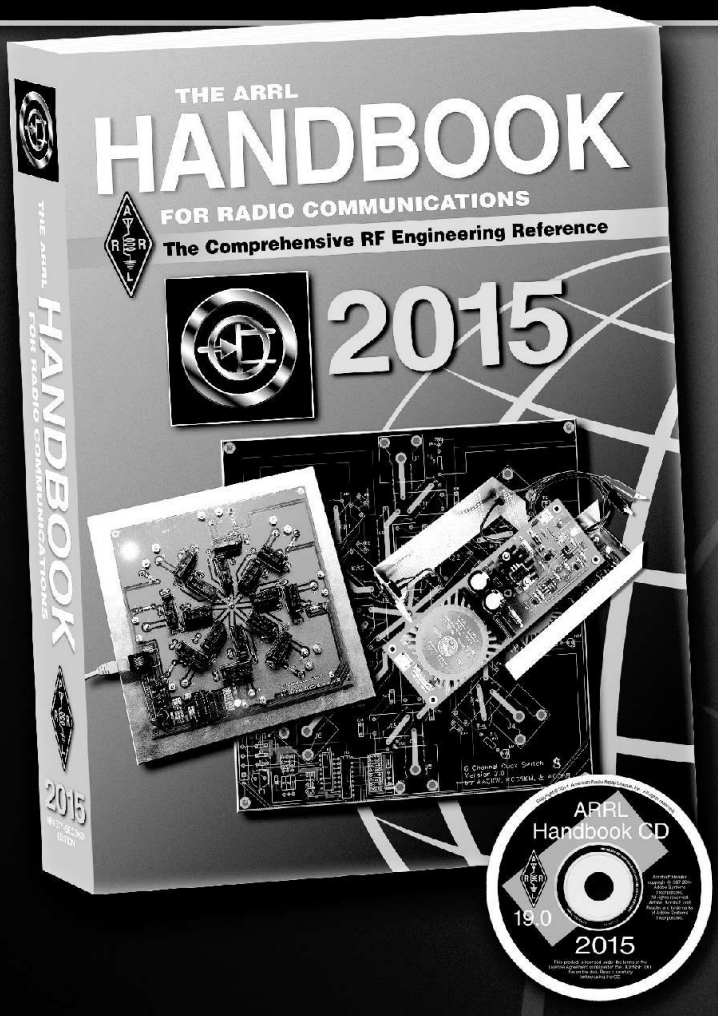

2015 Edition

Discover the theory, practical information and construction details to expand your knowledge and skill as an Amateur Radio operator and experimenter.

This 92nd edition of ***The ARRL Handbook*** is at the forefront of the growing field of wireless telecommunications. The book covers not only the fundamentals of radio electronics—analog and digital—but also practical circuit and antenna design, computer-aided design, digital operating modes, equipment troubleshooting, and reducing RF interference. Many projects and construction articles are included to help enhance your station and expand your participation as an active radio experimenter. Practical applications and solutions make ***The Handbook*** a must-have for hobbyists and technical professionals, finding its way onto workbenches, operating desks, and into university libraries and classrooms.

Dozens of contributors help ensure that each edition is updated and revised to reflect the latest advances and technologies:

New Projects

- Simple Adjustable Tracking Power Supply
- Tri-Band Moxon Yagi Antenna
- A Legal-Limit Bias-T
- An Eight-Channel Remote Control Antenna Switch

New Information

- Updated material on the state of Solar Cycle 24
- Recommended parts for modifying circuit designs and fine-tuning performance
- A package of useful applications on CD-ROM from Tonne Software, including a new version of the ELSIE™ filter design program
- Annual transceiver model review

CD-ROM Inside

Includes the fully searchable text and illustrations in the printed book, as well as expanded supplemental content, software, PC board templates, and other support files.

Softcover Book and CD-ROM
ARRL Order No. 1920
Only $49.95*

Hardcover Book and CD-ROM
ARRL Order No. 0218
BONUS! Save $10.00 while supplies last
Only $49.95* (retail $59.95)

Special Offer!

The BEST DEAL in Amateur Radio is back! Save $10.00 and get the Hardcover edition at the Softcover price, while supplies last.

*Shipping and handling charges apply. Sales Tax is required for all orders shipped to CT, VA, and Canada.
Prices and product availability are subject to change without notice.

ARRL The national association for AMATEUR RADIO®

ARRL 100 YEARS

www.arrl.org/shop

**Toll-Free US 888-277-5289,
or elsewhere +1-860-594-0355**

QEX 01/2015

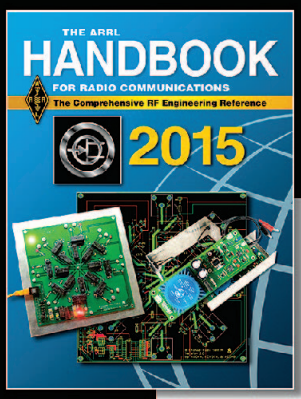

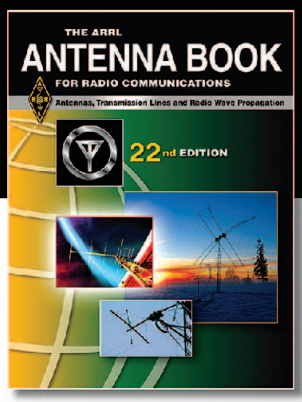

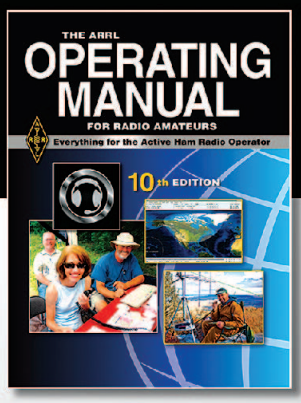

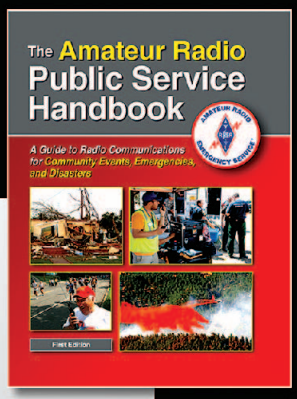

Stay in the Know!

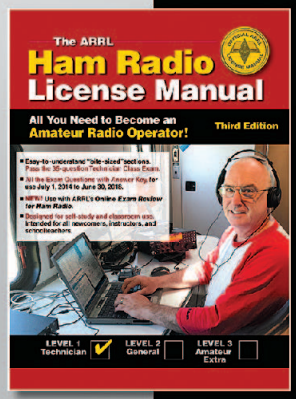

ARRL Publications and Journals
www.arrl.org/shop

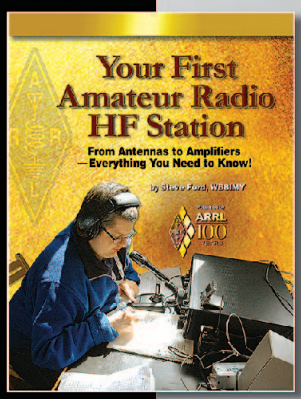

ARRL, the national association for Amateur Radio®
Devoted entirely to Amateur Radio

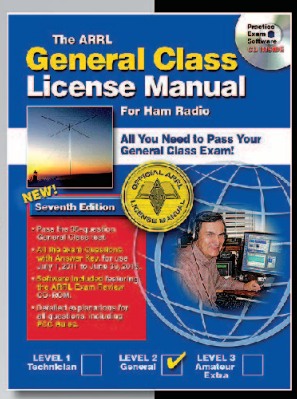

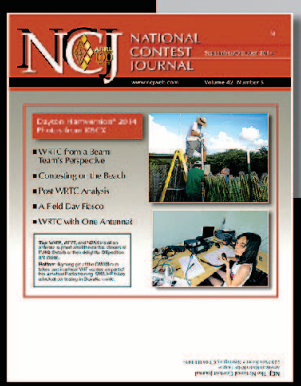

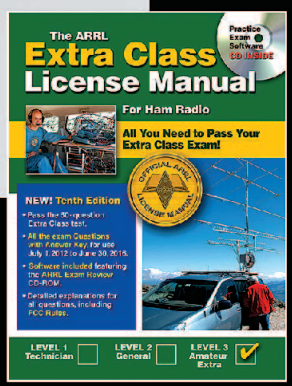

Quicksilver Radio

See Our Huge Display at Dayton Hamvention 2015. Visit Our Booths 462-463-464-465-469-470-471-472

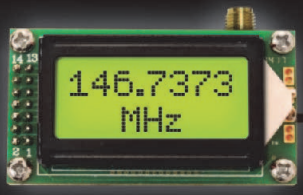

Frequency Counter 0-500 MHz

Affordable test equipment. Perfect for bench or field work. Standard SMA antenna jack. Bright, easy-to-read display.

Digital Voltmeter/ Ammeter

Two line display shows both current and voltage. Included shunt allows measurement up to 50A and 99V. Snaps into a panel to give your project a professional finish.

LED Volt Meters

0 to 99VDC Volt Meter. Available in blue, red, yellow, and green.
Sale Price $11.73
Pack of 4 $39.73

Digital Temperature Sensor

Two channel, includes two sensors. Reads in Fahrenheit or Celsius. Indoor/Outdoor use. Available in blue or red.
Sale Price $24.73

LCR and Impedance Meter

Newest Model. Analyzes coils, capacitors, and resistors. Indicates complex impedance and more.

Automatic Passive Component Analyzer

Analyzes coils, capacitors, and resistors.

Advanced Semiconductor Component Analyzer

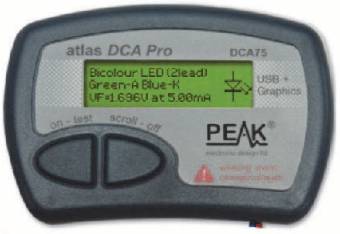

Analyzes transistors, MOSFETs, JFETs, IGBTs, and more. Graphic display. Enhanced functionality with included PC software.

Semiconductor Component Analyzer

Analyzes transistors, MOSFETs, JFETs and more. Automatically determines component pinout.

Capacitance and ESR Meter

Analyzes capacitors, measures ESR.

Quicksilver Radio Products

Sign up on our website for your **FREE** newsletter.
Ham Radio news,articles and special discounts.

www.qsradio.com